Effects of Aggressive Leachates on Modified Geosynthetic Clay Liners (GCLs)

Tarek Abichou[1], Christian Wireko[1], and Youneng Tang[1]
[1] *FAMU-FSU College of Engineering, Florida State University, Department of Civil and Environmental Engineering*
Email: abichou@eng.famu.fsu.edu, Phone: (850)410-6661

KEYWORDS: Municipal solid waste incinerator ash, Polymer-modified bentonite, Bentonite-polymer composite, Hydraulic conductivity, Swell index, Viscosity, Linear polymer, Water-soluble polymer, Crosslinked polymer, Superabsorbent polymer, Polymer elution

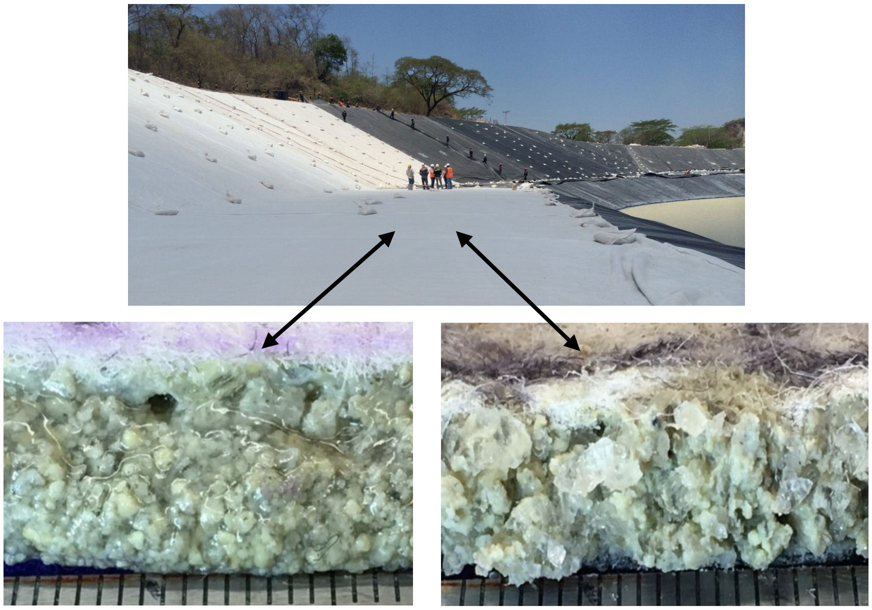

FINAL REPORT

Prepared for the
Environmental Research and Education Foundation

EREF

2020

Executive Summary

Motivation and Objectives

Geosynthetics clay liners (GCLs) are factory manufactured products consisting of a thin layer (< 10 mm) of natural or activated sodium bentonite (Na-B) either glued to a geomembrane or sandwiched between two geotextiles by an adhesive or fibers and have gained widespread use as alternative to compacted clay liners in waste containment facilities mainly due to ease of installation and increase in waste storage capacity (because of their relatively thinness). Municipal solid waste incinerator (MSW-I) ash is being co-landfilled in MSW landfills or mono-filled in several states in the U.S. Leachates from MSW-I ash landfills typically have elevated concentration of salts which can be detrimental to the performance of conventional bentonite (CB) GCLs as effective hydraulic barrier. To resist these high ionic strength leachates, polymer-modified bentonite (PMB) GCLs containing a blend of Na-B and various polymers have been introduced in recent years. To date, only a limited number of studies have been performed on PMB GCLs, and the effects of the aggressive leachates on the performance and design of these second generation GCLs have not been well understood.

The first objective of this study was to develop new alternative index tests or criteria to predict the long-term hydraulic performance of the PMB GCLs. The second objective was to mechanistically understand how aggressive leachates like MSW-I ash leachate affect the performance of these second generation GCLs.

Key Findings

Effect of Specimen Preparation on Index Properties of Polymer-Modified Bentonite GCLs

Based on the results of the swell index (SI) and loss on ignition (LOI) the following conclusions can be deduced:

- There are limitations in application of the ASTM D5890 standard procedure for preparing specimens for swell index (SI) testing, particularly for PMBs. For both the Na-B and PMBs used in the study, <100% of the specimen passed through the #100 sieve regardless of the amount of crushing performed using a mortar and pestle. For the Na-B, 0.2% of the initial mass of the specimen was retained on the #100 sieve, whereas up to ~4% of the specimen was retained on the #100 sieve for the PMBs.

- The SI and LOI of the portion of the PMBs passing #100 sieve was comparable to that of the Na-B, whereas the portion retained on #100 sieve had high SI (~50 to 550 mL/2 g) and LOI (~40 to 84%). These observations indicate that grinding and sieving of the PMBs per the ASTM D5890 lead to segregation of polymer.
- Alternative specimen preparation methods investigated in this study showed that unlike Na-B, crushing and sieving have significant influence on the SI of PMBs. However, the effect was more profound for PMBs containing crosslinked polymer due to the high swelling capacity of superabsorbent polymers.
- The results of this study suggest that, to measure representative SI values for PMBs, SI tests should be performed using uncrushed polymerized bentonite received from the manufacturer or retrieved from the GCL.

Hydraulic Conductivity of Polymer-Modified Bentonite GCLs to MSW-I Ash Leachates

Based on the findings of the study, the following conclusions are drawn:

- Hydraulic conductivity of the PMB GCLs permeated MSW-I ash leachates depends on the ionic strength of the leachate, the polymer loading as well as the type of polymer (i.e., whether the polymer is linear or crosslinked).
- The PMB GCLs used in this study had hydraulic conductivity lower than 1.0×10^{-10} m/s when permeated with the MSW-I ash leachate with ionic strength of 174 mM (regardless of the polymer type or polymer loading), whereas the CB GCLs had hydraulic conductivity greater than 5.0×10^{-8} m/s when permeated with the same leachate.
- However, all the PMB GCLs used in this study had hydraulic conductivity greater than 3.0×10^{-10} m/s when permeated with MSW-I ash leachate with ionic strength exceeding 600 mM.
- Similar to CB GCLs, prehydrating PMB GCLs with water improves the compatibility of PMB GCLs to MSW-I ash leachates. Prehydration with water seem to improve the performance of PMB GCL with higher polymer loading. The effect of polymer loading and polymer type on the hydraulic conductivity of water-prehdyrated PMB GCLs is currently being investigated.
- The relationship between swell index (SI) and hydraulic conductivity of PMB GCLs, a strong correlation existed between SI and hydraulic conductivity of PMB GCLs when the

PMB specimens used for the SI tests were not subjected to any form of crushing and sieving. This suggests that SI (measured using polymerized bentonite retrieved from the GCL) can be used to assess the compatibility of PMB GCLs at least qualitatively preliminarily to MSW-I ash leachates under low effective stress (< 40 kPa).

- At similar polymer loading, LPB GCLs have lower hydraulic conductivity than CPB GCLs when permeated with the same MSW-I ash leachate. This is because linear polymers easily dissolve and diffuse uniformly in the bentonite matrix, therefore are more efficient than crosslinked polymers in blocking flow during permeation.
- However, polymer elutes from LPB GCLs during permeation, regardless of the chemistry of the permeant solution (i.e. whether permeated with DI water or MSW-I ash leachate). This is because, unlike crosslinked polymers, linear polymers are water-soluble, therefore, easily migrate with the leachate during permeation.
- Polymer elution affected hydraulic conductivity of the LPB GCLs used in this study when permeated with MSW-I ash leachates with ionic strength ≥ 622 mM but had negligible impact on hydraulic conductivity of the LPB GCLs permeated with the MSW-I ash leachate with ionic strength of 174 mM.
- The results of this study also suggest that the polymer blockage mechanism previously hypothesized to control the hydraulic conductivity of PMB GCLs is only applicable to PMB GCLs containing crosslinked polymer because crosslinked polymers are water-insoluble therefore do not easily migrate with the permeation solution as linear polymers do. A study was conducted to investigate factors that influence polymer elution from LPB GCLs and the mechanism containing the chemical compatibility of LPB GCLs (after polymer elutes).

Investigating Factors Influencing Polymer Elution and the Mechanism Controlling Chemical Compatibility of a Polymer-Modified Bentonite GCL containing linear Polymer

Based on the findings of the study, the following conclusions are drawn:

- The linear polymer gel eluted during permeation of the LPB GCL, regardless of the permeant chemistry (i.e. whether with DI water of salt solution). However, the rate at which polymer eluted and the effect of polymer elution had on the final hydraulic conductivity of the LPB GCL depended on the concentration and valence of the dominant cation in permeant solution.

- The rate at which polymer eluted from the LPB GCL increased with the cation valance and concentration of the dominant cation in the permeant solution. When permeant with $CaCl_2$ solutions, polymer eluted at a rate nineteen times faster than with the NaCl solutions. This is because divalent cations can contract the polymer chains by crosslinking the functional groups within a polymer chain and/or between individual polymer chains which consequently reduces the polymer ability to absorb water, resulting in a lower viscosity polymer gel.
- The rate at which polymer eluted also increased with the average hydraulic gradient used during permeation. However, hydraulic gradient did not have any impact on the measured hydraulic conductivity of the LPB GCL.
- Free swell tests coupled with chemical analysis suggest that the long-term chemical compatibility of the LPB GCL is due to the ability of the polymer to scavenge cations from the solution which allows the bentonite to undergo osmotic swelling during the initial hydration period.

Compatibility Testing of Polymer-Modified Bentonite GCLs: Recommendations

- Eluted polymer can clog the effluent tube of the permeameter during permeation and cause an apparent decrease in measured hydraulic conductivity. Therefore, both the effluent and influent tubes require periodic check for potential clogging by eluted polymer when during hydraulic conductivity testing of LPB GCLs. A large diameter tubing (preferable ≥ ¼ in inner diameter tube) is recommended for the influent and effluent lines of the permeameter to reduce the risk of polymer clogging. The volumetric flow ratio (Q_{out}/Q_{in}) can be used along with the trend in measured hydraulic conductivity to check for polymer clogging, with $Q_{out}/Q_{in} < 0.75$ suggesting clogging.

Table of Contents

List of Figures

List of Tables

1 Introduction

1.1 Motivation and Objectives

Incineration of municipal solid waste (MSW), also known as waste-to-energy (WTE), has become a popular method for managing MSW due to the ability to significantly reduce the mass and volume of waste (by ~60 % and ~90% respectively), saving landfilling space (Chandler et al., 1997; Dou et al., 2017), and generating electricity and heat in the process (Allegrini et al., 2015). In countries like Sweden, Denmark, and Germany, more than 50% of MSW incinerator (MSW-I) ash by WTE plants is reused as a substitute for light aggregates used in construction applications (Dou et al., 2017). However, in the United States (US), majority of MSW-I ash is either disposed alone in an ash monofill or co-disposed with regular MSW (Oehmig et al., 2015; Moody and Townsend, 2017; Joseph et al., 2018; Li et al., 2019). MSW-I ash can contain high concentrations of heavy metals, chlorides and organic pollutants (Chandler et al., 1997; Sabbas et al., 2003; Lam et al., 2010). Thus, to protect groundwater quality, regulatory agencies in the US require MSW-I ash landfills to have at least a single-composite liner system consisting of a geomembrane overlying a 0.6 m thick compacted clay liner (CCL) having hydraulic conductivity $\leq 1.0 \times 10^{-9}$ m/s (Qian et al., 2001; Bonaparte et al., 2002). Regulatory agencies also allow the use of an alternative liner material if demonstrated to be "technically equivalent" to a CCL (Qian et al., 2001; Bonaparte et al., 2002). Geosynthetics clay liners (GCLs) are factory manufactured products consisting of a thin layer (< 10 mm) of natural or activated sodium bentonite (Na-B) either glued to a geomembrane or sandwiched between two geotextiles by an adhesive or fibers, and have gained widespread use as alternative to CCLs in waste containment facilities mainly due to ease of installation and increase in waste storage capacity (because of their relatively thinness) (Qian et al., 2001; Koerner, 2012; Rowe, 2020).

In the absence of a geomembrane, the hydraulic conductivity of conventional GCLs is primarily controlled by the Na-B (Petrov et al., 1997a; Shackelford et al., 2000; Jo et al., 2001; Kolstad et al., 2004b; Lee and Shackelford, 2005; Setz et al., 2017; Chen et al., 2018; Rowe, 2020). The dominant mineral in the Na-B used in GCLs is montmorillonite, which has Na^+ as the dominant interlayer cation (Norrish, 1954; Grim and Guven, 1978). When hydrated and permeated with water or a dilute solution, Na-B undergoes osmotic swelling due to "chemico-osmosis," i.e., the flow of H_2O from lower ion concentration (higher H_2O chemical potential) outside the interlayer region of the montmorillonite particles (tactoids) to higher ion concentration (lower H_2O chemical potential) inside the interlayer region of the montmorillonite particles, which results in the formation of a thick layer of ions and water molecules (so-called “diffuse double layer”) around the montmorillonite particles (Norrish, 1954; Olphen, 1963; Grim and Guven, 1978; McBride, 1994). Repulsive forces between individual hydrated particles causes the particles to form the so-called “house-of-cards” structure, an arrangement which minimizes repulsion between the particles (Olphen, 1963). This house-of-cards structure of the montmorillonite particles reduces intergranular pores spaces of the bentonite fabric and yields a tortuous flow path for the permeant solution, resulting in low hydraulic conductivity ($<1.0 \times 10^{-10}$ m/s) (Mesri and Olson, 1971; Shackelford et al., 2000; Jo et al., 2001; Ashmawy et al., 2002; Kolstad et al., 2004b; Chen et al., 2018).

However, when Na-B is hydrated and permeated with aggressive solutions (i.e. solutions with high ionic strength and/or predominance of polyvalent cations like Ca^{2+} and Mg^{2+}), osmotic swelling of Na-B is suppressed due to the low concentration gradient between the permeant solution and the interlayer region of the montmorillonite particles and/or due to cation exchange (i.e. replacement of the native Na^+ cations by polyvalent cations in the permeant solution) (McBride, 1994). This results in large intergranular pore spaces within the bentonite fabric and consequently high hydraulic conductivity ($> 1.0 \times 10^{-10}$ m/s) (Petrov and Rowe, 1997; Shackelford et al., 2000; Jo et al., 2001; Katsumi et al., 2001; Jo et al., 2004; Kolstad et al., 2004b; Jo et al., 2005; Lee et al., 2005; Bradshaw and Benson, 2014; Bradshaw et al., 2016; Chen et al., 2018; Wang et al., 2019). Leachate from landfills containing IA can have elevated concentration of salts (Ashmawy et al., 2002; Xia et al., 2015; Moody and Townsend, 2017; Li et al., 2019), which can be detrimental to the performance of conventional GCLs as effective hydraulic barrier.

Significant research has focused on improving the chemical compatibility of Na-B to aggressive solutions by chemically modifying or blending bentonite with organic molecules and polymers, which are hypothesized to either activated osmotic swelling, limit cation exchange or physically clog the intergranular pore spaces of the bentonite fabric, yielding low hydraulic conductivity (Onikata et al., 1996; Onikata et al., 1999; McRory and Ashmawy, 2005; Katsumi et al., 2008; Di Emidio, 2010; Scalia et al., 2014; Guler et al., 2018; Ozhan, 2018; Prongmanee et al., 2018; Salemi et al., 2018; Pandey et al., 2019; Prongmanee and Chai, 2019; Yu et al., 2019; Chai and Prongmanee, 2020). Most manufacturers sell GCLs containing bentonite dry blended or treated with proprietary polymers (Ashmawy et al., 2002; Scalia et al., 2014; Athanassopoulos et al., 2015; Salihoglu et al., 2016; Tian et al., 2016; Donovan et al., 2017; Tian and Benson, 2017; Tian et al., 2017; Chen et al., 2019; Tian et al., 2019; Zainab and Tian, 2020). These second generation commercial GCLs are collectively referred to herein as polymer-modified bentonite (PMB) GCLs. To date, only a limited number of studies have been performed on PMB GCLs, and the effects of the aggressive leachates on the performance and design of these second generation GCLs have not been well understood.

The first objective of this study was to develop new alternative index tests or criteria to predict the long-term hydraulic performance of the PMB GCLs. The second objective was to mechanistically understand how aggressive leachates like MSW-I ash leachate affect the performance of the second generation GCLs.

1.2 Background

1.2.1 Polymers used in polymer-modified bentonites and bentonite-polymer composites

Various types of polymers have been used as amendments for bentonites proposed for containment of aggressive solutions (Di Emidio, 2010; Scalia et al., 2014; Guler et al., 2018; Ozhan, 2018; Prongmanee et al., 2018; Salemi et al., 2018; Scalia et al., 2018a; Pandey et al., 2019; Prongmanee and Chai, 2019; Yu et al., 2019; Chai and Prongmanee, 2020; Fan et al., 2020). Polymers that have been used in literature for sealing applications can be generally grouped into two main categories, depending on the basic structure of the polymer, i.e. as linear polymer or crosslinked polymer.

Linear polymers are polymers in which monomeric units are covalently linked together to form a chain. Linear polymers (whether naturally occurring or synthetic) have a unique ability to disperse and swell in water to form a viscous polymer gel due to the presence of hydrophilic functional groups in their repeating units. For this reason, linear polymers are loosely referred to as water-soluble polymers (Chatterji and Borchardt, 1981; Billmeyer, 1984; Williams, 2007; Kadajji and Betageri, 2011; Rivas et al., 2018). Tian et al. (2019) used Fourier transform infrared (FTIR) spectroscopy to identify the polymer blended with bentonite in one commercial PMB GCL. The FTIR spectra of the polymer used in the PMB GCL matched (up to 80%) the spectra of anionic polyacrylamide, which is a commercial linear polymer. Sodium carboxymethyl cellulose (Na-CMC) polymer which was used by Di Emidio (2010) to develop “HYPER clay” also has a linear structure, and therefore classified as a linear polymer (Chatterji and Borchardt, 1981; Williams, 2007).

Crosslinked polymers are a network of linear polymer chains bonded together either physically (using methods such as heating/cooling, and etc.) or chemically (using special crosslinking agents or grafting techniques) (Buchholz and Graham, 1998; Zohuriaan-Mehr and Kabiri, 2008; Behera and Mahanwar, 2020). Unlike linear polymers, crosslinked polymers are not soluble in water due to presence of the crosslinkers but are capable of imbibing large amount of water when hydrated to form discrete polymer hydrogels, hence are commonly referred to as superabsorbent polymers (SAPs). However, SAPs also have a soluble fraction (so-called "extractables") which consists of residual monomers and low molecular weight polymer chains that were not successfully incorporate into the polymer network during manufacturing. The soluble fraction of SAPs is typically less than 20% (Buchholz and Graham, 1998; Zohuriaan-Mehr and Kabiri, 2008; Behera and Mahanwar, 2020). Scalia and Benson (2016) and Salemi et al. (2018) have experimented with blending sodium-polyacrylate (a commercially available SAP) with bentonite for aggressive leachate containment applications.

1.2.2 Compatibility indicator: Limitations of the traditional ASTM D890 procedure for measuring swell index of PMB GCLs

The hydraulic conductivity of GCLs typically is measured in the laboratory as per ASTM D6766. Based on these standards, a hydraulic conductivity test is continued until hydraulic and chemical equilibrium are achieved in order to reflect the long-term hydraulic conductivity of GCLs, which may require the test durations lasting from a few months to years (Petrov and Rowe, 1997; Shackelford et al., 2000; Katsumi et al., 2001; Kolstad et al., 2004b; Jo et al., 2005; Katsumi et al., 2007; Katsumi et al., 2008). The time required to reach chemical equilibrium can be even longer for PMB GCLs (Scalia et al., 2014; Razakamanantsoa and Djeran-Maigre, 2016; Tian et al., 2016; Donovan et al., 2017; Chen et al., 2019). Hence, quick and inexpensive index tests are often performed on the bentonite component of GCLs to assess indirectly the chemical and hydraulic compatibility of the GCL with the permeant liquid (Jo et al., 2001; Lee et al., 2005; Katsumi et al., 2008; Rosin-Paumier et al., 2010).

The swell index (SI) test (ASTM D5890) is a commonly used index test to assess the hydraulic performance and the chemical compatibility of GCLs to leachates. Two grams of bentonite are ground until 100 % passes the No. (#) 100 mesh, and a minimum of 65% passes the #200 mesh U.S. standard sieve. Numerous studies have shown that a correlation exists between SI and hydraulic conductivity of CB (Jo et al., 2001; Jo et al., 2004; Kolstad et al., 2004b; Olsta et al., 2004; Lee et al., 2005; Katsumi et al., 2008; Guyonnet et al., 2009; Chen et al., 2018). For CB GCLs, SI > 14 mL/2 g generally correlates to hydraulic conductivity < 1.0×10^{-10} m/s, whereas SI < 14 mL/2 g generally correlates to hydraulic conductivity > 1.0×10^{-10} m/s (Jo et al., 2001; Lee et al., 2005; Chen et al., 2018). However, the SI and hydraulic conductivity of PMB GCLs are not well correlated. For example, as shown in Figure 1, PMB GCLs with SI < 10 mL/2 g can still maintain low hydraulic conductivity (< 1.0×10^{-10} m/s) (Scalia et al., 2014; Salihoglu et al., 2016; Shen et al., 2016; Tian et al., 2016; Scalia et al., 2018a; Chen et al., 2019; Tian et al., 2019). In contrast, the hydraulic conductivity of PMB GCLs can be greater than 1.0×10^{-10} m/s when SI of PMB exceeds 20 mL/2g. The poor correlation between hydraulic conductivity and SI for PMB GCLs may be an indication that the procedure and specimen preparation for the SI test are not appropriate for PMB GCLs. For example, during sieve analysis of a PMB GCL, Oren et al. (2018) observed some gel-like materials retained on the #200 sieve which they attributed to the polymer additive(s) in the bentonite.

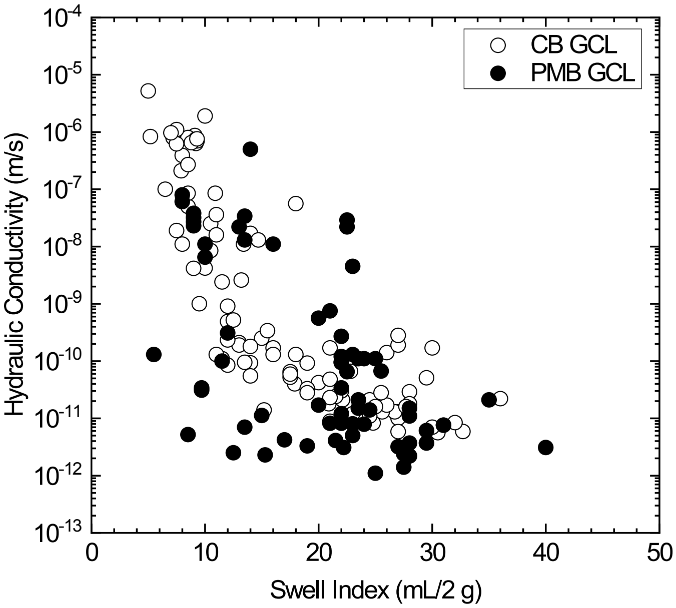

Figure 1. Relationship between swell index and hydraulic conductivity of conventional bentonite (CB) and polymer-modified bentonite (PMB) GCLs [Note: CB GCLs data from Jo et al. (2001); (Kolstad et al., 2004b); Lee et al. (2005); Katsumi et al. (2008); Setz et al. (2017); and Wang et al. (2019); and PMB GCLs data from Tian et al. (2016); Tian and Benson (2017); Tian et al. (2017); Chen et al. (2019); and Tian et al. (2019)]. Figure adapted from Wireko et al. (2020).

1.2.3 Mechanism proposed in literature for improved chemical compatibility of PMB GCLs

Studies conducted on PMB GCLs show they can have improved hydraulic performance as compared to CB GCLs when permeated with aggressive liquids (Salihoglu et al., 2016; Tian et al., 2016; Tian and Benson, 2017; Tian et al., 2017; Chen et al., 2019; Tian et al., 2019). For instance, Athanassopoulos et al. (2015) measured the hydraulic conductivity of a PMB GCL and CB GCL permeated with a bauxite liquor (with pH = 13 and ionic strength = 2350 mM) and a trona ash leachate (with pH = 11 and ionic strength = 1050 mM). The hydraulic conductivity of the PMB GCL to the bauxite liquor and trona ash leachate was less than 1.0×10^{-10} m/s, whereas the CB GCL had hydraulic conductivity greater than 1.0×10^{-8} m/s. However, the mechanism controlling the chemical compatibility of PMB GCLs is still not well understood mainly because polymer(s) used in PMB GCLs are proprietary, meaning crucial information about the specific polymer(s) used is not provided by the manufacturer (Razakamanantsoa et al., 2012; Razakamanantsoa and Djeran-Maigre, 2016; Tian et al., 2016; Scalia et al., 2018a; Chen et al., 2019; Tian et al., 2019);

Based on scanning electron microscope (SEM) images of PMB specimens hydrated with deionized (DI) water and $CaCl_2$ solutions, Tian et al. (2016) and (2019) hypothesized that hydraulic conductivity of PMB GCLs is controlled by blockage of the bentonite intergranular pores by the viscous polymer gel. However, the mechanism of polymer blockage does not totally explain the observed behavior of PMB GCLs reported in literature because, the migration of the polymer gel from the GCL (i.e. polymer elution) have been reported to occur during permeation of PMB GCLs regardless of the chemistry of the permeant liquid (Chen, 2015; Salihoglu, 2015; Tian and Benson, 2017; Tian et al., 2017; Geng, 2018; Reybrock, 2018; Chen et al., 2019; Tian et al., 2019). However, the impact polymer elution has on the hydraulic conductivity of PMB GCLs seem to depend on the chemical characteristics of the permeant.

Figure 2 shows hydraulic conductivity as a function of total mass of polymer eluted from a PMB GCL during with various salts solutions and synthetic trona leachate by Geng (2018). The PMB GCL had 5.1% polymer loading. Geng (2018) determined the total mass of polymer eluted using total organic carbon (TOC) concentration of the effluent samples collected during permeation. As shown in Figure 2, specimens of same PMB GCL can have significantly different hydraulic conductivities even when similar amount of polymer elutes during permeation. For instance, the final hydraulic conductivity of the PMB GCL specimen permeated with 300 mM

NaCl was ~8.0×10^{-11} m/s) whereas hydraulic conductivity of the specimen permeated with 50 mM $CaCl_2$ was ~3.3×10^{-7} m/s (more than 100 times higher), even though similar amount of polymer (925 mg versus 950 mg) eluted from both specimens during permeation. Moreover, there is no correlation between the hydraulic conductivity and mass of polymer eluted from the PMB GCL during permeation as shown in Figure 2. For example, hydraulic conductivity of the PMB GCL specimen permeated with 50 mM Mg [with anion ratio (Cl^-/SO_4^{-2}), R = 20] was more than three orders-of-magnitude higher than that of specimen permeated 50 mM $CaCl_2$ (2.0×10^{-10} m/s versus 3.3×10^{-7} m/s even though more polymer eluted from the specimen permeated with 50 mM Mg [with anion ratio (Cl^-/SO_4^{-2}), R = 20] as shown in Figure 2.

Similarly, Salihoglu (2015) measured the hydraulic conductivity of two PMB GCLs permeated with various CCP leachates and one MSW-I ash leachate. Salihoglu (2015) also quantified the amount of polymer eluted using TOC concentration of the effluent samples collected during permeation. For one of the PMB GCLs, the final hydraulic conductivity of the specimen permeated with a synthetic CCP leachate (with ionic strength of 177 mM) was 9.8×10^{-12} m/s whereas hydraulic conductivity of the specimen permeated the MSW-I ash leachate (with ionic strength of 1042 mM) was 1.3×10^{-10} m/s, even though the percentage polymer eluted from both specimens were almost the same. These aforementioned discrepancies suggest that some other mechanism may be responsible the improved chemical compatibility of PMB GCLs relative to CB GCLs even when polymer elutes.

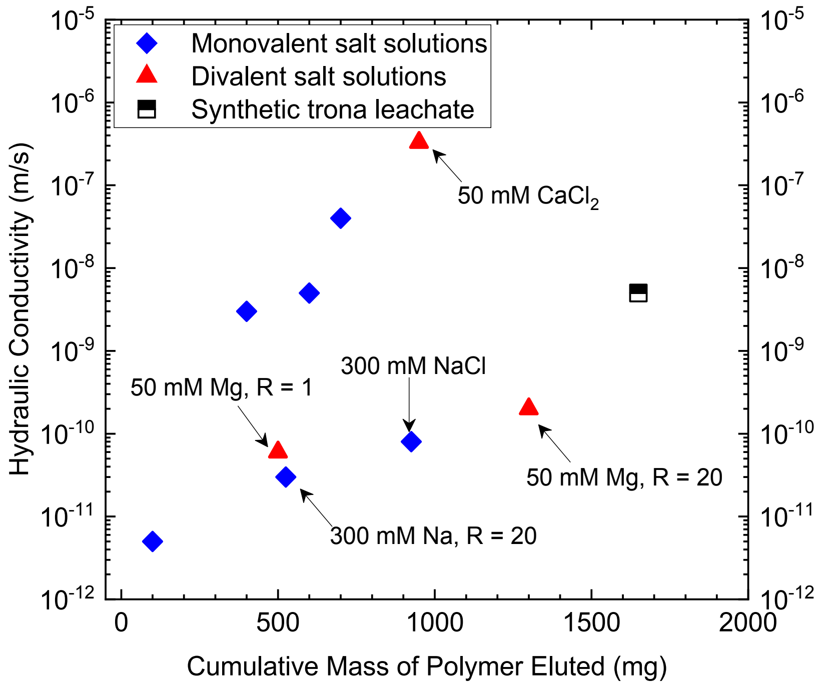

Figure 2. Hydraulic conductivity as a function of cumulative mass of polymer eluted from a polymer-modified bentonite (PMB) GCL with 5.1% polymer loading (by dry mass) during permeation with different inorganic salt solutions and leachate [Note: Data from Geng (2018). R = Anion ratio; defined as the ratio of the molar concentration of Cl^- to SO_4^{-2}. The reported hydraulic conductivity values were measured at an average effective stress of 20 kPa and hydraulic gradient of 130. Cumulative mass of polymer was calculated based on total organ carbon concentration in effluent samples collected during permeation].

2 Results and Discussion

2.1 Effect of Specimen Preparation on Index Properties of Polymer-Modified Bentonite GCLs

Note: A manuscript containing majority of the text, figures and tables in the section has been accepted for publication in Geotextiles and Geomembranes Journal:
Wireko C.[1], Zainab Z.[2], Tian K.[3], Abichou T.[1], 2020. "Effect of Specimen Preparation on the Swell Index of Bentonite-Polymer GCLs"
[1]Department of Civil and Environmental Engineering, Florida A&M University- Florida State University College of Engineering, 2525 Pottsdamer St., Tallahassee, FL, 32310-6064, USA; [2]Tetra-Tech AAI, Orlando, FL, USA; [3]Department of Civil, Environmental and Infrastructure Engineering, George Mason University, Fairfax, VA 22030, USA.

This section describes a study conducted to investigate the influence of crushing and sieving on the swell index (SI) of PMBs. Tests were conducted on seven PMB specimens prepared according to the ASTM standard method (D5890) and two other alternative methods. SI tests were performed using type II deionized (DI) water. Loss on ignition (LOI) tests were also conducted to quantify polymer content of the prepared specimens, in support of the explanations for the measured swell indices.

Seven PMBs designated herein as B-P1, B-P2, B-P3, B-P4, B-P5, B-P6, and B-P7 were investigated in this study. All the PMBs were produced by dry mixing of granular Na-B with proprietary polymer(s). Though the specific polymer(s) used in the PMBs was(were) not disclosed, the manufacturer specified that the bentonites used in B-P1, B-P2, B-P3, and B-P4 were blended with different linear polymer(s) (i.e., water-soluble polymers) at different polymer contents, whereas B-P5, B-P6, and B-P7 were comprised of crosslinked polymer(s) (i.e., superabsorbent polymers). Distinct swelling characteristics of the two classes of the PMBs were observed in this study, as demonstrated in subsequent sections.

2.1.1 Specimen preparation methods

2.1.1.1 Standardized swell index testing

The Na-B and PMB specimens were first prepared following the ASTM standard for the SI test (ASTM D5890). Twenty five grams of each specimen was ground to pass the #100 sieve using a conventional pestle and mortar. However, after extensive and iterative grinding and sieving, a small portion of PMBs would not pass through the #100 sieve. Of the portion that passed the #100 sieve, more than 65% also passed the #200 sieve, as required by the ASTM D5890. The portion that passed the #100 sieve is referred to herein as "ASTM-Passing #100 (ASTM-P)", whereas the portion that was retained on the #100 sieve is referred to herein as "ASTM-Retained #100 (ASTM-R)". The amounts of ASTM-P and ASTM-R for all seven PMBs are shown in Table 1. The mass of ASTM-R as percentage of the initial mass of specimen ranged from 0.1 to 4% for both Na-B and PMB specimens.

For the PMBs, the ASTM-R were white granules and had a gel-like texture, unlike the ASTM-P which were powder and grayish brown as shown in Figure 3a and b for B-P7. Oren et al. (2018) reported similar results for a sieve analysis of a PMB GCL. The physical appearance and texture of the ASTM-R suggested the material could be the polymer additives (Williams, 2007; Zohuriaan-Mehr and Kabiri, 2008; Mahon et al., 2019; Behera and Mahanwar, 2020) which was segregated from the PMBs during sieving. To verify this, free swell tests (using DI water) and loss on ignition (LOI) tests were performed on the ASTM-R.

Table 1. Amounts of 25.0 g Na-B and PMB specimens retained and passing the #100 sieve after Crushing

Material	Mass retained #100 sieve (g)	Mass passing # 100 sieve (g)	Percentage mass retained # 100 sieve (%)
Na-B	0.05	24.95	0.20
B-P1	0.03	24.97	0.12
B-P2	0.54	24.46	2.2
B-P3	0.41	24.59	1.6
B-P4	0.99	24.01	4.0
B-P5	0.56	24.44	2.2
B-P6	0.60	24.40	2.4
B-P7	0.50	24.50	2.0

2.1.1.2 Alternative swell index methods

Observations of the specimens prepared following the ASTM standard method revealed that crushing and sieving the PMBs, as required by ASTM D5890, resulted in the retention of some material on the #100 sieve (Table 1), which appeared to be the polymer additives (see Figure 3b). Hence, alternatives to the standardized method as defined in Table 2 were explored as possible specimen preparation methods for SI testing of B-P GCLs.

For Alternative 1 (AL1), specimens of Na-B and PMBs were not subjected to any crushing and sieving to prevent the potential separation of polymer and bentonite, i.e., the specimens were used as they were received from the manufacturer. Specimens prepared using this method are referred to herein as “AL1 specimens.”

For Alternative 2 (AL2), 50 g of each specimen was ground and sieved until approximately half of the specimen passed the #100 sieve. This method was developed to assess the influence of the #100 sieve on polymer segregation. The portion that passed the #100 sieve is referred to herein as “Alternative 2-Passing #100 (AL2-P),” and the portion that retained on the #100 sieve is referred to herein as “Alternative 2-Retained #100 (AL2-R).”

2.1.2 Swell Index Tests

Swell index (SI) tests on the ASTM-P, AL1, AL2-P and AL2-R specimens were performed following the procedure outlined in ASTM D5890. Two grams of the specimen was oven-dried and added into a 100 mL graduated cylinder filled with 90 mL of DI water or synthetic leachate. The specimen was added in increments of 0.1 g into the graduated cylinder. The cylinder then was filled to the 100 mL mark with the same hydrating liquid. The SI (mL/2g) was measured as the volume of the swollen specimen in the graduated cylinder after 24 h. For the Na-B and all the PMBs, SI tests were conducted in triplicates, and averages were reported.

For the ASTM-R specimens, an earlier attempt to measure the SI following the traditional procedure resulted in the clogging of the top of the graduated cylinder. This further suggested that the portion of the PMBs retained on the #100 sieve was polymer, because unlike bentonite, polymers have a much lower density (0.9 – 1.3 g/cm^3) (Billmeyer, 1984), and therefore settle at a slower rate. Based on this observation, the procedure adopted for the ASTM-R specimens was as follows: 0.2 g of ASTM-R specimen (due to the small quantity of specimen) were added to an empty 100 mL graduated cylinder and then DI water was gradually added in increments of 1 mL every 10 min. The tests were performed until no swelling was observed after adding the water and the SI (mL/0.2 g) was then recorded as the final volume of the swollen specimen.

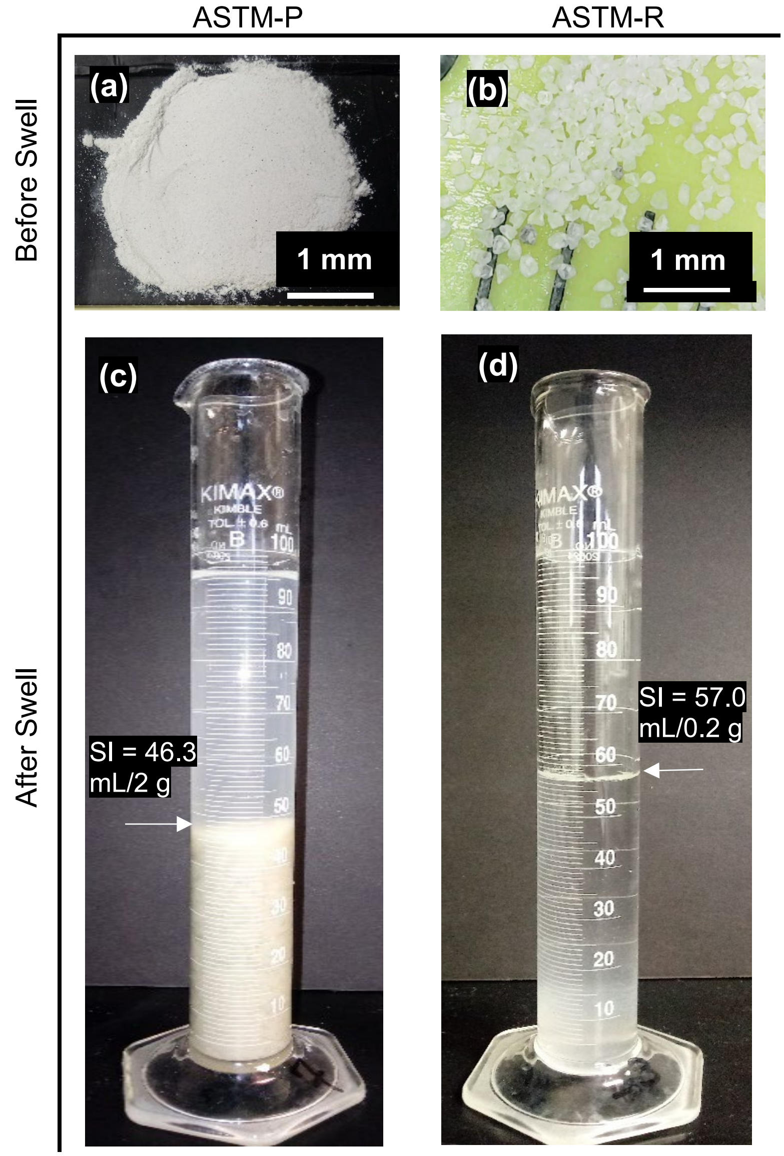

Figure 3. Comparison of swell indices of B-P7 specimens before (a and b) and after (c and d) swell test, prepared following ASTM standard method which includes the specimens passing the #100 sieve (ASTM-P) and retained on the #100 sieve (ASTM-R). (Note: above the 57 mL mark of the graduated cylinder for the ASTM-R there is no extra water).

Table 2. Specimen preparation methods used in this study

Method	Method Components	Designation	Crushing and Sieving
ASTM Standard	ASTM-Passing #100	ASTM-P	Passing #100 sieve (min 65% passing # 200 sieve)
	ASTM-Retained #100	ASTM-R	Retained #100 sieve (Remnants of ASTM specimen)
Alternative 1	Not applicable	AL1	None
Alternative 2	Alternative 2-Passing #100	AL2-P	Passing #100 sieve (50% of total AL2 specimen)
	Alternative 2-Retained #100	AL2-R	Retained #100 sieve (50% of total AL2 specimen)

2.1.3 Loss on Ignition Tests

The loss on ignition (LOI) test is widely used to determine the polymer content of PMBs (Scalia et al., 2014; Tian et al., 2016; Scalia and Benson, 2017; Chen et al., 2019; Tian et al., 2019). LOI tests were conducted in this study to determine the polymer content of the specimens prepared by different methods (i.e., ASTM-P, ASTM-R, AL1, AL2-P, and AL2-R). The specimens obtained from each preparation method were first oven-dried to a constant mass at 105 ± 5 ^{0}C. The specimens then were ignited at 550 ± 5 ^{0}C for 4 h using a muffle furnace. During the LOI test, polymer additives were assumed to be the only constituents that are combusted completely. The percentage of mass loss of the specimen was reported as the LOI.

Three replicate tests were conducted using approximately 5 g of the ASTM-P, AL1, AL2-P, and AL2-R specimens. LOI tests were also conducted on the ASTM-R specimens to quantify the polymer content of the portion of PMBs segregated by the #100 sieve when following the ASTM D5890. However, the mass of the ASTM-R specimens used for the LOI tests varied from 0.1 to 0.2 g due to the limited quantity of the specimen, as shown in Table 1.

2.1.4 Results of tests performed on specimens prepared following the ASTM standard method

Results of the SI and LOI tests conducted on Na-B and PMB specimens prepared following the ASTM standard method (ASTM-P and ASTM-R) are summarized in Table 3. SI results given in Table 3 were performed using DI water. Images of the SI tests performed on the ASTM-P and ASTM-R specimens for B-P7 are shown in Figure 4. The ASTM-P specimen (Figure 3a), when hydrated, formed a grayish brown gel (see Figure 3c), whereas the ASTM-R specimen (Figure 3b) formed a clear gel (see Figure 3d). To compare SI results of the ASTM-P and ASTM-R specimens, the measured SI of the ASTM-R specimens (mL/0.2 g) were linearly converted to mL/2 g by multiplying the measured SI of the ASTM-R specimens by a factor of 10 as given in Table 3. For instance, because the swell volume of 0.2 g of the ASTM-R specimen for B-P7 was 55.0 mL (see Figure 3d) and 43.6 mL for 2 g of the ASTM-P specimen (see Figure 3c), 2 g of the ASTM-R specimen was projected to have a swell volume of 570.0 mL.

Table 3. Swell index and loss on ignition (LOI) test results of specimens prepared following ASTM standard method

Material	ASTM-P		ASTM-R		
	Swell index (mL/2 g)	LOI (%)	Swell index (mL/0.2 g)	Projected swell index (mL/2 g)	LOI (%)
Na-B	28.7	1.3	NM	NM	NM
B-P1	28.7	1.2	NM	NM	50
B-P2	30.3	1.2	5.0	50	46
B-P3	30.3	1.4	9.0	90	72
B-P4	31.0	1.3	15.0	150	71
B-P5	31.0	1.9	7.0	70	44
B-P6	50.1	2.9	40.0	400	54
B-P7	46.3	4.0	57.0	570	84

Note: NM = Not measured due to limited quantity of specimen.

2.1.4.1 Swell index

The SI of the ASTM-P and ASTM-R specimens are compared in Figure 4. The SI of the ASTM-R specimens of the PMBs were significantly greater (2 to 11 times) than the SI of the ASTM-P specimens. For instance, for B-P4, the SI of the ASTM-P specimen was approximately 31 mL/2 g, whereas the SI of the ASTM-R specimen was approximately 150 mL/2 g. Similarly, for B-P6, the SI of the ASTM-P specimen was approximately 51 mL/2 g, compared to 400 mL/2 g for the ASTM-R specimen.

Visual inspection of the ASTM-R specimens before and after the swell tests also suggested that two distinct types of polymers were used in the PMBs investigated in this study (see Figure 5). ASTM-R specimens for B-P2, B-P3, and B-P4 formed a viscous gel when hydrated with DI water (as shown in Figure 5c for B-P3), suggesting that B-P2, B-P3, and B-P4 comprised linear polymer(s) (water-soluble polymers). Water-soluble polymers have a unique property of modifying the viscosity of aqueous solutions (Williams, 2007). On the other hand, ASTM-R specimens for B-P5, B-P6, and B-P7 formed discrete non-viscous hydrogels when hydrated with DI water (as shown in Figure 5d for B-P7). This indicates that the Na-B contained in B-P5, B-P6, and B-P7 were blended with crosslinked polymer(s) (SAP). A granule of SAP can absorb and retain a large amount of water to form a discrete hydrogel (Buchholz and Graham, 1998; Zohuriaan-Mehr and Kabiri, 2008; Mahon et al., 2019; Behera and Mahanwar, 2020).

The difference in polymer type explains the difference in SI between the ASTM-R specimens for the PMBs. For example, the SI of the ASTM-R specimen for B-P7 was more than 3 times the SI of the ASTM-R specimen for B-P4 (550 mL/2 g vs. 150 mL/2 g). SAP (crosslinked polymers) have higher swelling capacity compared to water-soluble polymers (linear polymers) (Buchholz and Graham, 1998; Williams, 2007). For instance, Scalia et al. (2014) reported that a commercial SAP had an SI of approximately 1790 mL/2 g in DI water. Results of the SI tests and examination of the swollen ASTM-R specimens revealed that the portion of the PMBs retained on the #100 sieve mainly comprised polymer (as shown in Figure 3 and Figure 5).

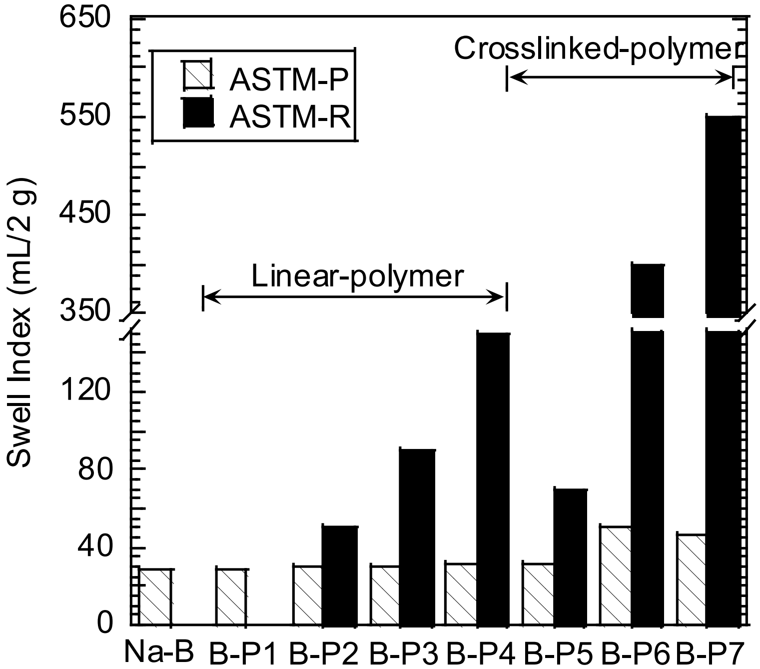

Figure 4. Comparison of swell indices of Na-B and PMB specimens prepared following ASTM standard method which includes the specimens passing the #100 sieve (ASTM-P) and retained on the #100 sieve (ASTM-R) (Note: the swell index of ASTM-R (in mL/2 g) was predicted based on swell index measured using 0.2 g of specimen; the swell index of the ASTM-R specimen for Na-B and B-P1 was not measured due to limited quantity of the specimen retained on the #100 sieve).

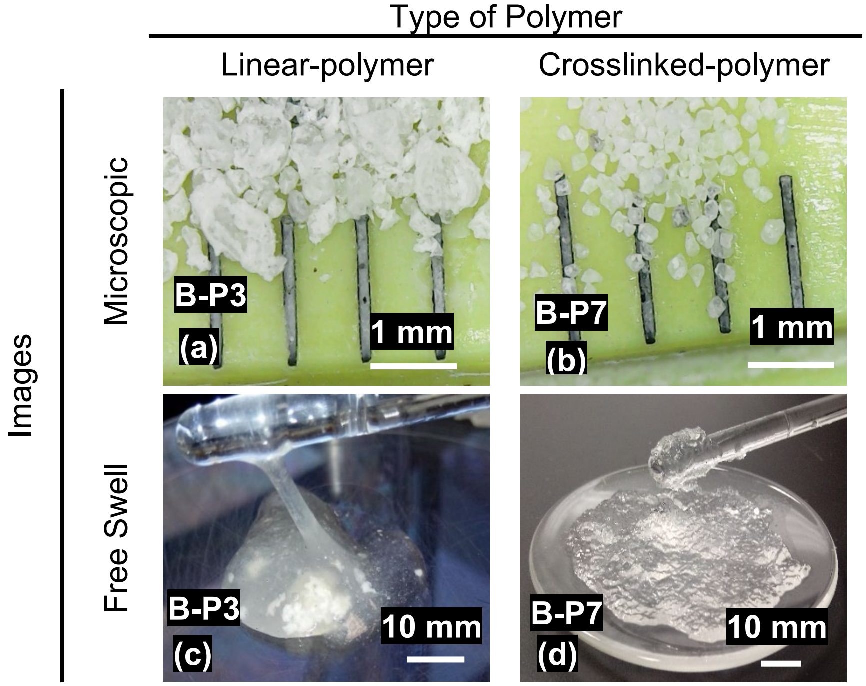

Figure 5. Images of ASTM-Retained #100 (ASTM-R) specimens of B-P3 and B-P7 before (a and b) and after (c and d) swell index test.

2.1.4.2 Loss on ignition

The LOI results for the ASTM-P and ASTM-R specimens for the Na-B and the PMBs are shown in Figure 6. The Na-B had an LOI of 1.3 %, which is similar to the LOI of Na-B (~1.6%) previously reported (Scalia et al., 2014; Tian et al., 2016). The LOI of the ASTM-P specimens for the PMBs containing linear polymer (i.e., B-P1, B-P2, B-P3, and B-P4) was similar to the LOI of the Na-B (1.2 to 1.3 %), whereas the LOI of the ASTM-P specimens for the PMBs containing crosslinked polymer (i.e., B-P5, B-P6, and B-P7) ranged from 1.8 to 4.0%. The ASTM-R specimens for all the PMBs showed significantly higher LOI (>40%) than the ASTM-P specimens. The significantly higher LOI of the ASTM-R specimens for the PMBs indicates that the ASTM-R specimens were primarily composed of polymer. The results of the LOI tests on the ASTM-P and ASTM-R specimens agree with the results of the SI tests (compare Figure 4 and Figure 6).

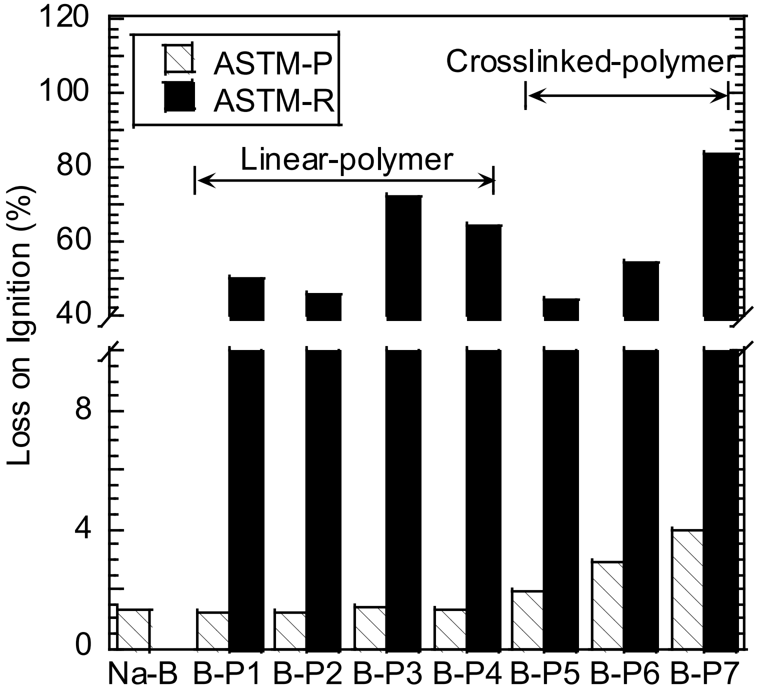

Figure 6. Loss on ignition (LOI) of Na-B and PMB specimens prepared following ASTM standard method for the specimen passing the #100 sieve (ASTM-P) and retained on the #100 sieve (ASTM-R).

Images of the ASTM-P and ASTM-R specimens for the Na-B and B-P6 before and after the LOI test, shown in Figure 7, support the contention that polymer was segregated from the PMBs during the grinding and sieving process. The ASTM-P specimen for Na-B before and after the LOI test looked similar, and no ash was seen in the ignited specimen, as shown in Figure 7a and d. Fewer ash residues were observed for the ASTM-P specimen of B-P6 after the LOI test (Figure 7e), whereas the ASTM-R specimen for B-P6 turned from white-gray granules to black ash after the LOI test, indicating burning of polymer (Fina and Camino, 2011). These observations correlate with the results of the LOI tests seen in Figure 6, i.e., the LOI of the ASTM-P specimens for the PMBs is similar to that of the Na-B, whereas LOI of the ASTM-R specimens for the PMBs is significantly higher than that of the ASTM-P specimens.

Overall, these observations indicate that polymer was segregated by the #100 sieve during crushing and sieving of the PMBs as per the ASTM D5890 specimen preparation method. The polymer segregation resulted in unrepresentative measured SI, which may explain the poor correlation between SI (performed in accordance with ASTM D5890) and hydraulic conductivity of B-P GCLs previously observed in literature (Scalia et al., 2014; Salihoglu et al., 2016; Shen et al., 2016; Tian et al., 2016; Scalia et al., 2018a; Chen et al., 2019; Tian et al., 2019).

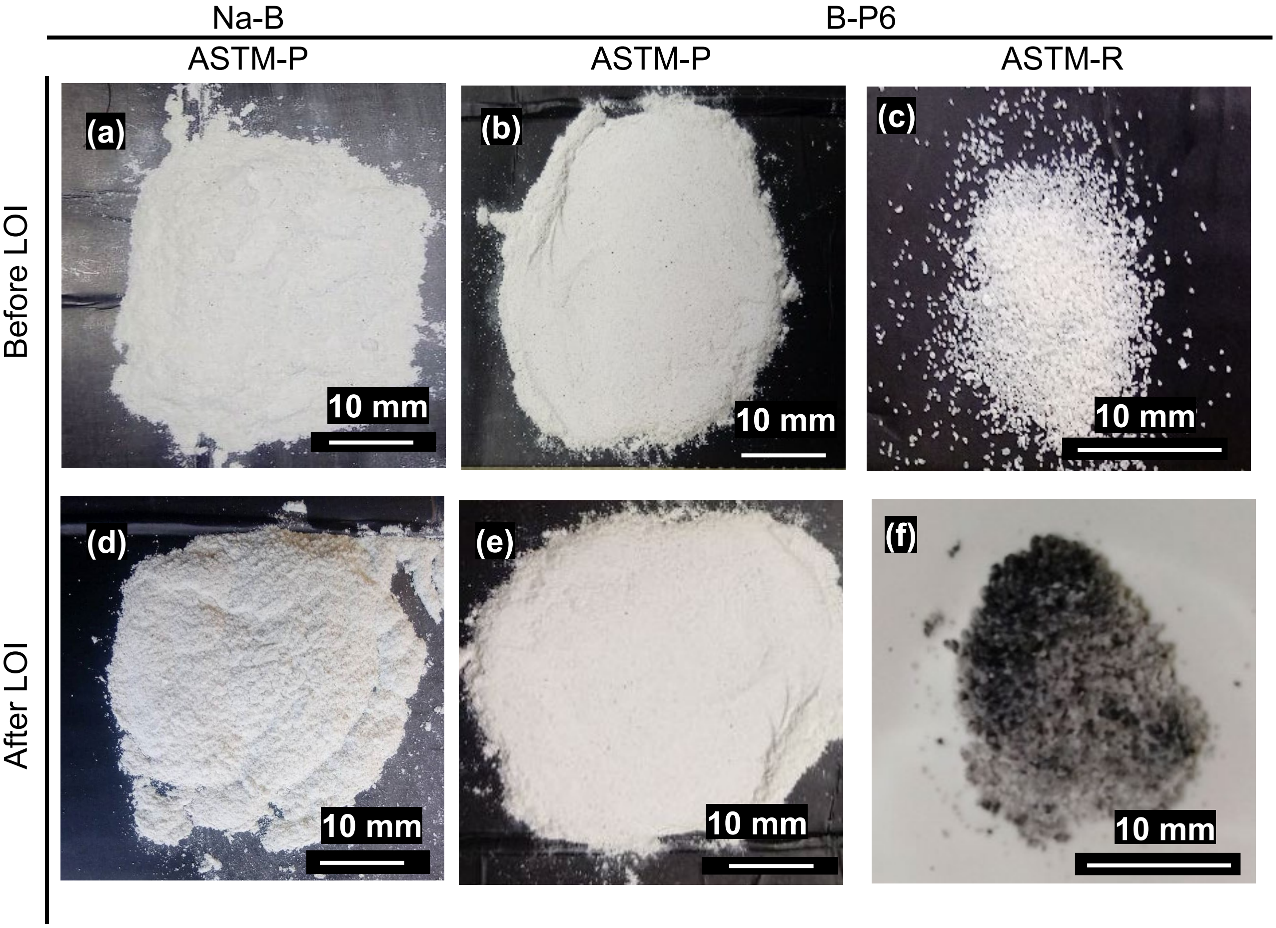

Figure 7. Images of Na-B and B-P6 specimens prepared following ASTM standard method for the specimens passing the #100 sieve (ASTM-P) and retained on the #100 sieve (ASTM-R) before and after loss on ignition test.

2.1.5 Results of tests performed on specimens prepared using alternative methods

The SI and LOI results for the alternatives AL1, AL2-P, and AL2-R for the Na-B and PMBs are summarized in Table 4. The SI results given in Table 4 were based on tests performed using DI water.

2.1.5.1 Swell index

The SI using Na-B specimens prepared with all the different methods had similar results, ranging from 28.5 mL/2 g to 31.0 mL/2 g (Figure 8). Scalia et al. (2018b) showed that the SI of Na-B is not sensitive to the granule size of the specimen. In contrast, the SI for the PMB specimens prepared by AL1 were higher than that of the AL2-P specimens but lower than the SI of the AL-R specimens, as shown in Figure 8. The SIs of the ASTM-P and AL2-P specimens for the PMBs containing liner polymer (i.e., B-P1, B-P2, B-P3, and B-P4) were similar to the SI of the Na-B specimens, whereas the SI of the AL1 and AL2-R specimens were slightly higher. Sato et al. (2017) showed that linear polymer (water-soluble polymer) enhances the swelling capacity of bentonite.

Images of specimens for Na-B and B-P3 after SI testing are shown in Figure 9. A glass rod (see Figure 9) was used to demonstrate the stickiness (which relates to viscosity) of the swollen specimen. For the Na-B specimens, the swollen gel of the ASTM-P and AL1 specimens did not stick to the glass rod as shown in Figure 9a and b. This suggests that the Na-B specimens formed a low viscosity gel after swelling. For B-P3, visual examination of the swollen ASTM-P and AL1 specimens, shows that the AL1 specimen was more viscous than the ASTM-P specimen (compare Figure 9c and d).

The SI of the PMBs containing crosslinked polymer (B-P5, B-P6, and B-P7) varied for specimens prepared with the different methods (see Figure 8). For example, the SI of ASTM-P specimens for B-P5 and B-P7 were similar to that of the Na-B specimens, whereas the SI of the AL1 and AL2-R specimens were much higher than the SI of the Na-B specimens.

Swollen ASTM-P and AL1 specimens for B-P7 are compared in Figure 9. The hydrogels formed in the ASTM-P specimen were significantly smaller (see Figure 9e) compared to the hydrogels formed in the AL1 specimen (see Figure 9f). This explains why the AL1 and AL2-R specimens had significantly higher SI than the ASTM-P and AL2-P specimens.

The results of the SI tests performed on the specimens obtained from the alternative methods show that the polymer additive(s) in the PMBs were screened out by the #100 sieve during the sieving process, which affected the measured SIs. This effect was more profound for the PMBs containing crosslinked polymers due to the high swelling capacity of SAP.

Table 4. Swell index and loss on ignition results of Na-B and PMB specimens prepared following the alternative methods 1 and 2

Material	AL1		AL2-P		AL2-R	
	Swell index (mL/2 g)	LOI (%)	Swell index (mL/2 g)	LOI (%)	Swell index (mL/2 g)	LOI (%)
Na-B	28.5	0.9	31.0	1.2	29.3	1.1
B-P1	30.6	1.3	29.2	1.1	31.3	2.0
B-P2	31.4	2.0	29.3	1.4	35.5	3.5
B-P3	31.8	2.2	29.0	1.4	34.2	3.5
B-P4	37.7	4.5	29.2	1.9	35.2	7.7
B-P5	40.1	2.5	29.5	1.4	40.3	6.4
B-P6	51.4	4.6	29.7	1.4	61.8	8.7
B-P7	52.4	5.9	30.7	1.8	66.3	11.2

Note: The swell index tests were performed using DI water.

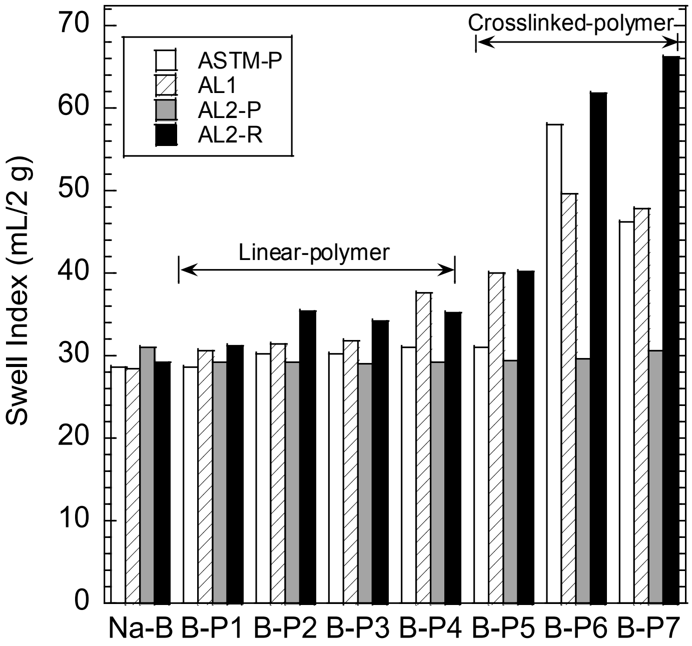

Figure 8. Comparison of swell indices of Na-B and PMB specimens prepared following ASTM standard method (ASTM-P) with alternative 1 (AL1) and alternative 2 passing the #100 sieve (AL2-P) and retained on the #100 sieve (AL2-R).

2.1.5.2 Loss on ignition

The LOI of the specimens prepared by the ASTM standard method and the alternatives are shown in Figure 10. The LOI of Na-B specimen prepared following the ASTM standard method (ASTM-P) was similar to the LOI of the specimens obtained following alternatives (AL1, AL2-P, and AL2-R), indicating that the specimen preparation methods used in this study did not have any influence on the measured LOI of the unamended Na-B.

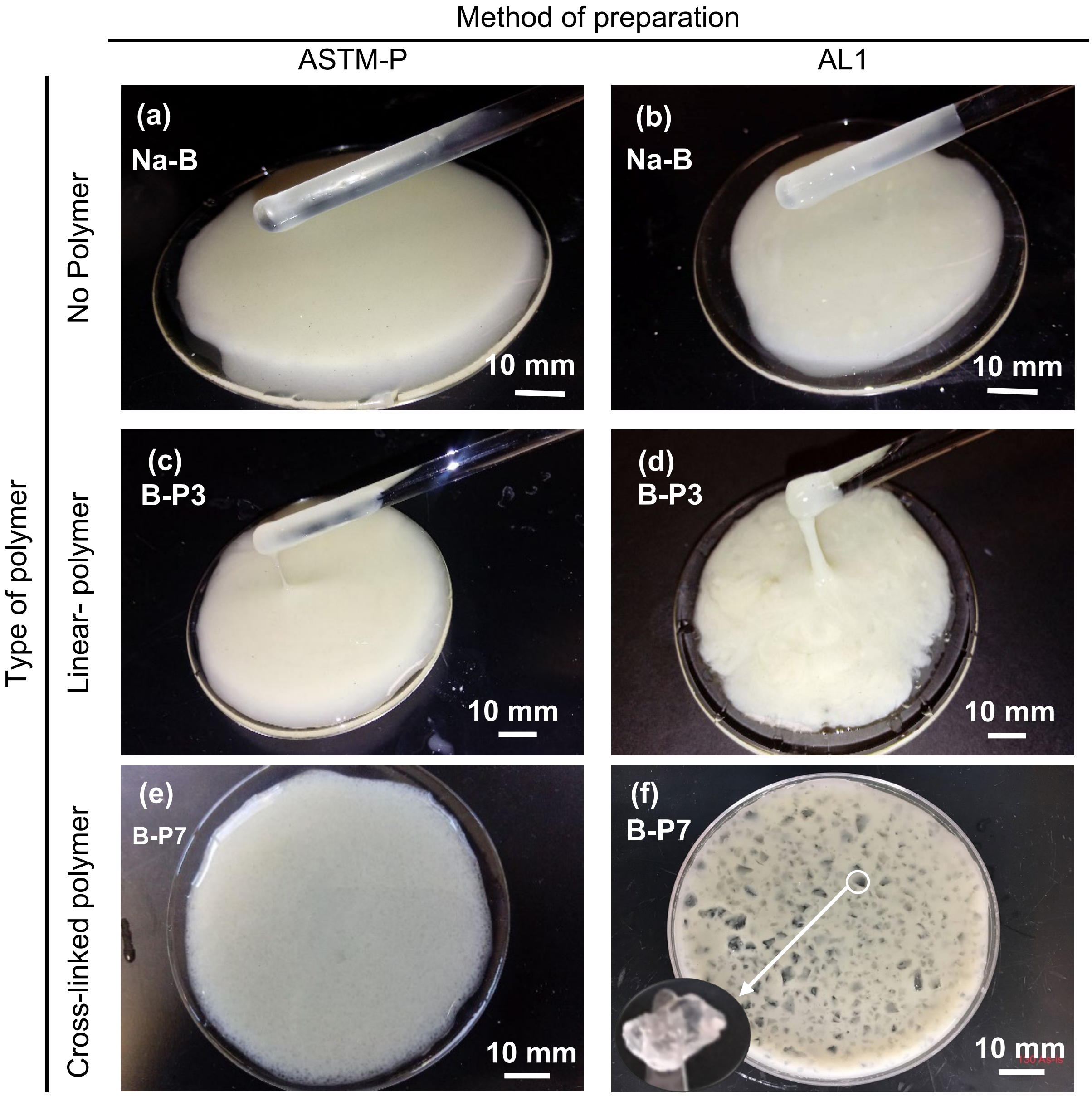

Figure 9. Images of Na-B, B-P3 and B-P7 prepared following the ASTM standard method (ASTM-P) and the alternative 1 (AL1) after swell index test.

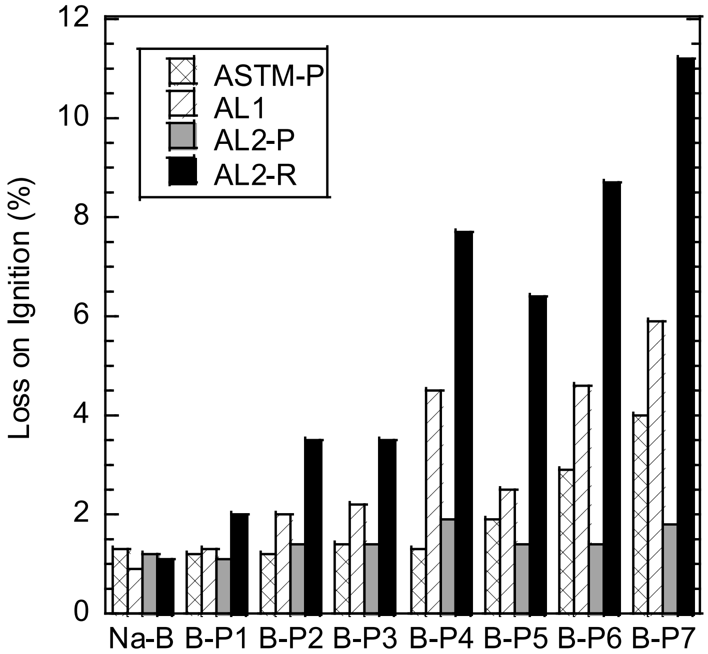

Figure 10. Comparison of loss on ignition values of Na-B and PMB specimens prepared following ASTM standard method (ASTM-P) with the alternative 1 (AL1) and alternative 2 [i.e. passing the #100 sieve (AL2-P) and retained the #100 sieve (AL2-R)].

However, for the PMBs, the LOI of the AL1 and AL2-R specimens were significantly higher than the LOI of the ASTM-P and AL2-P specimens (see Table 4 and Figure 10). The LOI of the AL2-P specimens for the PMBs were similar to that of the Na-B, whereas the LOI of AL2-R specimens were much higher than the LOI of the AL2-P specimens. For example, the LOI of the AL2-R specimen for B-P6 was ~8.7%, whereas the LOI of the AL2-P specimen was ~1.4% (which is comparable to the LOI of the Na-B). This result shows that, after screening approximately half of the initial mass of the AL2 specimen through the #100 sieve, the portion of the specimen that passed the #100 sieve mainly comprised bentonite, whereas the polymer was retained on the #100 sieve.

Images of the B-P6 specimens before and after the LOI test are shown in Figure 11. The AL2-P specimens before (Figure 11b) and after (Figure 11e) the LOI test looked similar. The same observation was made for Na-B specimens after the LOI test (see Figure 11a and d). However, the AL1 and AL2-R specimens had a significant amount of ash residues after the LOI test (see Figure 11d and f), which as previously stated indicates polymer combustion (Fina and Camino, 2011).

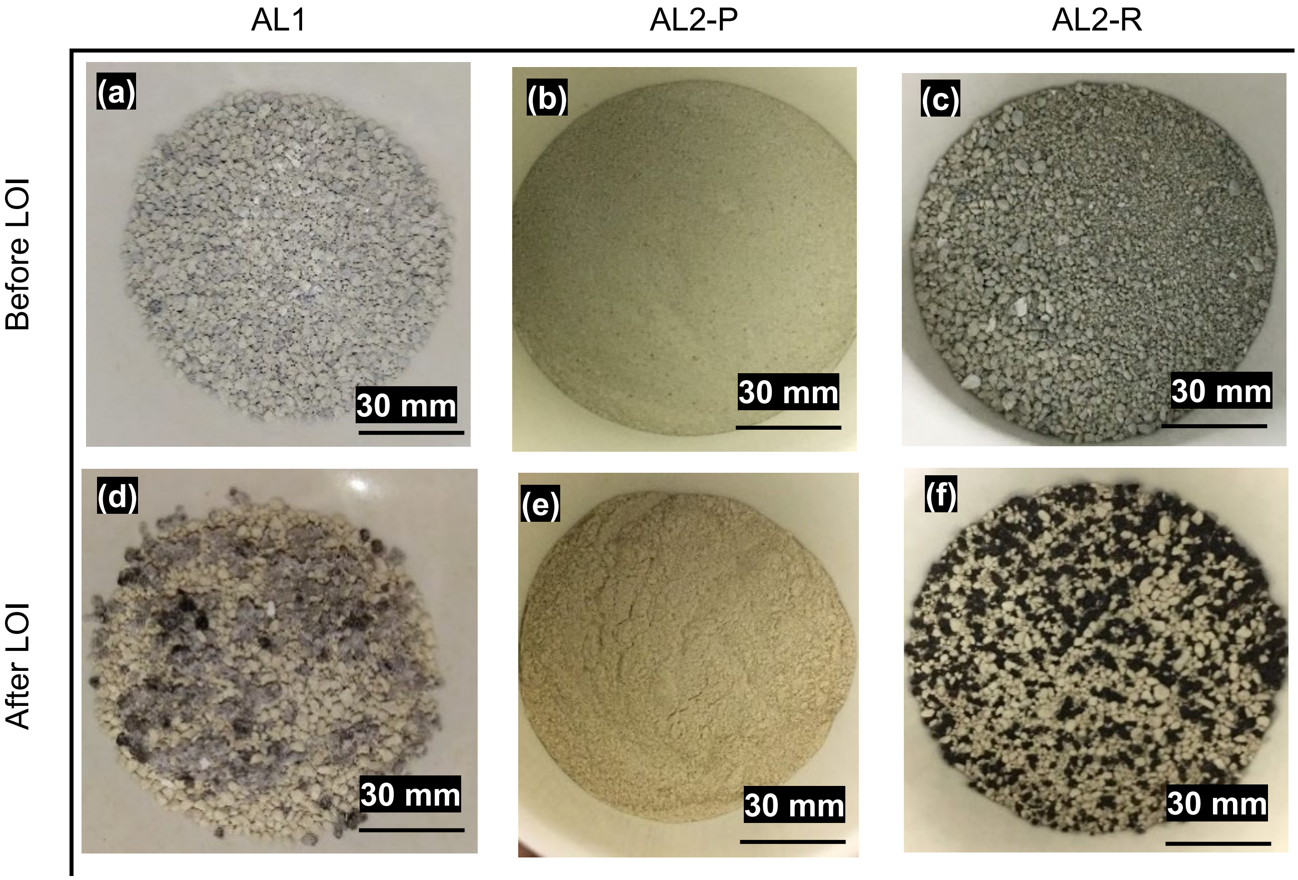

Figure 11. Images of B-P6 specimens prepared following alternative 1 (AL1) and alternative 2 (AL2-P and AL2-R) before and after loss on ignition test.

2.2 Hydraulic Conductivity of Polymer-Modified Bentonite GCLs to MSW-I Ash Leachates

Note: A manuscript containing majority of the text, figures and tables in the section is currently under review in Waste Management Journal:
Wireko C.[1], Abichou T.[1], Tian K.[2], Zainab B.[3], Zhang Z.[1], 2020. "Effect of Incineration Ash on the Hydraulic Conductivity of Bentonite-Polymer Composite Geosynthetic Clay Liners"
[1]Department of Civil and Environmental Engineering, Florida A&M University-Florida State University College of Engineering, 2525 Pottsdamer St., Tallahassee, FL, 32310-6064, USA; 2Department of Civil, Environmental and Infrastructure Engineering, George Mason University, Fairfax, VA 22030, USA; [3]Tetra-Tech AAI, Orlando, FL, USA.

This section describes a study where hydraulic conductivity of six needle-punched PMB GCLs was evaluated using five different synthetic leachates representative of leachates from landfills where MSW-I ash is either disposed alone or co-disposed with MSW. The PMB GCLs were obtained from two manufacturers and were identified to contain either linear polymer or crosslinked polymer dry blended with granular Na-B at different polymer loading (ranging from 0.5 to 5.5% by dry mass). As control, comparable hydraulic conductivity tests were also performed on two CB GCLs (one from each manufacturer) containing the same untreated Na-B as the bentonite used in the PMB GCLs. The effect of the polymer type on the temporal behavior of the PMB GCLs and some factors that influence the compatibility of PMB GCLs to MSW-I ash leachates are also discussed in this section. Free swell tests were also performed on bentonite extracted from the CB and PMB GCLs using the permeant solutions. Bentonite extracted from the PMB GCLs were not crushed or sieved to avoid loss of polymer additives as shown in Section 2.1.

Table 5 summarizes results of the hydraulic conductivity and free swell tests performed in this study. The hydraulic conductivity and pore volumes of flow (PVF) values reported in Table 5 were calculated using the final thickness and dry mass of the GCL specimen, except for the ongoing tests where the initial properties were used. The cumulative mass of polymer eluted during permeation of the PMB GCLs is also reported in Table 5. The cumulative mass of polymer eluted is expressed as a percentage of the initial amount of polymer in the GCL (which was estimated using initial polymer loading and the dry mass of bentonite) and also reported in Table 5.

Table 5. Summary of hydraulic conductivity tests on GCLs and free swell tests on bentonite extracted from the GCLs

GCL	Hydrating solution	Permeating solution	Swell index[b] (mL/2 g)	Average σ'	Average i[c]	Time elapsed[d]	k[c] (m/s)	PVF[c]	ASTM D6766 Termination criteria met?			Cumulative mass of polymer eluted[e] (mg)	Percentage of initial polymer eluted[e] (%)
									Hydraulic	EC	pH		
BA	DI water	DI water[a]	24.5	20 kPa	196	110.0 days	2.2×10^{-11}	12.6	Yes	N/A	N/A	N/A	N/A
	CD-MIN	CD-MIN	8.3	30 kPa	160	1.0 h	3.2×10^{-7}	9.2	Yes	Yes	Yes	N/A	N/A
	CD-AVG	CD-AVG	8.2	30 kPa	177	0.1 h	5.3×10^{-7}	6.1	Yes	Yes	Yes	N/A	N/A
	AM-AVG	AM-AVG	7.7	30 kPa	165	0.2 h	4.2×10^{-7}	7.1	Yes	Yes	Yes	N/A	N/A
	CD-MAX	CD-MAX	7.2	30 kPa	160	0.2 h	4.6×10^{-7}	7.0	Yes	Yes	Yes	N/A	N/A
	AM-MAX	AM-MAX	6.0	39 kPa	231	0.1 h	4.4×10^{-7}	5.1	Yes	Yes	Yes	N/A	N/A
BB	DI water	DI water[a]	26.5	39 kPa	277	39.0 days	2.0×10^{-11}	5.8	Yes	N/A	N/A	N/A	N/A
	CD-MIN	CD-MIN	6.0	30 kPa	177	3.1 h	3.0×10^{-7}	5.5	Yes	Yes	Yes	N/A	N/A
	CD-AVG	CD-AVG	5.5	30 kPa	177	0.1 h	3.7×10^{-7}	6.0	Yes	Yes	Yes	N/A	N/A
	AM-AVG	AM-AVG	5.5	30 kPa	160	0.2 h	6.7×10^{-7}	7.1	Yes	Yes	Yes	N/A	N/A
	CD-MAX	CD-MAX	5.3	30 kPa	160	0.2 h	9.5×10^{-7}	9.5	Yes	Yes	Yes	N/A	N/A
	AM-MAX	AM-MAX	5.0	39 kPa	290	0.1 h	4.2×10^{-7}	5.0	Yes	Yes	Yes	N/A	N/A
LPBA-0.5	DI water	DI water[a]	31.2	20 kPa	153	119.0 days	2.2×10^{-11}	4.6	Yes	N/A	N/A	-	-
	CD-MIN	CD-MIN	24.8	39 kPa	220	53.0 days	6.7×10^{-11}	11.7	Yes	Yes	Yes	12.0	5.4
	CD-AVG	CD-AVG	8.5	30 kPa	126	8.4 h	1.7×10^{-8}	11.0	Yes	Yes	Yes	1.7	0.7
	AM-AVG	AM-AVG	8.3	30 kPa	121	12.0 h	1.9×10^{-8}	6.6	Yes	Yes	Yes	0.6	0.2
	CD-MAX	CD-MAX	7.5	39 kPa	265	0.1 h	1.3×10^{-7}	5.1	Yes	Yes	Yes	2.0	1.0
	AM-MAX	AM-MAX	6.0	39 kPa	232	0.1 h	3.8×10^{-7}	5.5	Yes	Yes	Yes	1.0	0.5
LPBA-1.5	DI water	DI water[a]	33.3	20 kPa	187	395.0 days	7.8×10^{-12}	10.8	Yes	N/A	N/A	-	-
	CD-MIN	CD-MIN	27.0	30 kPa	174	98.0 days	2.4×10^{-11}	6.9	Yes	Yes	Yes	58.4	13.3
	CD-AVG	CD-AVG	9.8	30 kPa	150	2.6 days	1.5×10^{-9}	11.0	Yes	Yes	Yes	15.8	2.9
	AM-AVG	AM-AVG	8.8	39 kPa	290	1.0 h	2.2×10^{-8}	5.4	Yes	Yes	Yes	4.8	0.9
	CD-MAX	CD-MAX	8.8	39 kPa	257	1.2 h	1.3×10^{-8}	4.5	Yes	Yes	Yes	5.3	0.9
	AM-MAX	AM-MAX	7.0	39 kPa	261	0.1 h	2.9×10^{-7}	2.7	Yes	Yes	Yes	4.1	0.7
	Tap water	AM-MAX	N/A	30 kPa	162	52.0 days	2.1×10^{-9}	29.1	Yes	Yes	Yes	33.9	6.2

Note: σ' = Effective stress, i = Hydraulic gradient, k = Hydraulic conductivity, PVF = Pore volumes of flow, N/A = Not applicable, - = Not measured, D. = Duplicate. Gravity heads were used to apply cell pressure (20 kPa) and hydraulic gradient for long-term testing of the GCL specimen permeated with DI water

[a] In the GCL designation, the first letter(s) indicates: B = Bentonite, LPB = Linear polymer-bentonite, CPB = Crosslinked polymer-bentonite. And the last letter indicates the manufacturer (A or B)

[b] Test still ongoing

[c] For the CB GCL, specimens used for swell index testing were crushed and sieved according to ASTM D5890, whereas uncrushed specimen were used for the PMB GCL based on results of the study described in Section 2.1 of this report

[d] Calculated based on the final thickness and dry mass of the GCL (except of ongoing tests where the initial properties were used)

[e] Does not include the period of hydration (2 days) and the time in-between readings (required to refill the influent canister with the permeation solution)

[f] Calculated by integrating the product of the total organic carbon (TOC) concentration (in mg/L) and the volume (in L) of effluent samples collected during permeation. And the percentage of initial polymer eluted was estimated based on the initial mass of polymer in the GCL specimen

Table 5. (*continued*)

GCL[a]	Hydrating solution	Permeating solution	Swell index[c] (mL/2 g)	Average σ'	Average i[d]	Time elapsed[e]	k[d] (m/s)	PVF[d]	ASTM D6766 Termination criteria met?			Cumulative mass of polymer eluted[f] (mg)	Percentage of initial polymer eluted[f] (%)
									Hydraulic	EC	pH		
LPBA-3.7	DI water[b]	DI water[b]	35.3	20 kPa	155	107 days	2.4×10^{-12}	2.0	Yes	N/A	N/A	-	-
	CD-MIN[b]	CD-MIN[b]	30.0	30 kPa	126	51 days	3.5×10^{-12}	1.3	Yes	No	No	-	-
	CD-AVG	CD-AVG	12.8	39 kPa	237	1.2 days	1.6×10^{-9}	17.7	Yes	Yes	Yes	49.3	3.1
	AM-AVG	AM-AVG	10.0	39 kPa	217	2 days	1.9×10^{-9}	12.8	Yes	Yes	Yes	18.4	1.4
	CD-MAX	CD-MAX	11.8	39 kPa	237	1.0 h	2.2×10^{-8}	4.9	Yes	Yes	Yes	14.2	0.8
	AM-MAX	AM-MAX	10.0	39 kPa	234	0.1 h	2.5×10^{-7}	2.1	Yes	Yes	Yes	0.9	0.1
LPBB-4.4	DI water	DI water	30.0	20 kPa	239	348 days	6.6×10^{-12}	10.4	Yes	N/A	N/A	-	-
	CD-MIN	CD-MIN	23.3	-	-	-	-	-	-	-	-	-	-
	CD-AVG	CD-AVG	8.0	39 kPa	310	46 days	3.4×10^{-10}	45.6	Yes	Yes	Yes	82.2	4.6
	AM-AVG	AM-AVG	7.0	39 kPa	295	61 days	1.9×10^{-9}	25.7	Yes	Yes	Yes	365.8	20.3
	AM-AVG	AM-AVG (D)	N/A	39 kPa	244	9.8 days	2.1×10^{-9}	17.8	Yes	Yes	Yes	-	-
	CD-MAX	CD-MAX	6.3	39 kPa	269	78 days	1.3×10^{-9}	44.4	Yes	Yes	Yes	214.8	14.0
	AM-MAX	AM-MAX	4.8	39 kPa	265	0.5 h	4.6×10^{-8}	5.0	Yes	Yes	Yes	14.3	1.1
CPBA-3.4	DI water[a]	DI water[a]	38.8	20 kPa	163	102 days	5.1×10^{-12}	3.4	Yes	N/A	N/A	-	-
	CD-MIN	CD-MIN	28.5	39 kPa	234	96 days	3.9×10^{-11}	13.4	Yes	Yes	Yes	-	-
	CD-AVG	CD-AVG	9.5	39 kPa	212	2.5 h	1.3×10^{-8}	3.9	Yes	Yes	Yes	-	-
	AM-AVG	AM-AVG	9.3	39 kPa	228	0.4 h	1.0×10^{-7}	5.0	Yes	Yes	Yes	-	-
	CD-MAX	CD-MAX	8.5	39 kPa	217	0.1 h	1.2×10^{-7}	3.2	Yes	Yes	Yes	-	-
	AM-MAX	AM-MAX	7.0	39 kPa	215	0.2 h	2.8×10^{-7}	2.8	Yes	Yes	Yes	-	-
	Tap water	AM-MAX	N/A	39 kPa	224	65 days	1.7×10^{-10}	39.0	Yes	Yes	Yes		
CPBA-5.5	DI water[a]	DI water[a]	55.0	20 kPa	153	388 days	9.3×10^{-12}	12.0	Yes	N/A	N/A	-	-
	CD-MIN	CD-MIN	30.5	39 kPa	185	131 days	2.6×10^{-11}	15.0	Yes	Yes	Yes	-	-
	CD-AVG	CD-AVG	10.0	39 kPa	223	10 h	2.6×10^{-9}	7.5	Yes	Yes	Yes	-	-
	AM-AVG	AM-AVG	10.0	39 kPa	210	12 h	7.2×10^{-8}	9.7	Yes	Yes	Yes	-	-
	CD-MAX	CD-MAX	10.3	39 kPa	217	6.0 h	9.4×10^{-8}	7.0	Yes	Yes	Yes	-	-
	AM-MAX	AM-MAX	8.0	39 kPa	201	0.2 h	7.4×10^{-7}	2.0	Yes	Yes	Yes	-	-

Note: σ' = Effective stress, i = Hydraulic gradient, k = Hydraulic conductivity, PVF = Pore volumes of flow, N/A = Not applicable, - = Not measured, D. = Duplicate. Gravity heads were used to apply cell pressure (20 kPa) and hydraulic gradient for long-term testing of the GCL specimen permeated with DI water

[a] In the GCL designation, the first letter(s) indicates: B = Bentonite, LPB = Linear polymer-bentonite, CPB = Crosslinked polymer-bentonite. And the last letter indicates the manufacturer (A or B)

[b] Test still ongoing

[c] For the CB GCL, specimens used for swell index testing were crushed and sieved according to ASTM D5890, whereas uncrushed specimen were used for the PMB GCL based on results of the study described in Section 2.1 of this report

[d] Calculated based on the final thickness and dry mass of the GCL (except of ongoing tests where the initial properties were used)

[e] Does not include the period of hydration (2 days) and the time in-between readings (required to refill the influent canister with the permeation solution)

[f] Calculated by integrating the product of the total organic carbon (TOC) concentration (in mg/L) and the volume (in L) of effluent samples collected during permeation. And the percentage of initial polymer eluted was estimated based on the initial mass of polymer in the GCL specimen

2.2.1 Hydraulic conductivity test results

2.2.1.1 Temporal behavior and ASTM D6766 termination criteria

Figure 12 uses LPBB-4.4 and CPBA-5.5 permeated with CD-MAX (I = 1097 mM) as examples to compare the observed trends in measured hydraulic conductivity values, polymer elution and termination criteria exhibited by the LPB GCLs and CPB GCLs used in this study during permeation with the synthetic IA leachates with ionic strength ≥ 622 mM. Both GCLs exhibited different trends in hydraulic conductivity evolution (compare Figure 12a to Figure 12c), but a similar trend in termination criteria as shown in Figure 12b and Figure 12b.

For LPBB-4.4, hydraulic conductivity to CD-MAX was initially ($<1.0 \times 10^{-11}$ m/s) but increased sharply to the 10^{-10} m/s range after (20 days of permeation) as shown in Figure 12a. This abrupt increase in hydraulic conductivity is attributed to polymer elution based on visual analysis of the effluent collected immediately after the jump in hydraulic conductivity. The concentration of polymer in effluent was estimated to be ~655 mg/L (corresponding to ~37 mg of polymer and 2.4 % of the initial mass of polymer in the specimen). Hydraulic conductivity remained steady (within the 10^{-10} m/s range) until about 12 PVFs where hydraulic conductivity started to decrease to the 10^{-12} m/s range (Figure 12a). The decreasing trend in hydraulic conductivity continued (for 30 days) until about 15 PVFs when hydraulic conductivity began to increase back into the 10^{-10} m/s range. During the period of decreasing hydraulic conductivity, the volumetric flow ratio (Q_{out}/Q_{in}) was mostly < 0.75 as shown in Figure 12a, which suggested that the decrease in hydraulic conductivity was due to clogging of the effluent tube (⅛ in inner diameter tube) by the eluting polymer gel. TOC analysis of effluents collected between 12 and 18 PVFs showed a spike in the concentration of polymer in the effluents compared to the effluent collected prior to the drop in the hydraulic conductivity. Steady state conditions were achieved after 35 PVFs with an average hydraulic conductivity of about 1.3×10^{-9} m/s, which is approximately three orders-of-magnitude higher than the initial hydraulic conductivity.

In contrast, the hydraulic conductivity of CPBA-5.5 permeated with CD-MAX was initially high (~3.3×10^{-7} m/s) but decreased gradually into the 10^{-8} m/s range (Figure 12c). This gradual decrease in hydraulic conductivity of CPBA-5.5 can be attributed to the gradual swelling of the crosslinked polymer hydrogels during permeation, which decreases the size of intergranular flow channels within the bentonite-polymer composite matrix. SAP have been shown to swell at a slower rate when ionic strength of the hydrating solution is high (Lee and Wu, 1996; Zhu et al., 2014). Hydraulic conductivity of CPBA-5.5 to CD-MAX, however, remained steady at approximately 9.0 × 10^{-8} m/s, after 3 PVFs.

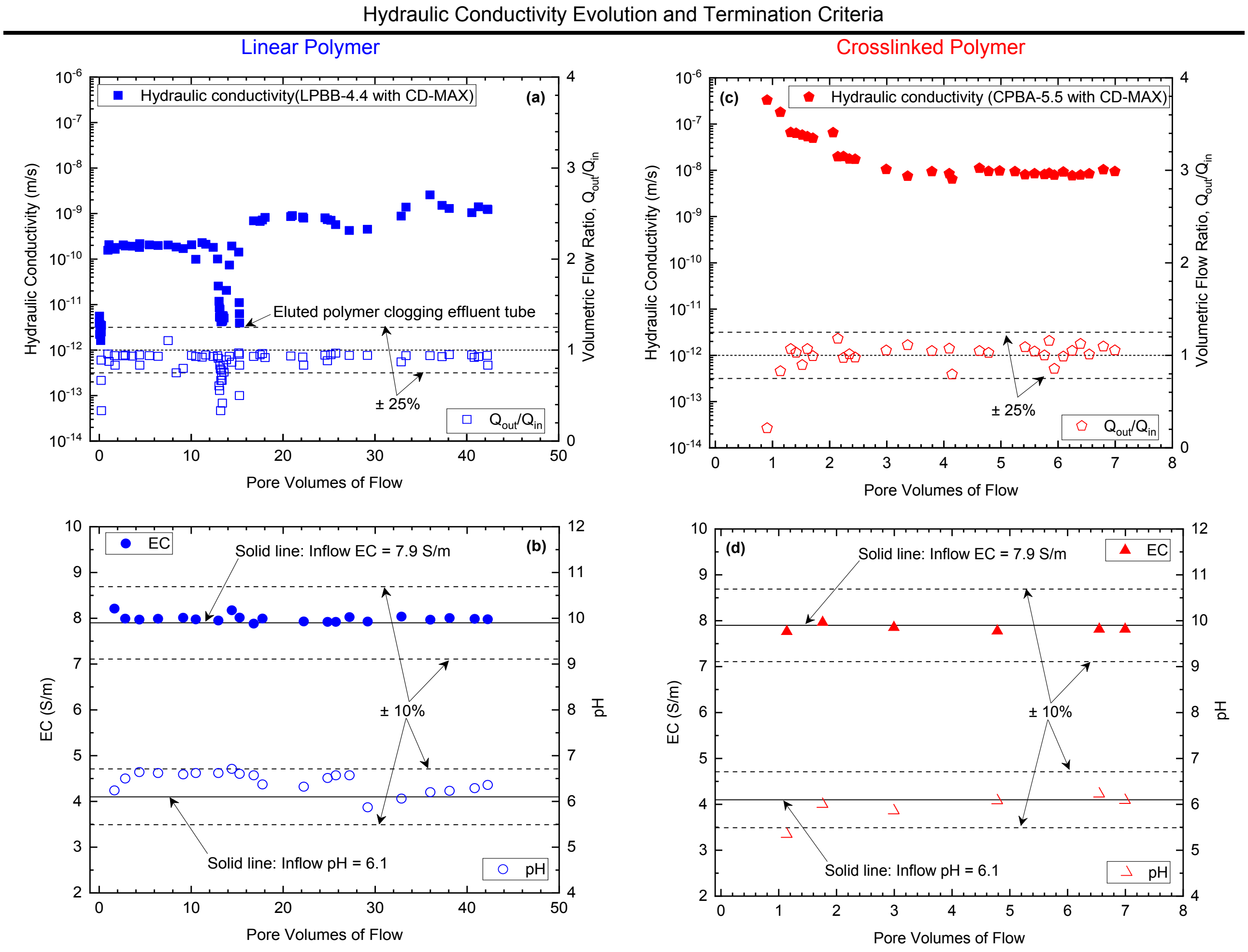

Figure 12. Hydraulic conductivity, volumetric flow ratio, influent and effluent electrical conductivity (EC) and pH as a function of pore volumes of flow for (a) LPBB-4.4 and (b) CPBA-5.5 permeated with CD-MAX (*I* = 1097 mM) (Note: The numerical suffix in the PMB GCL designation is polymer loading given in percent dry mass of bentonite. CD = Co-Disposal, Max = Maximum, *I* = ionic strength).

Interestingly, there was not much difference between the EC and pH of the influent leachate and effluents collected during permeation of either LPBB-4.4 or CPBA-5.5 with CD-MAX as shown in Figure 12b and Figure 12d. This suggests that chemical equilibrium was achieved immediately after permeation was initiated. A similar trend in the chemical equilibrium evolution was observed in this study for all the PMB GCLs permeated with the MSW-I ash leachates with ionic strength ≥ 622 mM, and have also been reported in literature for both CB and PMB GCLs permeated with aggressive solutions (Jo et al., 2005; Lee and Shackelford, 2005; Chen, 2015; Salihoglu, 2015).

2.2.1.2 Effect of MSW-I ash leachate chemistry on hydraulic conductivity

The hydraulic conductivity data in Table 5 are plotted in Figure 13a as a function of ionic strength of the permeant solutions for all GCL specimens used in this study. Hydraulic conductivity of the GCL specimens permeated with DI water are assigned an ionic strength of ~ 0 mM. As shown in Figure 13a, hydraulic conductivity of the CB GCLs (BA and BB) was greater than 1.0×10^{-7} m/s when permeated with all the MSW-I ash leachates used in this study, which is more than three orders-of-magnitude higher than when permeated with DI water. Similar hydraulic conductivity values have been reported in literature for CB GCLs permeated with leachates with ionic strength >100 mM (Ashmawy et al., 2002; Shackelford et al., 2010; Chen et al., 2018). The high hydraulic conductivity of the CB GCLs can be attributed to the shrinkage of the double layer thickness of Na-B associated with high concentration of monovalent cations and abundance of divalent cations in the MSW-I ash leachates used in this study (Petrov and Rowe, 1997; Shackelford et al., 2000; Jo et al., 2001; Jo et al., 2005; Lee and Shackelford, 2005). These limitations of Na-B are the driving force behind the development of modified bentonites and BPCs that can be more compatible with aggressive solutions.

Figure 13a shows that the hydraulic conductivity of the PMB GCLs was consistently lower than that of the CB GCLs when permeated with the MSW-I ash leachates, except for the PMB GCL specimens permeated with AM-MAX (I = 1978 mM), where only PMB GCLs with polymer loading > 4% had a relatively lower hydraulic conductivity than the CB GCLs (compare Figure 13b and Figure 13c). All the PMB GCL specimens permeated with CD-MIN (I = 174 mM) had hydraulic conductivity lower than 1.0×10^{-10} m/s (see

Figure 13a). However, all of the PMB GCLs used in this study had hydraulic conductivity greater than 1.0×10^{-10} m/s when permeated with MSW-I ash leachates with ionic strength ≥ 622 mM. This dramatic increase in hydraulic conductivity of the PMB GCLs with ionic strength can be partly attributed to the Cl-rich nature of the MSW-I ash leachates used in this study (see Section 4.2).

In a study conducted by Chen et al. (2019), hydraulic conductivity of one PMB GCL with polymer loading of 1.9% was approximately 1.0×10^{-10} m/s when permeated with CCP leachates with ionic strength of 755.0 mM. Whereas in this study, hydraulic conductivity of PMB GCL with polymer loading up to 5.5% was greater than 3.0×10^{-10} m/s when permeated with CD-AVG (with ionic strength of 622.4 mM). Tian et al. (2017) found that hydraulic conductivity of a PMB GCL (with polymer loading of 5.1%) permeated with pure Na_2SO_4 solution with 300 mM Na^+ was 3.1×10^{-12} m/s, whereas hydraulic conductivity of duplicate specimens of the same PMB GCL permeated with pure NaCl solution with 300 mM Na^+ was 4.5×10^{-9} m/s and 6.1×10^{-10} m/s (which is more than two orders of magnitude higher). This suggest that the reason for the lower hydraulic conductivity of the PMB GCL (with polymer loading with 1.9%) permeated with CCP leachate with ionic strength of 755.0 mM in Chen et al. (2019) may be because, that particular CCP leachate consisted of only SO_4^{-2} species (with no Cl^- species).

2.2.1.3 Effect of initial polymer loading and polymer type on hydraulic conductivity

Hydraulic conductivities of the PMB GCLs permeated with the MSW-I ash leachates are plotted as a function of polymer loading in Figure 13d-e to highlight the effect initial polymer loading has on the compatibility of PMB GCLs to MSW-I ash leachates. Hydraulic conductivities of the CB GCLs permeated with the same MSW-I ash leachates are also shown in Figure 13d-e for comparison.

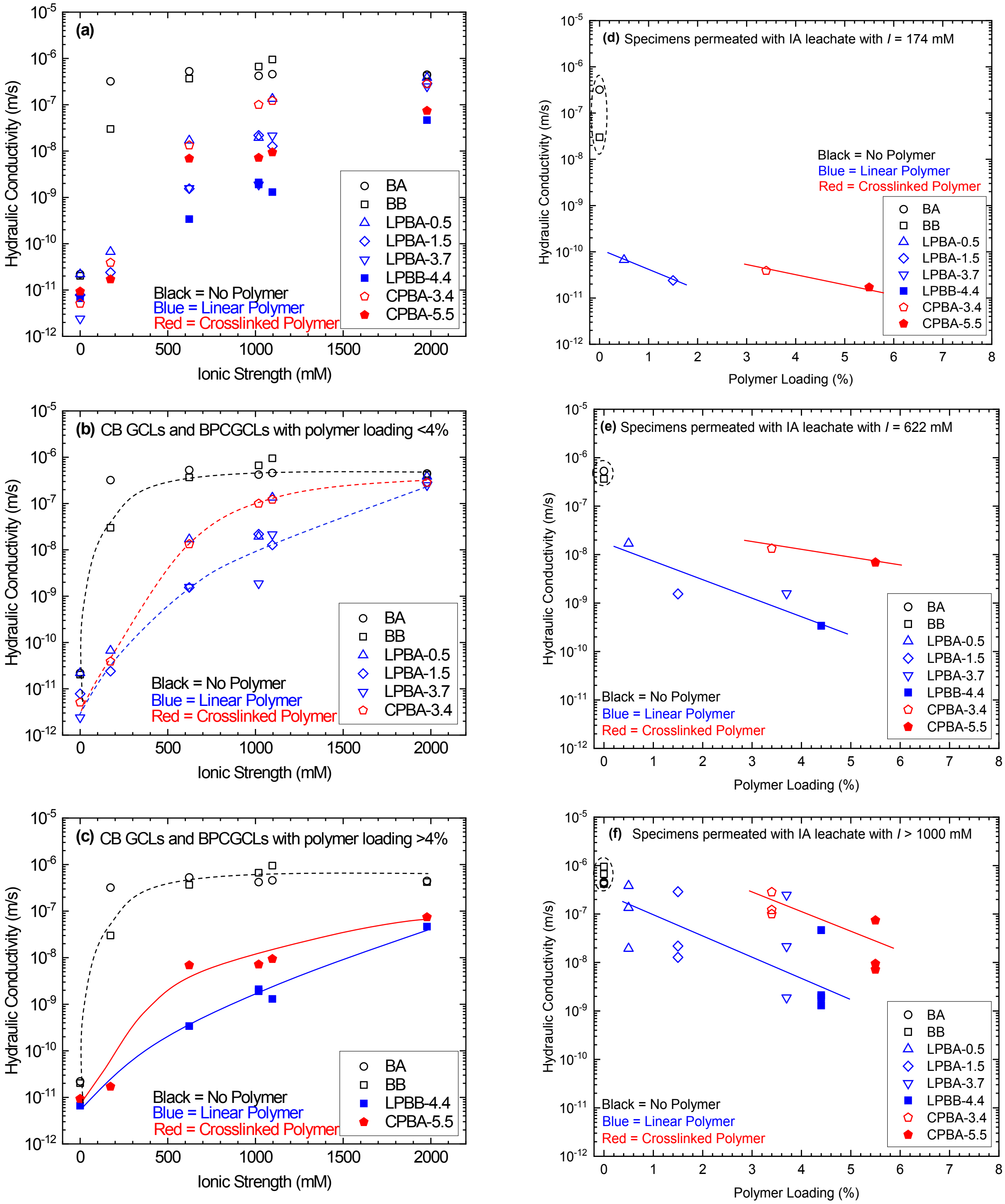

Figure 13. Hydraulic conductivity of the GCLs used in this study as a function of (a-c) ionic strength (*I*) of incineration ash (IA) leachates and (d-f) initial polymer loading of GCL specimens permeated with the IA leachates (Note: Hydraulic conductivity of the GCLs permeated with DI water plotted on 0 mM).

As shown in Figure 13d-e, hydraulic conductivity generally decreases with increasing polymer loading, regardless of the polymer type. For instance, hydraulic conductivity of LPBA-0.5 (with only 0.5% polymer loading) was more than three orders-of-magnitude lower than that of BA when permeated with CD-MIN (I = 174 mM). This result indicate that the polymer additives increase the chemical resistance of PMB GCLs to the MSW-I ash leachates. However, more polymer is required to maintain low hydraulic conductivity ($< 1.0 \times 10^{-10}$ m/s) as ionic strength of the MSW-I ash leachate increases (compare Figure 13d to Figure 13f). Tian et al. (2016) and Chen et al. (2019) have reported a similar decreasing trend of hydraulic conductivity with increasing polymer loading for PMB GCLs permeated with LLW and CCP leachates respectively.

The trends in measured hydraulic conductivities of the PMB GCLs shown in Figure 13 also indicates that, the type of polymer blended with the bentonite has significant influence on the compatibility of a specific PMB GCL to a given MSW-I ash leachate. For example, even though LPBA-3.7 and CPBA-3.4 had similar polymer loading (3.7% versus 3.4%) and contained the same untreated bentonite, geotextiles and reinforcement, the hydraulic conductivity of LPBA-3.7 was consistently lower than that of CPBA-3.4 (compare the trend lines in Figure 13b), except for the specimens permeated with DI water and AM-MAX where the hydraulic conductivities of both GCLs were comparable. Similarly, hydraulic conductivity of LPBB-4.4 was consistently lower than that of CPBA-5.5 when permeated with MSW-I ash leachates with ionic strength ≥ 622 mM (see Figure 13c and f), even though CPBA-5.5 had higher polymer loading than LPBB-4.4.

The reason for the relatively lower hydraulic conductivity values measured for the LPB GCLs is possibly due to the difference in nature of swelling of the polymers. A visual comparison of the cross section of LPBA-3.7 and CPBA-3.4 after permeation with ASH-AVG in Figure 14 shows that, linear polymers easily dissolve and diffuse uniformly within the bentonite matrix as shown in Figure 14a, however, crosslinked polymers form discrete polymer hydrogels, therefore require more polymer to guarantee even distribution within the bentonite matrix as shown in Figure 14b. Thus, at the similar loading, linear polymers were more efficient in blocking flow than crosslinked polymers for the PMB GCLs and MSW-I ash leachates used in this study.

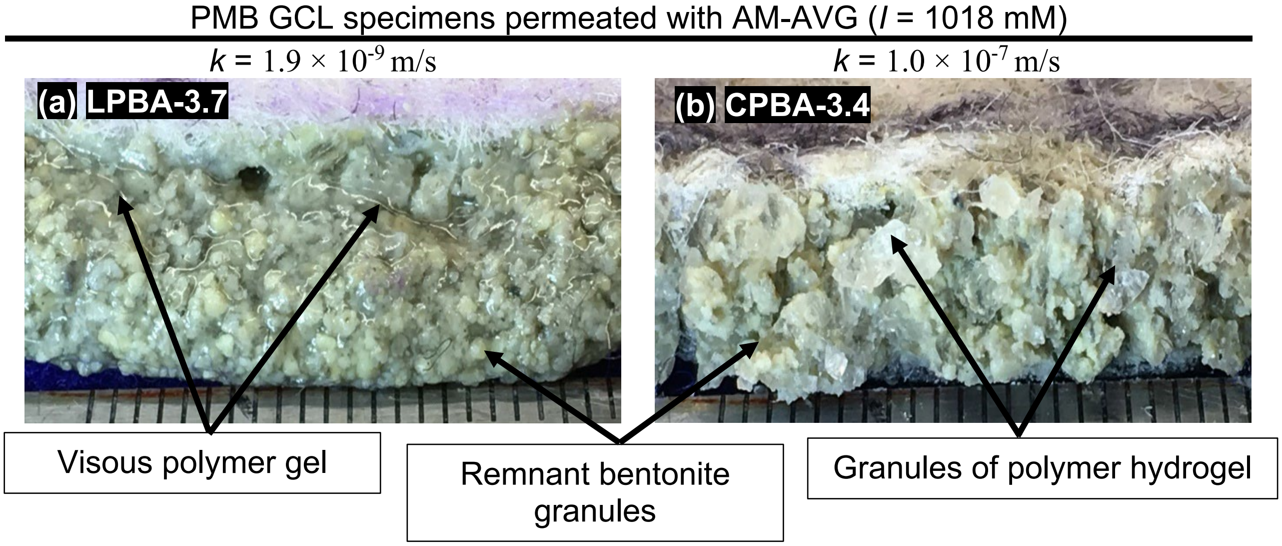

Figure 14. Cross sections of (a) linear polymer-bentonite composite (LPB) and (b) crosslinked polymer-bentonite composite (CPB) GCL specimens after permeation with AM-AVG (I = 1018 mM) [Note: The scale each image is the mm. The numerical suffix in the GCL designation is polymer loading in given percent dry mass of bentonite. AM = Ash monofill, AVG = Average, I = ionic strength, k = Hydraulic conductivity].

2.2.1.4 Effect of initial hydrating liquid on hydraulic conductivity

Hydraulic conductivity of all the PMB GCLs used in the study was high (> 1.0×10^{-10} m/s) when hydrated and permeated with the MSW-I ash leachates with ionic strength ≥ 622 mM. Hence, additional hydraulic conductivity tests were conducted on selected GCLs to investigate the effect of the initial hydrating liquid on the compatibility of PMB GCLs to MSW-I ash leachates. Figure 15 compares the hydraulic conductivity of GCL specimens of LPBA-1.5 and CPBA-3.4 directly hydrated and permeated with the strongest MSW-I ash leachate with ionic strength of 1978 mM, i.e., AM-MAX (leachate-hydrated specimens) to specimens of the same GCLs which were hydrated with tap water before permeating with AM-MAX (water-hydrated specimens). As shown in Figure 15, hydraulic conductivity of the water-hydrated specimens was at least two orders-of-magnitude lower than the leachate-hydrated specimens all the GCLs.

As shown in Figure 15, the final water content of the water-hydrated specimen was higher than that of the leachate-hydrated specimen for both GCLs. This suggest that the lower hydraulic conductivity of the water-hydrated specimen can be attributed to the increased water associated bentonite and polymer due to initial exposure to water which results in a more tortuous flow path of the permeant liquid which has been widely reported in the literature for CB GCLs as well as PMB GCLs (Daniel and Shan, 1993; Petrov et al., 1997a; Ruhl and Daniel, 1997; Vasko et al., 2001; Ashmawy et al., 2002; Jo et al., 2004; Katsumi et al., 2004; Shackelford et al., 2010; Chen et al., 2018; Chen et al., 2019).

An interesting observation in Figure 15 is that, hydraulic conductivity of water-hydrated specimen of CPBA-3.4 was one order-of-magnitude lower than that of LPBA-1.5 (2.1×10^{-9} m/s versus 1.3×10^{-10} m/s), even though both GCLs has similar hydraulic conductivities (both ~3.0×10^{-7} m/s) when directly permeated with AM-MAX. This suggests that much lower hydraulic conductivity values can be achieved for water-hydrated specimens of PMB GCLs with higher polymer loading (>3.4%) when permeated with the same leachate. The effect of polymer loading and polymer type on the hydraulic conductivity of water-hydrated GCLs is currently been investigated.

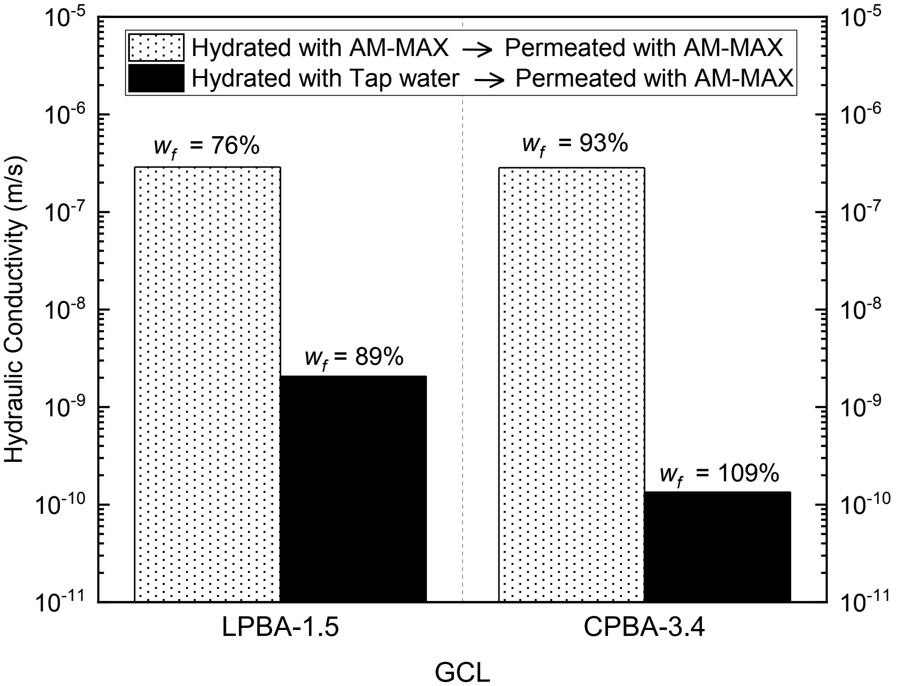

Figure 15. Comparison of hydraulic conductivity of leachate-hydrated (hydrated with AM-MAX) and water-hydrated (hydrated with tap water) and polymer-modified bentonite (PMB) GCL specimens permeated with AM-MAX (I = ~1978 mM) [Note: w_f = final water content. AM = Ash monofill, Max = Maximum, I = ionic strength. In the GCL designation, the first letter(s) indicates: B = Bentonite, LPB = Linear polymer-bentonite, CPB = Crosslinked polymer-bentonite. The last letter in the GCL designation indicate the manufacturer (A or B), whereas the numerical suffix in the bentonite-polymer composite GCL designation is polymer loading in percent dry mass of bentonite].

2.2.2 Free swell test results

The swell indices of bentonite extracted from PMB GCLs are compared in Figure 16 to the swell indices of bentonite extracted from CB GCLs from manufacturer A and B. As shown in Figure 16, swell index (SI) of the bentonite in BA and BB, decreased from 24.5 mL/2 g and 26.5 mL/2 g in DI water to 8.3 mL/2 g and 6.0 mL/2 g respectively in CD-MIN (I = 174 mM). This dramatic decrease in swelling of the (untreated) bentonite in BA and BB can be attributed to the inability of the bentonite to undergo osmotic swelling due to the low concentration gradient between the interlayer regions of the montmorillonite particles of the bentonite and the hydrating liquid (Shackelford et al., 2000; Egloffstein, 2001; Jo et al., 2001; Kolstad et al., 2004a). In contrast, the swell indices of the PMBs were greater than 20 mL/2 g when hydrated with CD-MIN (I = 174 mM). Furthermore, for all the liquids used in this study, the swell indices of the BPCs were consistently higher than the CBs except for MSW-I ash leachates with $I \geq 622$ mM where some of the PMBs and CBs had comparable swell indices as shown in Figure 16.

The improved chemical resistance and swelling of the PMBs in the synthetic MSW-I ash leachates can be attributed to the polymer additives because, for each manufacturer, the untreated bentonite used in the CB GCL is the same as the bentonite used in the PMB GCLs. Other researchers have made similar observations regarding the effect polymers have on the swelling of bentonite in aggressive liquids (Katsumi et al., 2008; Di Emidio et al., 2011; Scalia et al., 2014; Sato et al., 2017).

The trends in the swell indices shown in Figure 16 also indicate that, for the same bentonite and the same hydrating liquid, SI increases with polymer loading. For example, the SI of LPBA-0.5 (with 0.5% polymer lading) hydrated with AM-MAX was ~6.0 mL/2 g (comparable with that of BA), whereas the SI of LPBA-3.7 (with 3.7% polymer lading) was ~10 mL/2 g in the same leachate. This suggests that the chemical resistance of the untreated bentonite increases with as the quantity of polymer added to the bentonite increases. Sato et al. (2017) and Di Emidio (2010) reported similar increase in swelling of bentonite with increasing polymer dosage in single- and multi-species salts solutions and sea water. However, SI of all the PMBs was lower than 14 mL/2 g when hydrated in the synthetic MSW-I ash leachates with $I \geq 622$ mM.

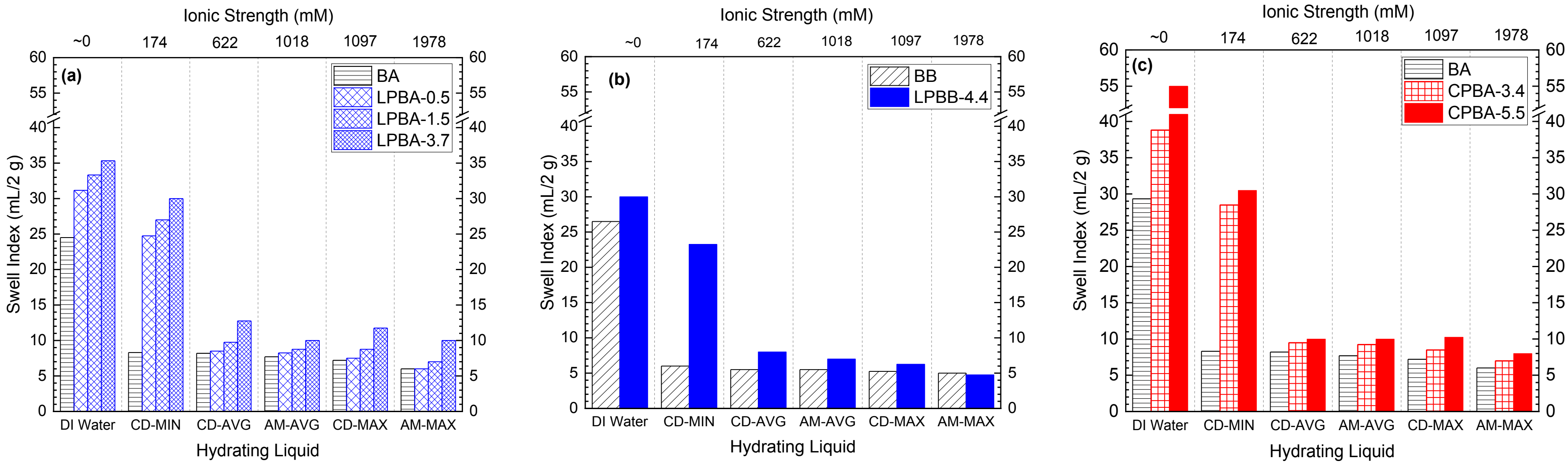

Figure 16. Comparison of the swell indices of the conventional bentonite (CB) GCL to the swell indices of polymer-modified bentonite (PMB) GCLs containing (a and b) linear polymer and (c) crosslinked polymer hydrated with DI water and MSW-I ash leachates [Note: For the CB GCL, specimens used for swell index testing were crushed and sieved according to ASTM D5890, whereas uncrushed specimens were used for the PMB GCLs].

2.2.3 Relationship between swelling and hydraulic conductivity of PMB GCLs

Figure 17a shows the relationship between swell index (SI) and hydraulic conductivity of the PMB GCLs used in this study. SI and hydraulic conductivity data for the CB GCLs reported in Table 5 were also included and shown Figure 17b. The trend lines in Figure 17a and Figure 17b were obtained through nonlinear regression analysis of the SI and hydraulic conductivity data reported in Table 5.

The trend line in Figure 17a shows that, similar to CB GCLs, hydraulic conductivity of the PMB GCLs is inversely related to SI of the bentonite component of the GCL (also see Figure 17b). Generally, SI >20 mL/2 g corresponds to hydraulic conductivity $< 1.0 \times 10^{-10}$ m/s, whereas SI <14 mL/2 g corresponds to hydraulic conductivity $> 1.0 \times 10^{-10}$ m/s. Katsumi et al. (2007) and (2008) reported as similar trend in the relationship between SI and hydraulic conductivity for conventional bentonites and modified bentonites permeated with single-species salts solutions, multispecies salts solutions and real inorganic waste leachates.

This result shows that, SI (measured using uncrushed specimen retrieved from the GCL) can be used to at least qualitatively asses the compatibility of PMB GCLs to MSW-I ash leachates under low effective stress (< 40 kPa). The trend lines in Figure 17 also suggests that the previously reported poor correlation between SI (measured per ASTM D 5890) of PMBs and hydraulic conductivity of PMB GCLs, shown in Figure 1, can be attributed to the segregation of the polymer additive from the composite material during specimen preparation.

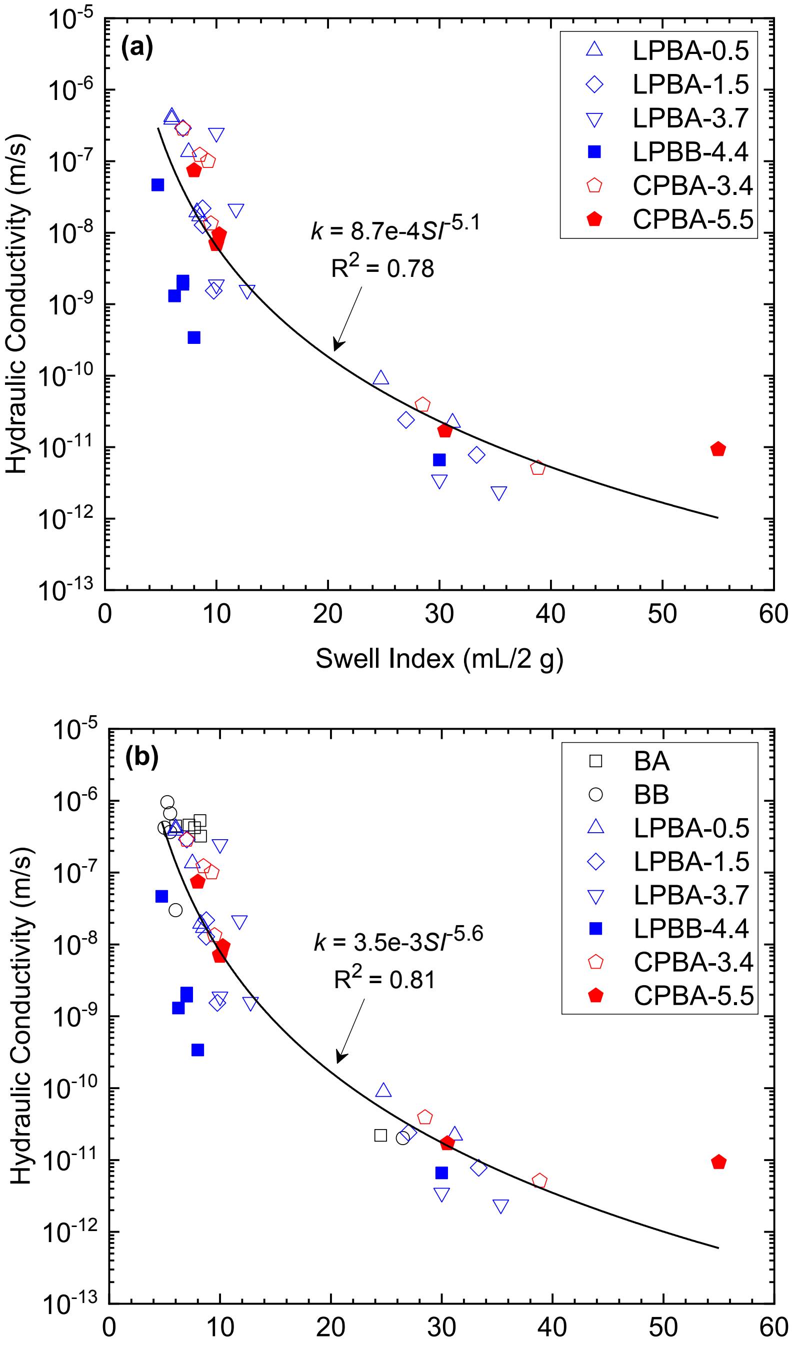

Figure 17. Hydraulic conductivity (*k*) as a function of swell index (*SI*) for (a) only polymer-modified bentonite (PMB) GCLs and (b) both conventional bentonite (CB) and PMB GCLs permeated with MSW incineration ash leachates. [Note: For the CB GCLs (BA and BB), specimens used for swell index testing were crushed and sieved according to ASTM D5890, whereas uncrushed specimens were used for the PMB GCLs].

2.2.4 Mechanism controlling hydraulic conductivity of polymer-modified bentonite GCLs to MSW-I ash leachates

A simplified schematic of the CB and PMB GCLs used in this study is shown in Figure 18 to illustrate the distribution of bentonite granules and polymer in the GCLs used in this study when hydrated with the MSW-I ash leachates. Hydrating a CB GCL with MSW-I ash leachate resulted in the formation of large intergranular pores of the bentonite granules in the GCL as shown in Figure 18a. Hydrating the a PMB GCL with MSW-I leachate results in the formation of a viscous polymer gel in the case of LPB GCL (see Figure 18b) or discrete polymer hydrogels in the case of CPB GCLs (as shown in Figure 18c). The viscous polymer gel or discrete hydrogels occupy the intergranular pores of the bentonite granules as shown in Figure 18d and e.

During permeation, the large intergranular pores in the bentonite fabric are responsible for conducting flow (Mesri and Olson, 1971; Shackelford et al., 2000; Jo et al., 2001; Ashmawy et al., 2002; Kolstad et al., 2004b; Chen et al., 2018), which typically results in high hydraulic conductivity immediately after permeation with MSW-I ash leachate as depicted in Figure 19. These intergranular pores will be physically occupied by discrete granules of polymer hydrogel for CBP GCLs which yields a more tortuous flow path for the permeant solution, reducing the flow rate and resulting in low hydraulic conductivity. However, because swelling capacity of crosslinked polymer (SAPs) diminishes rapidly in high ionic strength solutions and solutions rich in divalent cations (Lee and Wu, 1996; Zhu et al., 2014) (see Figure 20), more polymer is required to occupy all the intergranular voids in the bentonite fabric as shown in Figure 19.

In the case of the LPB GCLs, due to the mobility of the polymer gel formed during hydration, some of the polymer gel eventual elutes during permeation as reported in Table 5. Polymer elution from the LPB GCLs used in this study, resulted in two possible outcomes as shown in Figure 21. Outcome 1 (Figure 21b): polymer elution resulted in high hydraulic conductivity either immediately during permeation or after some time (see Figure 12a). Outcome 2 (Figure 21c).: Hydraulic conductivity of the LPB GCL remains low even after polymer elutes from the GCL Figure 21c.

The evolution of measured hydraulic conductivity for LPBA-0.5 specimens permeated with CD-MIN (I = 174 mM) and CD-AVG (I = 622 mM) is shown in Figure 22 to illustrate the two possible outcomes depicted in Figure 21. As shown in Figure 21 hydraulic conductivity of the specimen permeated with CD-AVG increased immediately after flow was initiated and remained in the 10^{-8} m/s range until termination after ~11.8 PVFs. The estimated total mass of polymer eluted from the specimen was ~1.7 mg which corresponds to only 0.7% of the initial mass of polymer that was in the specimen (see Table 5). however, for the specimen permeated with CD-MIN, hydraulic conductivity of the was initially ~2.0× 10^{-10} m/s, then, decreased slightly to ~7 × 10^{-11}m/s which is only 2.8 times lower [which is within the range of reproducibility identified by Daniel et al. (1997) for hydraulic conductivity testing of GCLs], and then remained in the 10^{-11}m/s range even after more than 5% of the initial amount of polymer in the specimen eluted. Similar observations were made for all the LPB GCLs used in this study and suggests that the impact that polymer elution had on the final hydraulic conductivity of the LPB GCLs depended on the chemistry of the permeant solution. Polymer elution was detrimental to the hydraulic conductivity of the LPB GCLs when ionic strength of the permeant solution is high.

The results of this study also suggest that the polymer blockage mechanism previously hypothesized to control the hydraulic conductivity of PMB GCLs is only applicable to PMB GCL containing crosslinked polymer because crosslinked polymers are water-insoluble therefore do not easily migrate with the permeation solution as linear polymers do. A study was conducted to investigate factors that influence polymer elution from LPB GCLs and the mechanism containing the chemical compatibility of LPB GCLs (after polymer elutes). The result of that study is discussed in the next section (i.e. Section 2.3)

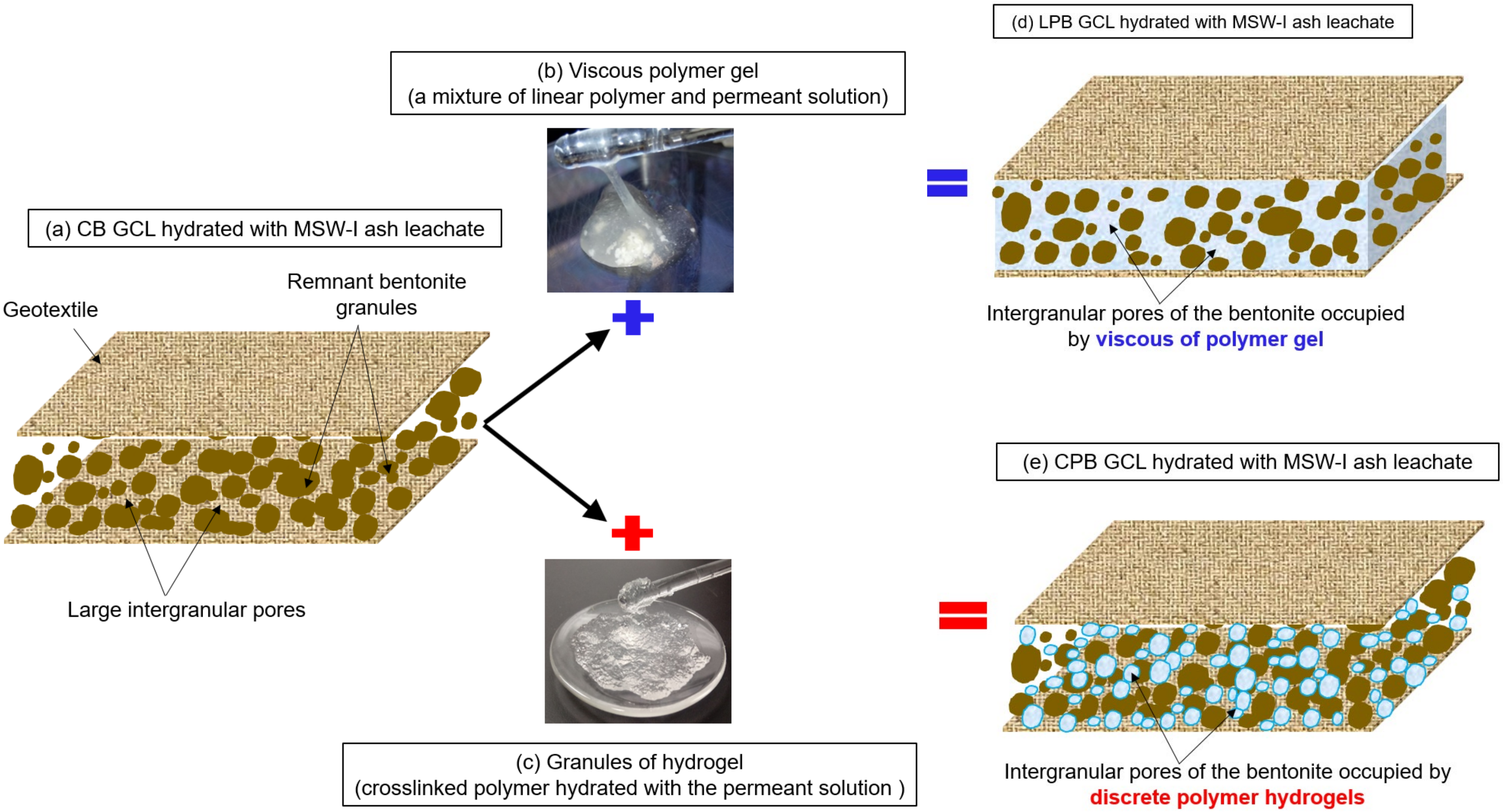

Figure 18. Schematic of GCL containing (a) conventional granular bentonite (CB) (d) linear polymer bentonite (LPB) composite (e) crosslinked polymer (CPB) bentonite composite when hydrated with MSW-I ash leachate [Note: (a) large intergranular pores due to suppressed osmotic swelling of bentonite. (b) The permeant solution mixes with linear polymer to form a viscous polymer gel which occupies the bentonite intergranular pores as shown in (d). (c) Crosslinked polymer imbibes the permeant solution, swells and fill the bentonite intergranular pores in as shown in (e)].

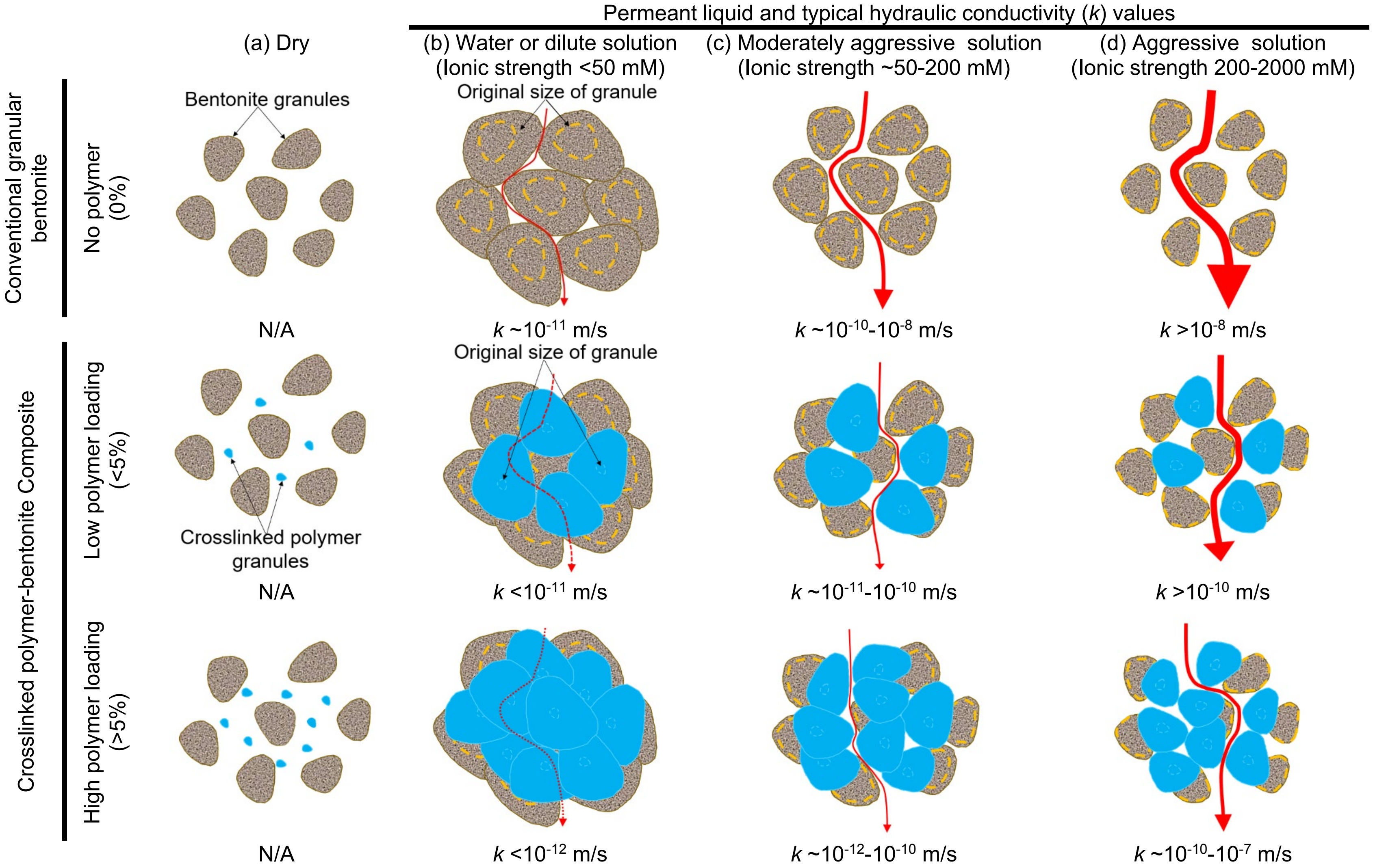

Figure 19. Conceptual models of physicochemical mechanism controlling the hydraulic conductivity of conventional bentonite (CB) polymer-modified bentonite (PMB) GCLs containing crosslinked polymer when permeated with (b) water or dilute solution (ionic strength of 50-200 mM), (d) moderately aggressive solution (ionic strength of 50-200 mM), and (d) aggressive solution (ionic strength 200-2000 mM).

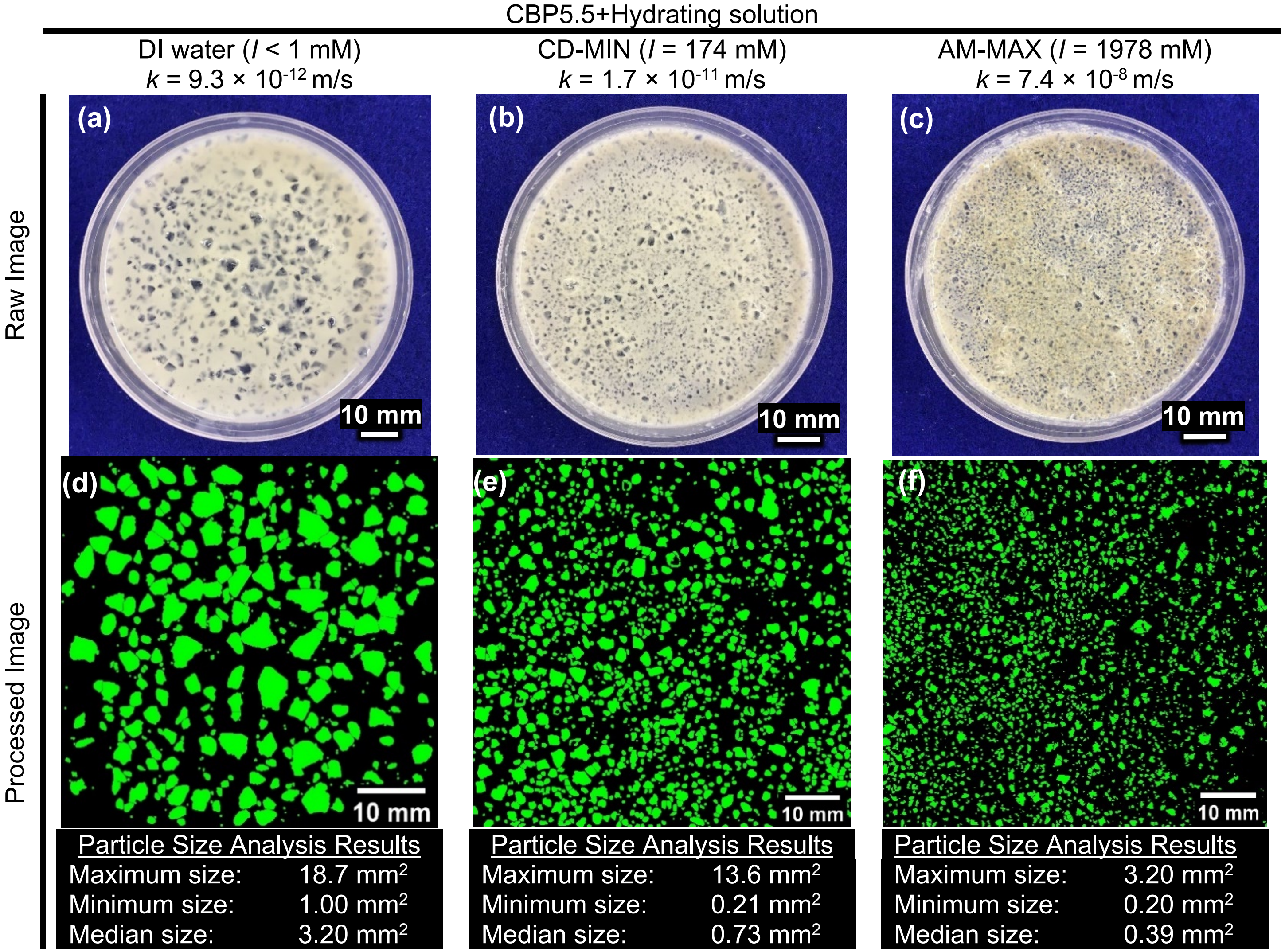

Figure 20. Raw images (a-c) and processed images (c-f) of hydrated bentonite extracted from CPB-5.5 which contains a blend of bentonite and crosslinked polymer (Note: k = hydraulic conductivity; I = ionic strength. Images c-f were processed and analyzed using ImageJ software. The sizes of the particles in images c-f were estimated by approximating the shape of the particles with spheres).

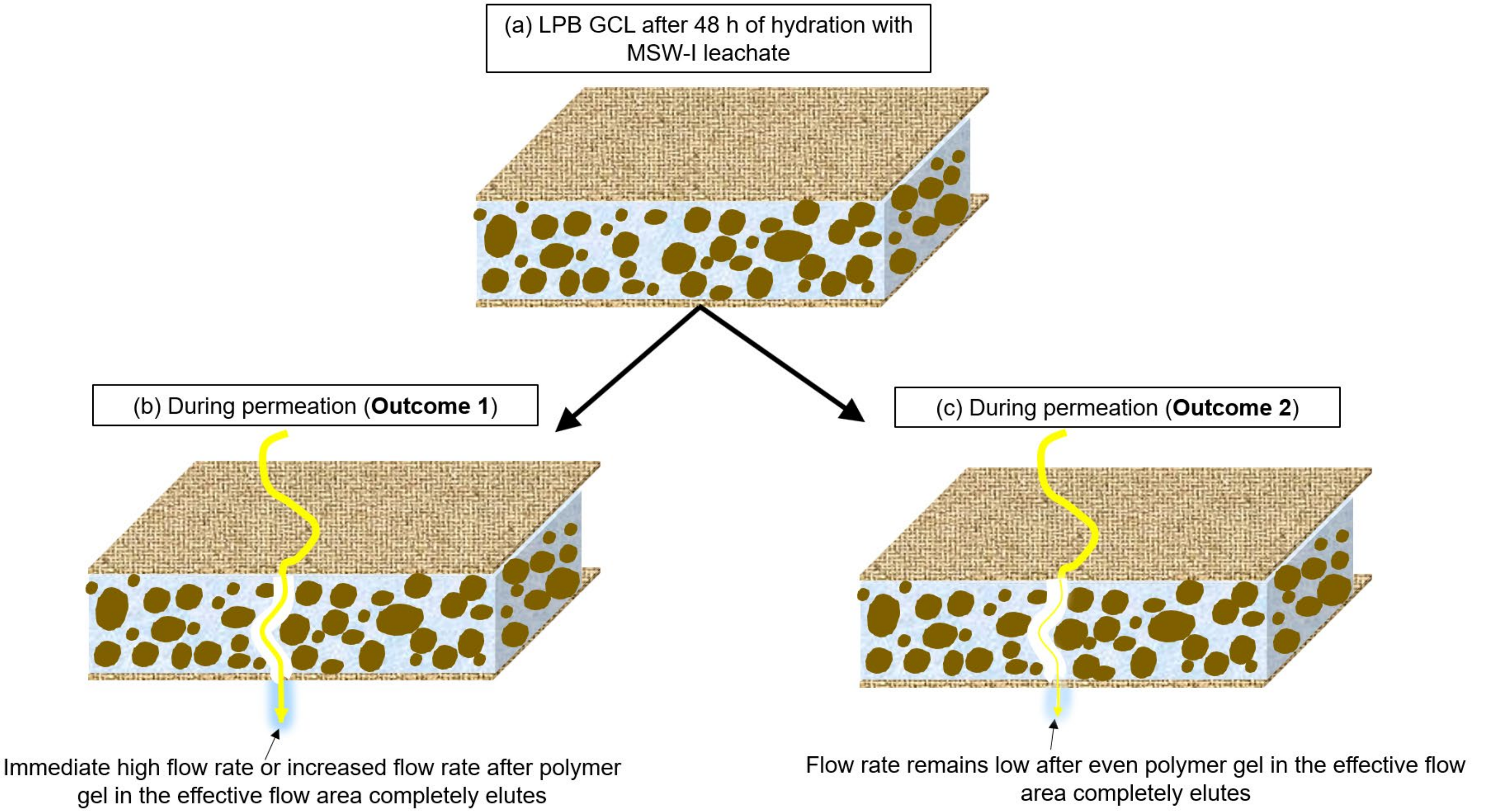

Figure 21. Effect of polymer elution on the hydraulic conductivity of polymer-modified bentonite (PMB) GCLs containing linear polymer when permeated with MSW-I ash leachate (Note: LPB = Linear polymer bentonite).

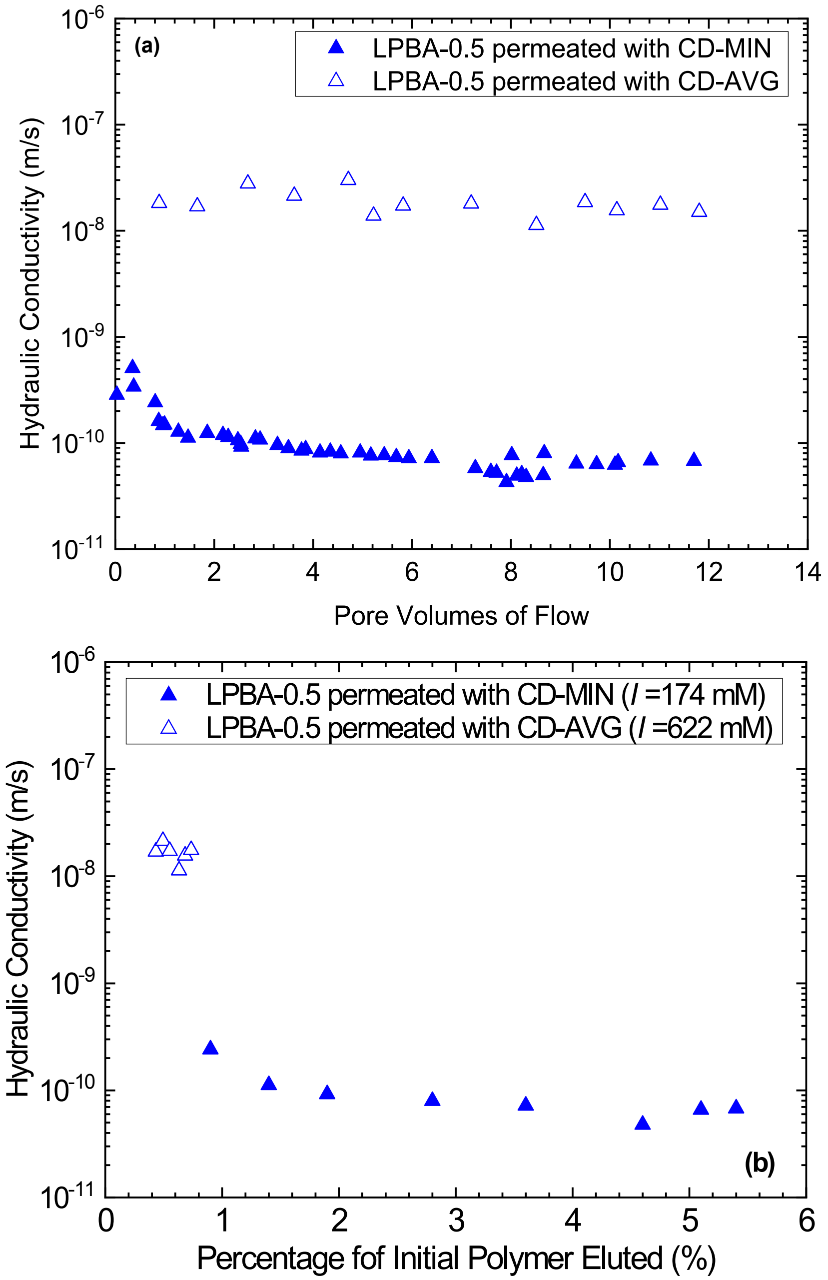

Figure 22. Hydraulic conductivity as a function of (a) pore volumes of flow and (b) percentage of initial polymer eluted from specimens of LPBA-0.5 (a PMB GCL containing linear polymer) permeated with CD-MIN (I = 174 mM) and CD-AVG (I = 622 mM) [Note: The percentage of initial polymer eluted is calculated as the cumulative mass of polymer eluted as a percentage of the initial mass of polymer. The cumulative mass of polymer eluted is determine by integrating

2.3 Investigating Factors Influencing Polymer Elution and the Mechanism Controlling Chemical Compatibility of a Polymer-Modified Bentonite GCL containing linear Polymer

Note: A manuscript containing majority of the text, figures and tables in the section is currently under review in Geotextiles and Geomembranes Journal:
Wireko C.[1], Abichou T.[1], 2020. “Investigating the Mechanism Controlling the Chemical Compatibility and Hydraulic Conductivity of a Bentonite-Polymer Composite GCL”
[1]Department of Civil and Environmental Engineering, Florida A&M University-Florida State University College of Engineering, 2525 Pottsdamer St., Tallahassee, FL, 32310-6064, USA;

Based on the observations made during the study described in the previous section (i.e. Section 2.2), a study was conducted to investigate factors that influence polymer elution and the mechanism controlling chemical compatibility of PMB GCLs containing linear polymer (LPB GCLs) by performing a series of hydraulic conductivity and index tests on one commercially available LPB GCL with 4.4% polymer loading (LPBB-4.4) using DI water, varying concentrations of NaCl and $CaCl_2$ solutions. Comparative tests were also performed on one CB GCL (BB) produced by the same manufacturer. The CB GCL contained the same (untreated) granular bentonite and had the same physical properties as the LPB GCL (see Table 7 in Section 4 of this report). Polymer elution during permeation was quantified using the TOC concentration in the effluent samples collected during hydraulic conductivity testing of the LPB GCL. Physicochemical factors that affect polymer elution were investigated by performing viscosity tests on slurries of bentonite extracted from the LPB GCL and duplicate hydraulic conductivity tests on LPB GCL using varying average hydraulic gradient (at an average effective stress of 39 kPa). Based on the results of the hydraulic conductivity and index tests, a new mechanism controlling the observed long-term chemical compatibility of LPB GCLs was proposed and supported with additional cation analysis.

2.3.1 Hydraulic conductivity and free swell test results

Results of the hydraulic conductivity and free swell tests performed on the LPB GCL and CB GCL are summarized in Table 6 and also plotted in Figure 23 for comparison. The total mass of eluted polymer reported in Table 6 was calculated by integrating the measured mass of polymer in each effluent sample, while the percentage of polymer eluted was estimated based on the initial polymer loading (4.4%) and the dry mass of bentonite in the LPB GCL (after subtracting the measured dry mass of the geotextiles). The final water content and change in bulk GCL height are also reported in Table 6.

The trends in measured swell index and hydraulic conductivity in Figure 23 shows improved chemical resistance and hydraulic performance of the LPB GCL (as expected) relative to the performance of the CB GCL when hydrated and permeated salt solutions (especially in the NaCl). For example, the hydraulic conductivity of the CB GCL to 500 mM NaCl was ~2.0×10^{-7} m/s, whereas that of the PMB GCL to 500 mM NaCl was ~1.4×10^{-10} m/s, an improvement of more than three orders-of-magnitude (see Table 6). Also, the hydraulic conductivity of the PMB GCL to both 50 and 200 mM $CaCl_2$ was more two orders-of-magnitude lower than that of the CB GCL.

This improved chemical resistance and hydraulic performance of LPB can be attributed to the linear polymer additive because the LPB GCL was manufactured using the same (untreated) bentonite in the CB GCL. As shown in Figure 23a and b, the presence of the linear polymer seems to increase the swelling capacity of the bentonite [also compare the final water content and relative change in bulk GCL height of the LPB GCL (reported in Table 6) to that of the CB GCL]. Other researchers have also reported improved swelling of bentonite treated with linear polymers (Di Emidio et al., 2008; Katsumi et al., 2008; Di Emidio, 2010; Di Emidio et al., 2011; Scalia et al., 2014; Sato et al., 2017; Prongmanee et al., 2018; Xu et al., 2018; Prongmanee and Chai, 2019; Yu et al., 2019; Chai and Prongmanee, 2020; Fan et al., 2020).

As reported in Table 6, polymer eluted from the LPB GCL regardless of the chemistry of the permeant solution (either with DI water or salt solution). However, the rate at which polymer eluted and the effect of polymer elution had on the final hydraulic conductivity of the LPB GCL depended on the concentration and valence of the dominant cation in permeant solution. The underlying mechanism for the observation made on hydraulic behavior and chemical compatibility of the LPB GCL will be discussed later.

Table 6. Summary of hydraulic conductivity and free swell tests on a PMB GCL containing linear polymer and a CB GCL using DI water, NaCl and $CaCl_2$ solutions

							ASTM D6766 Termination criteria met?					
GCL[a]	Permeant solution	Swell index[c] (mL/2 g)	Average i[c]	Duration[d]	PVF[e]	k[e] (m/s)	Hydraulic	Chemical	ΔH[f] (mm)	w_f (%)	Cumulative mass of polymer eluted[g] (mg)	Percent initial polymer eluted[g] (%)
LPBB-4.4	DI water[b]	30.0	219	91 days	1.4	3.7×10^{-12}	Yes	N/A	N/A	N/A	191.4	14.8
	500 mM NaCl	10.5	284	62 days	17.6	1.4×10^{-10}	Yes	Yes	0.0	99	487.7	33.8
	2000 mM NaCl	3.0	308	3.8 h	9.7	1.7×10^{-8}	Yes	Yes	-0.1	81	224.0	15.8
	50 mM $CaCl_2$	11.0	263	40 days	10.0	1.5×10^{-9}	Yes	Yes	0.8	124	279.8	20.5
	50 mM $CaCl_2$ (D1)	11.0	490	48 days	16.7	2.2×10^{-9}	Yes	Yes	0.7	107	336.8	23.6
	50 mM $CaCl_2$ (D2)	11.0	957	9 days	32.8	2.6×10^{-9}	Yes	Yes	0.5	113	239.8	17.3
	200 mM $CaCl_2$	7.5	265	14.6 h	10.7	1.9×10^{-9}	Yes	Yes	0.4	87	683.7	44.0
	500 mM $CaCl_2$	5.0	293	1.5 h	20.9	5.8×10^{-8}	Yes	Yes	0.3	86	450.4	35.3
BB	DI water[a]	26.0	234	39 days	4.3	2.0×10^{-11}	Yes	N/A	N/A	N/A	N/A	N/A
	200 mM NaCl	9.5	278	0.2 h	5.4	1.3×10^{-7}	Yes	Yes	0.2	107	N/A	N/A
	500 mM NaCl	6.0	327	0.4 h	25.7	2.0×10^{-7}	Yes	Yes	0.0	99	N/A	N/A
	1000 mM NaCl	5.0	316	0.4 h	28.0	2.9×10^{-7}	Yes	Yes	-0.2	89	N/A	N/A
	50 mM $CaCl_2$	7.0	272	0.1 h	4.1	1.9×10^{-7}	Yes	Yes	0.1	101	N/A	N/A
	200 mM $CaCl_2$	5.5	314	0.4 h	26.7	2.3×10^{-7}	Yes	Yes	-0.1	115	N/A	N/A
	500 mM $CaCl_2$	5.0	272	0.2 h	7.6	2.1×10^{-7}	Yes	Yes	-0.3	84	N/A	N/A

Note: i = Hydraulic gradient, k = Hydraulic conductivity, PVF = pore volumes of flow, N/A = Not applicable, D = Duplicate ΔH = Change in bulk GCL thickness, w_f = final water content . All k tests were conducted under an average effective stress of 39 kPa

[a] In the GCL designation, the first letter(s) indicates: B = Bentonite, LPB = Linear polymer-bentonite, And the last letter indicates the manufacturer (A or B)

[b] Tests with DI water still ongoing

[c] For the CB GCL, specimens used for swell index testing were crushed and sieved according to ASTM D5890, whereas uncrushed specimen were used for the PMB GCL as recommended by Wireko et al. (2020)

[d] Does not include the period of hydration (2 days) and the time in-between readings (required to refill the influent canister with the permeation solution)

[e] Calculated based on the final thickness of the bulk GCL specimen (except of ongoing tests where the initial thickness was used)

[f] Calculated as the difference between the initial and final thickness of the bulk GCL specimen

[g] Calculated by integrating the product of the total organic carbon (TOC) concentration (in mg/L) and the volume (in L) of effluent samples collected during permeation. And percentage of initial polymer eluted was estimated based on the initial mass of polymer in the GCL specimen

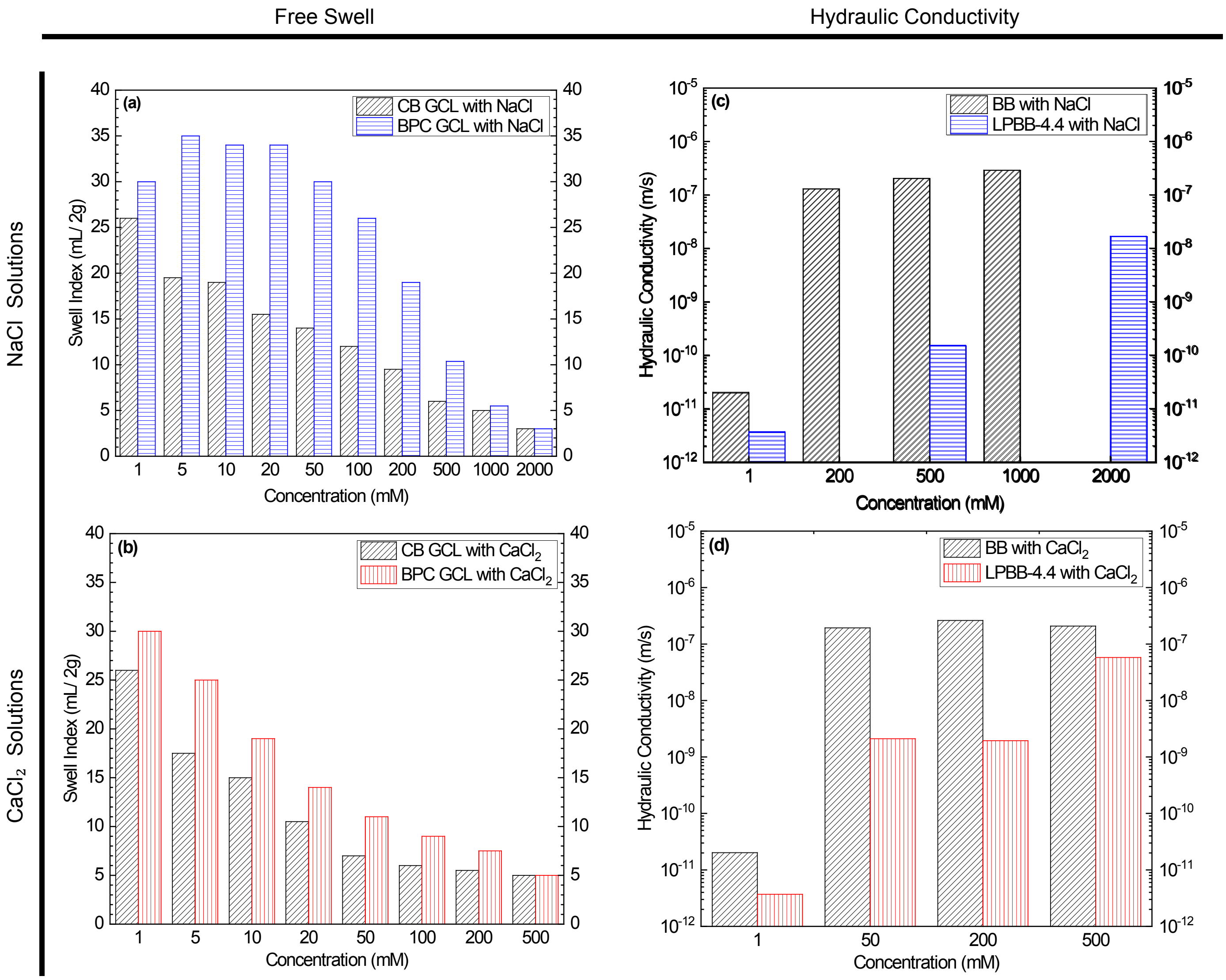

Figure 23. Results of the free swell (a and b) and hydraulic conductivity (c and d) tests performed on a polymer-modified bentonite (PMB) and conventional bentonite (CB) GCL specimens using NaCl solutions and $CaCl_2$ solutions. (Note: Results of the test performed using DI water is shown on 1 mM for comparison. For the CB GCL, specimens used for swell index testing were crushed and sieved according to ASTM D5890, whereas uncrushed specimen were used for the PMB GCL)

2.3.2 Observations on the evolution of hydraulic conductivity of polymer-modified bentonite GCLs containing linear polymer

Hydraulic conductivity versus PVF for the LPB GCL specimens permeated with DI water and 50 mM $CaCl_2$ solutions is shown in Figure 24 to highlight how chemistry of the permeant solution affects evolution of the hydraulic conductivity of the LPB GCL. As mentioned before, polymer elution occurred during all the hydraulic conductivity tests on the LPB GCL regardless of chemistry of permeating solution. However, the consistency of the eluting polymer appeared to be different for the different permeant solutions. For instance, the effluent tubes of the permeameter were clogged with a highly viscous (thick) polymer gel eluting from the LPB GCL when permeated with DI water which resulted in an apparent decrease in hydraulic conductivity (see Figure 24a). During that test, the effluent tubes were unclogged to allow for flow into the effluent side of the GCLs. (Note: the closed black arrows in Figure 24a indicate events where the effluent tubes were unclogged). The eluting polymer from the specimen permeated with 50 mM $CaCl_2$ on the other hand appeared significantly less viscous and did not cause clogging of the effluent tubes. However, hydraulic conductivity increased gradually (from ~2.2×10^{-11} m/s, to 1.5×10^{-9} m/s) as the test progressed due to polymer elution. Reybrock (2018) also reported that during hydraulic conductivity testing of two BPC GCLs, tests with dilute leachates required periodic unclogging of effluent tube whereas test with aggressive leachates did not require unclogging of effluent tubes.

Figure 25 shows images of influent and effluent samples from hydraulic conductivity test on LPB GCL specimens permeated with DI water (Figure 24a) and 50 mM $CaCl_2$ (Figure 24b) solution. The turbidity of the effluent as compared to the influent is an indication that the polymer gel migrated from the LPB GCL during permeation. One can also visually observe the difference in consistency between the effluents from each test indicating that the viscosity of the eluting polymer gel is a function of the chemistry permeating solution, as will be discussed in the next section.

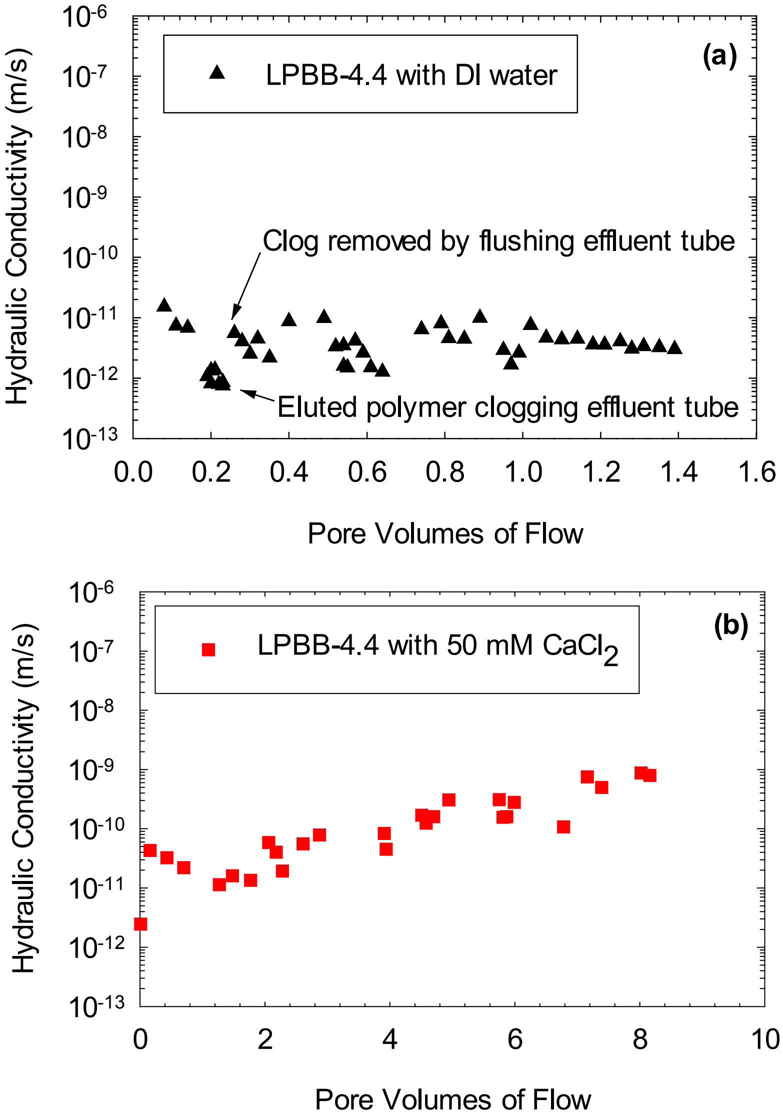

Figure 24. Hydraulic conductivity as a function of pore volumes of flow for specimens of a polymer-modified bentonite GCL containing linear polymer permeated with (a) DI water, (b) 200 mM NaCl, and (c) 50 mM $CaCl_2$ solution (Note: The black filled arrows indicate points where the effluent tube was unclogged).

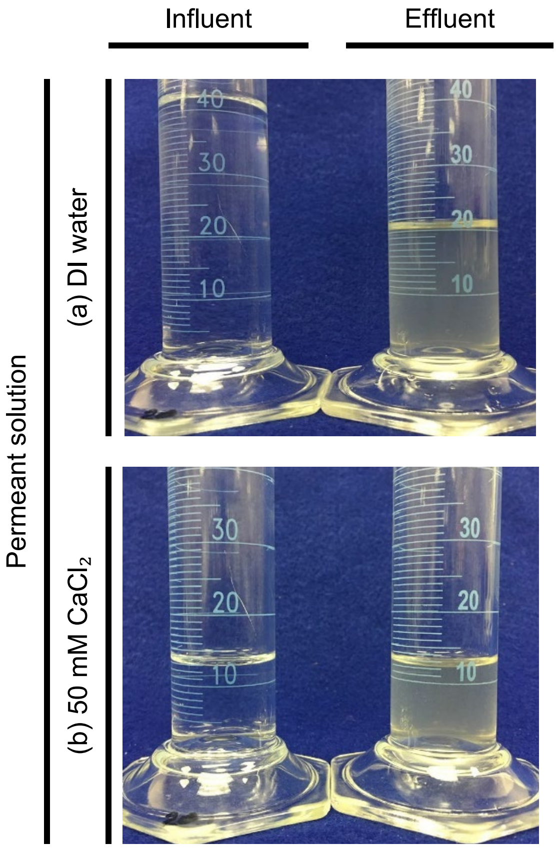

Figure 25. Influent and effluent from hydraulic conductivity test on specimens of a polymer-modified bentonite GCL containing linear polymer (LPBB-4.4) permeated with (a) DI water, (b) 50 mM $CaCl_2$ solution.

2.3.3 Polymer elution and hydraulic conductivity of linear polymer-modified bentonite GCLs

2.3.3.1 Effect of cation concentration and valance on the rate of polymer elution

Figure 26 shows the rate of polymer elution as a function of concentration for hydraulic conductivity tests performed on LPBB-4.4 using the NaCl and $CaCl_2$ solutions. The rate of polymer elution was calculated by dividing the total mass of polymer eluted (in mg) reported in Table 6 by the cross-sectional area of the GCL specimen (in m^2) and the test duration (in seconds). All tests had a non-zero polymer elution rate, suggesting polymer elutes regardless of the chemistry of the permeant. However, the rate at which polymer eluted increases as the concentration of the permeant solution increases. Moreover, the slope of the rate of polymer elution curve for specimens of LPBB-4.4 permeated with the $CaCl_2$ solutions is approximately nineteen times that of the NaCl solutions (as shown in Figure 26), which is an indication of the difference in interactions between the polymer and the Na^+ and Ca^{2+} cations. Polyvalent cations can contract the polymer chains by crosslinking the functional groups within a polymer chain and/or between individual polymer chains (Peng and Wu, 1999). This consequently reduces the polymer ability to absorb water resulting in a lower viscosity polymer gel, which is less resistant to flow (Katchalsky, 1964; Mungan, 1972; Martin, 1975; Muller et al., 1979; Durst et al., 1981; Huber, 1993; Peng and Wu, 1999; Schweins and Huber, 2001; Schweins et al., 2006).

Figure 27 shows the results of the viscosity tests performed on slurries of bentonite extracted from BB and LPBB-4.4 (1:10 solid to liquid ratio) prepared with DI water and solutions with increasing NaCl and $CaCl_2$ concentrations. The difference in polymer elution rate is associated with viscosity of the gel formed by the polymer and the permeating solution. The additional viscosity provided by the polymer decreases dramatically for $CaCl_2$ solution as the concentration reaches 50 mM. For the NaCl solutions, however, viscosity of the LPB slurries was high than the viscosity of the CB with DI water until the concentration of Na was greater than 200 mM. The difference in viscosity between the CB and LPB is a manifestation of the additional viscosity provided by the polymer (see the shaded regions in Figure 27). This difference in viscosity of the polymer gel (i.e. the polymer-influent mixture) formed in the pore space between the bentonite granules in the GCL significantly affects the rate at which polymer elutes from the LPB GCL.

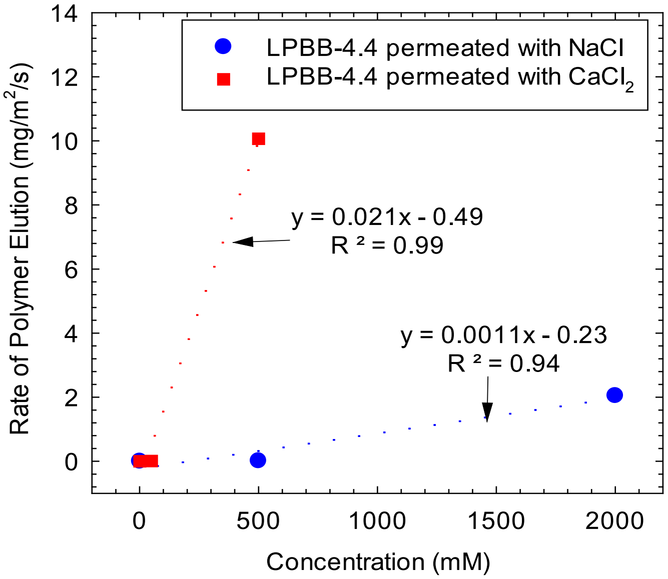

Figure 26. Rate of polymer elution from specimens of a polymer-modified bentonite GCL containing linear (LPBB-4.4) as a function of NaCl or CaCl$_2$ concentration with DI water shown on 1 mM [Note: The rate of polymer elution was calculated by dividing the total mass of polymer eluted (in mg) by the cross-sectional area of the GCL specimen (in m^2) and the test duration (in seconds). Shows only data for GCL specimens permeated using comparable hydraulic gradient (263 – 305)].

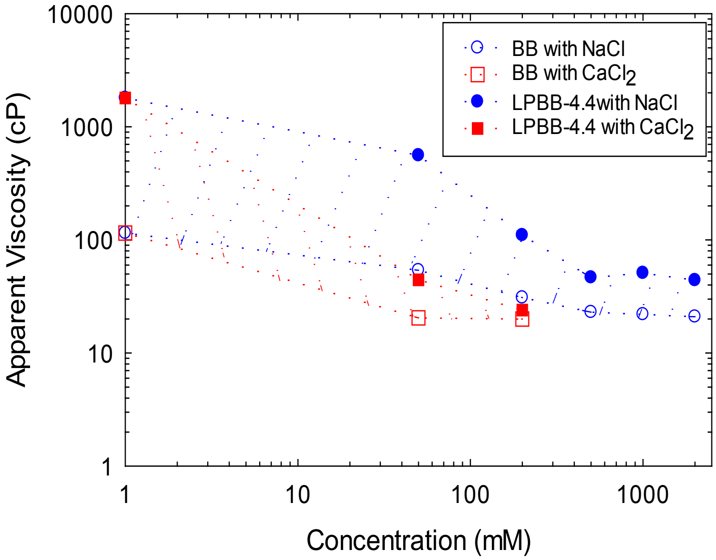

Figure 27. Apparent viscosity of slurries of bentonite extracted from a conventional bentonite (i.e. BB) and a polymer-modified bentonite GCL containing linear polymer (i.e. LPBB4.4) slurries (1:10 solid to liquid ratio) as a function of concentration of NaCl or CaCl$_2$ with DI water shown on 1 mM (Note: the shaded region represents additional viscosity induced by the presence of the polymer).

2.3.3.2 Effect of hydraulic gradient on the rate of polymer elution

The results of the duplicate hydraulic conductivity tests reported in Table 6 are shown in Figure 28 along with data from Petrov (1995) for a CB GCL permeated with distilled water, tap water and NaCl solutions at different average hydraulic gradient (but comparable average effective stress). As shown in Figure 28, hydraulic conductivity of the LPB GCL permeated with 50 mM $CaCl_2$ at average hydraulic gradient of 263, 490 or 957 was practically equal ($1.5 – 2.6 \times 10^{-9}$ m/s). This result is consistent with the observations in literature for GCLs (Petrov, 1995; Petrov and Rowe, 1997; Petrov et al., 1997a, b; Shackelford et al., 2000) and implies that the range of hydraulic gradient used in this study (including Section 2.2) did not have any significant influence of the final hydraulic conductivity reported for the LPB GCLs.

However, hydraulic gradient had a profound influence on the rate at which polymer eluted from the LPB GCL and the duration of the test. To illustrate this, hydraulic conductivity is shown as a function of PVF and the time elapsed in Figure 29a and b for specimens of the LPB GCL permeated with 50 mM $CaCl_2$ solution using an average hydraulic gradient 490 and 957. As shown in Figure 29a and b, the temporal behavior and final hydraulic conductivity of the specimens permeated with an average hydraulic gradient 490 and 957 were comparable to that of the specimen permeated using an average hydraulic gradient 263 which is shown in Figure 24c (also see Figure 28 and Table 6). However, the hydraulic conductivity of the specimen permeated with average hydraulic gradient of 490 was with the order 10^{-12} m/s for 32 days before starting to increase and eventually reaching steady state after 48 days, whereas hydraulic conductivity reached steady state after just in 7 days for the specimen permeated with average hydraulic gradient of 957.

The rate of polymer elution is shown in Figure 30 as a function of the average hydraulic gradient used for the duplicate hydraulic conductivity tests performed on the LPB GCL using 50 mM $CaCl_2$ solution. As shown in Figure 30 the rate at which polymer elutes increases as the average hydraulic gradient increase, which consequently had significant impact on the duration of the hydraulic conductivity test (see Table 6).

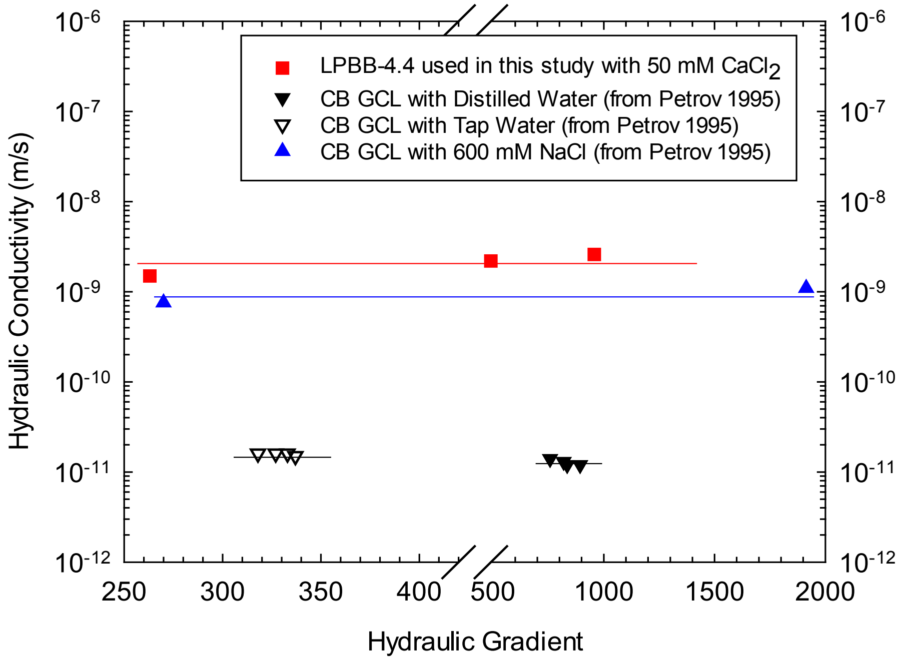

Figure 28. Hydraulic conductivity versus hydraulic gradient for specimens of a polymer-modified bentonite GCL containing linear polymer used in this study and conventional bentonite (CB) GCL from literature. [Note: CB GCL data from Petrov (1995). The reported hydraulic conductivity values for both CB and BPC GCLs were measured at an average effective stress of 34–38 kPa].

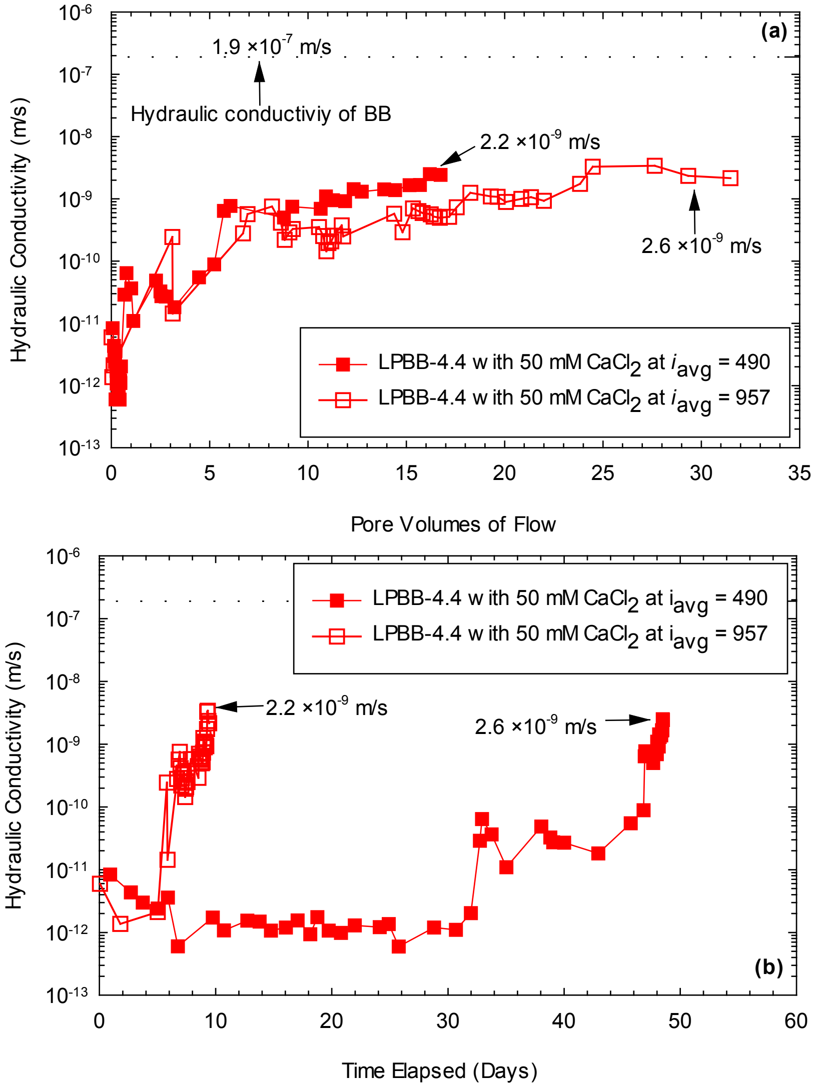

Figure 29. Hydraulic conductivity as a function of (a) pore volumes of flow and (b) time elapsed for specimens of a polymer-modified bentonite GCL containing linear (LPBB-4.4) permeated with 50 mM $CaCl_2$ at an average hydraulic gradient (i_{avg}) of 490 or 957. [Note: Hydraulic conductivity of the conventional bentonite (CB) GCL (i.e BB) permeated with 50 mM $CaCl_2$ is shown with a dashed line in a and d respectively for comparison].

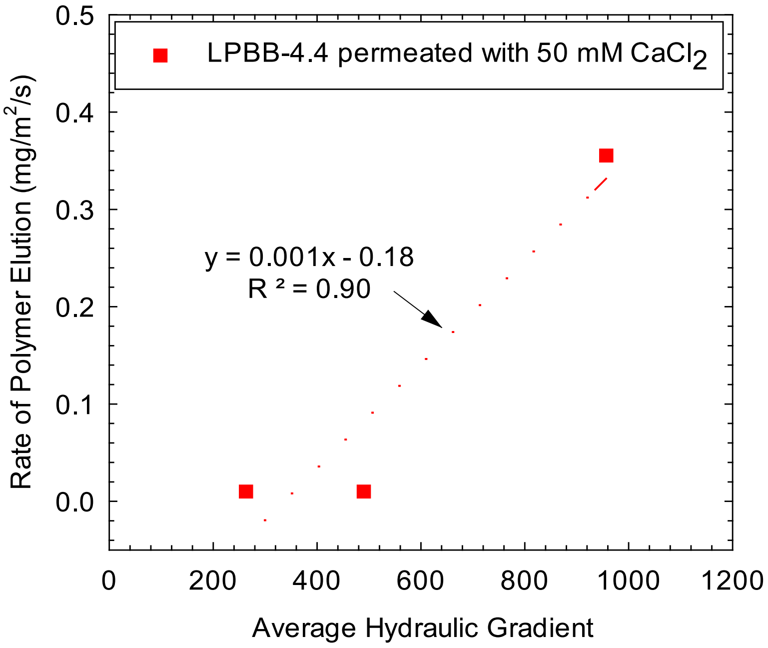

Figure 30. Rate of polymer elution from specimens of a polymer-modified bentonite GCL containing linear (LPBB-4.4) permeated with 50 mM $CaCl_2$ solutions at different hydraulic gradients. [Note: The rate of polymer elution was calculated by dividing the total mass of polymer eluted (in mg) by the cross-sectional area of the GCL specimen (in m^2) and the test duration (in seconds)].

2.3.3.3 Effect of polymer elution on hydraulic conductivity of liner-polymer bentonite modified GCLs

As reported in Table 6, polymer eluted from the LPB GCL regardless of the chemistry of the permeant solution (either with DI water or salt solution). However, the impact that polymer elution had on the final hydraulic conductivity of the LPB GCL depended on the chemical properties of the permeant solution. The hydraulic conductivity results plotted in Figure 31 as a function of the total mass of polymer eluted from each LPB GCL specimen permeated with DI water, the NaCl and $CaCl_2$ solutions. As mentioned before, hydraulic conductivity of the PMB GCL is not at all correlated with the total mass of polymer eluted from the GCL. For instance, hydraulic conductivity of the LPB GCL specimen permeated with 500 mM NaCl was ~1.4×10^{-10} m/s, whereas hydraulic conductivity the specimen permeated with 2000 mM NaCl was ~1.7×10^{-8} m/s even though twice as much polymer eluted from the specimen permeated with 500 mM NaCl (487.7 mg) compared to the specimen permeated with 2000 mM NaCl (224.0 mg).

Moreover, hydraulic conductivity of the LPB GCL specimen permeated with 500 mM NaCl was more than two orders of magnitude lower than the specimen permeated with 500 mM $CaCl_2$ even though similar amount of polymer eluted from both specimens as shown in Figure 31 (also see Table 6). This suggests that the same LPB GCL can have different hydraulic conductivities even when the same amount of polymer is retained in the GCL. Salihoglu (2015) also made similar observations (also see data reported in Figure 2). Therefore, the improved hydraulic performance of the LPB GCL cannot be explained by the polymer blockage mechanism previously hypothesized by Tian et al. (2016) and (2019). A new hypothesis or mechanism of bentonite-polymer-permeant interactions is proposed in the next section to explain the improvement in chemical compatibility and hydraulic conductivity of the LPB GCL (even when polymer elutes).

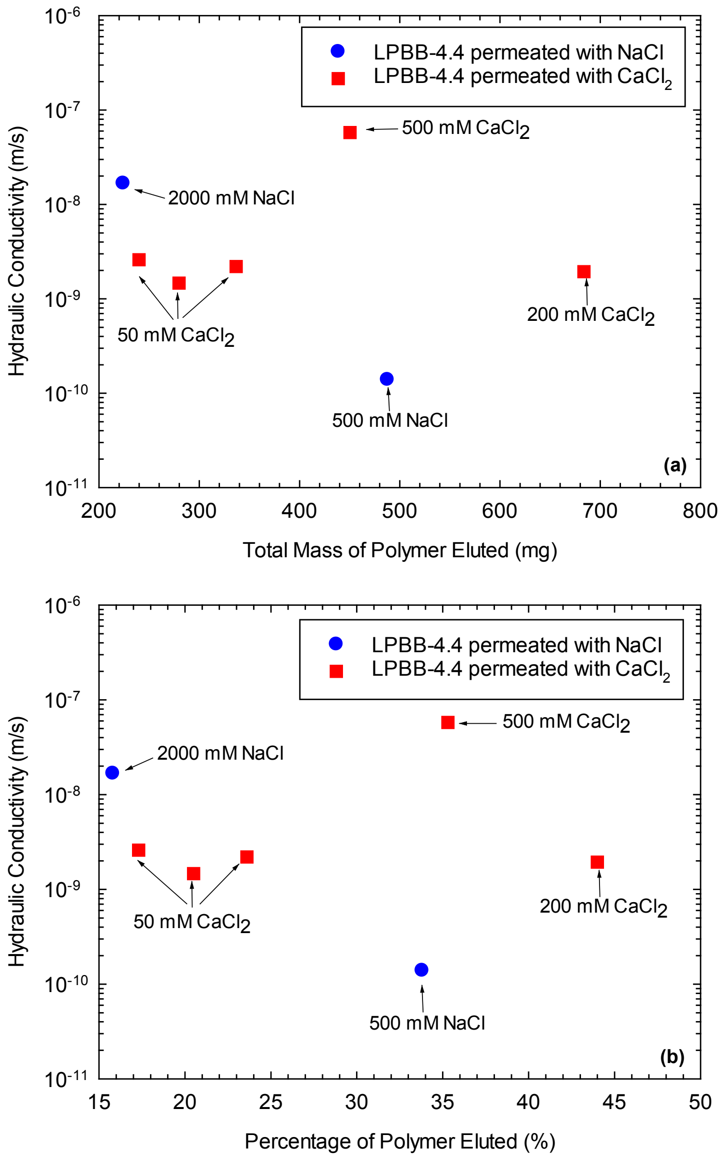

Figure 31. Hydraulic conductivity of polymer-modified bentonite (PMB) GCL specimens as function of (a) the total mass of polymer eluted and (b) the percentage of polymer eluted after permeation with NaCl and $CaCl_2$ solutions. [Note: The total mass of polymer eluted was calculated by integrating the product of the total organic carbon (TOC) concentration (in mg/L) and the volume of effluent (in L) samples collected during permeation. Percentage of polymer eluted was estimated by based on the total mass of polymer eluted and initial mass of polymer in the GCL specimen.].

2.3.4 Proposed mechanism controlling long-term chemical compatibility of polymer-modified bentonite GCLs containing linear polymer

2.3.4.1 Proposed mechanism

Based on the results of the hydraulic conductivity and index tests, the following mechanism, conceptually depicted in Figure 32, is proposed to explain the long-term chemical compatibility of LPB GCLs (containing a blend of bentonite and linear polymer) as compared to CB GCLs (without polymers): when the LPB GCL is hydrated with weak liquid (with low to moderate ionic strength and/or low concentration of divalent cations), the polymer scavenges cations from the permeant solution (see Figure 32c) and mixes with the solution to form a gel. During this initial stage, two different liquid phases occupy the void space between the bentonite granules: (1) a newly formed polymer gel (polymer-permeant) that has a higher concentration of cations associated with the polymer (Figure 32c), and (2) an additional solution that fills the remainder of the void space (Figure 32d). This second solution is characterized by lower ionic strength and lower cation concentration than the incoming permeant, because some of the cations in the permeant solution become associated with the polymer gel (see Figure 32c). This more dilute solution (not associated with the polymer) is available for the bentonite granules to hydrate and swell. During this initial stage, the montmorillonite particles can undergo osmotic swelling due to the reduced cation concentrations in hydrating pore solution (as shown Figure 32e). As the polymer gel is pushed out of the pore space during permeation by the moving permeant (at a rate dependent on the viscosity of the polymer gel) the so-called “house-of-card structure” attained by montmorillonite particles (Olphen, 1977; Ashmawy et al., 2002; Katsumi et al., 2004) and increase in tightly bound water molecules due to osmotic swelling of the bentonite (Jo et al., 2004) that occurred during the initial hydration period controls the hydraulic conductivity of the GCL. This phenomenon is analogous to the improvement in the hydraulic conductivity of CB GCLs when they are prehydrated with water or dilute solution before permeation with waste leachate. However, when the PMB GCL is hydrated with very aggressive liquid, as shown Figure 32f, the amount of polymer may not be enough to scavenge all the cations (see Figure 32g and h). Therefore, osmotic swelling of the bentonite is suppressed (see Figure 32i), causing significant increase in hydraulic conductivity when the front of polymer gel breaks through the GCL during permeation.

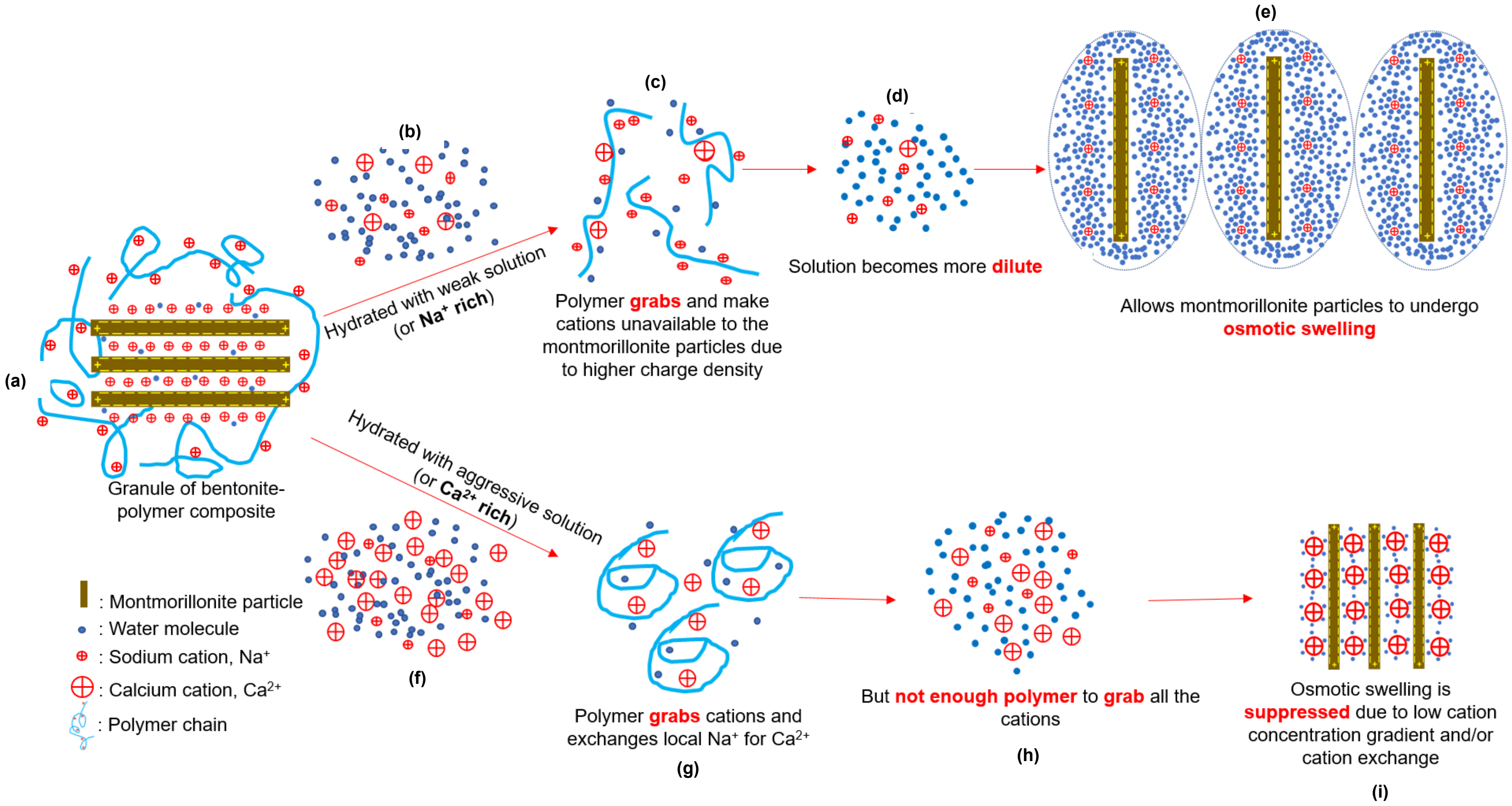

Figure 32. Hypothesized mechanism of interaction between polymer-modified bentonite containing linear polymer and hydrating solution

2.3.4.2 Theory behind proposed mechanism

The ability of linear (water-soluble) polymers to scavenge cations is well studied in literature due to their application in environmental and industrial applications like recovery of metals from waste water (Rivas et al., 2003; Rivas et al., 2009; Mukherjee et al., 2018; Rivas et al., 2018). In a polymer-cation aqueous system, functional groups of the polymer interact with the cations mainly through electrostatic forces and the formation of coordination bonds (Rivas et al., 2003; Rivas et al., 2018). Intrinsic properties of the polymer like the physical structure of the polymer, the molecular weight of the polymer, and the nature of the functional group have significant impact on how the polymers interacts with cations (Rivas and Moreno-Villoslada, 2000; Rivas et al., 2003; Rivas et al., 2009; Rivas et al., 2011; Rivas et al., 2018). External factors like the surrounding pH, temperature and the valence of the cation can also influence polymer-cation interactions (Moreno-Villoslada and Rivas, 2003; Rivas et al., 2003; Rivas et al., 2009; Rivas et al., 2011). Generally, water-soluble polymers have a stronger affinity to polyvalent cations than monovalent cations (Moreno-Villoslada and Rivas, 2002; Rivas et al., 2003). However, in a very low pH (<3) environment, interactions between the polymer and polyvalent cations is limited due to charge screening of the functional groups on the polymer chain by abundant H^+ ions (Rivas et al., 2003; Rivas and Aguirre, 2007). Increasing concentration of polymer (i.e. polymer mass per unit volume solution) increases the number reactive sites available for the polymer to bind cations (Rivas and Moreno-Villoslada, 2000; Rivas et al., 2011).

2.3.4.3 Support for proposed mechanism: Free swell tests coupled with cation analysis

To demonstrate the mechanism of polymer scavenging cations, free swell tests were performed by gradually mixing 2 g of PMB or CB GCL (in increments of 0.5g) with 50 mL of NaCl or $CaCl_2$ solution in centrifuge tube. After allowing the bentonite to swell and settle for 24 h, the supernatant (i.e. the liquid above the bentonite gel) was decanted and analyzed for Na^+ or Ca^{2+}. For the LPB, the supernatant, believed to be a mixture of polymer gel and the hydrating solution as shown in Figure 33a, was decanted into a different centrifuge tube (see Figure 33b) and then centrifuged for 6 h to separate the polymer gel from the hydrating (free) solution (i.e. the solution not associated with the polymer) as shown in Figure 33c.

Figure 34 shows the results of the cation analysis performed on the hydrating solution retrieved from free swell tests on the LPB and CB specimens performing using 50 mM, 100 mM and 500 mM NaCl, and 10 mM, 20 mM and 50 mM $CaCl_2$ solutions. The result shows the mass of Na^+ or Ca^{2+} in the supernatant (hydrating solution) relative to the initial mass of the Na^+ or Ca^{2+} in the test solution. The mass of cation was determined by multiplying the concentration of cation by the volume of the supernatant. As shown in Figure 34a and Figure 34b, the relative mass of Na^+ or Ca^{2+} in the hydrating solution of the LPB was consistently lower than the CB for all the test solutions, and supports the hypothesis that the polymer binds to some of the cations in the test solution making them unavailable to the bentonite during initial hydration. The results of the free swell tests coupled with cation analysis explains the observed chemical resistance and relatively lower hydraulic conductivity of the LPB GCL compared to the CB GCL shown in Figure 23 (also see Table 6).

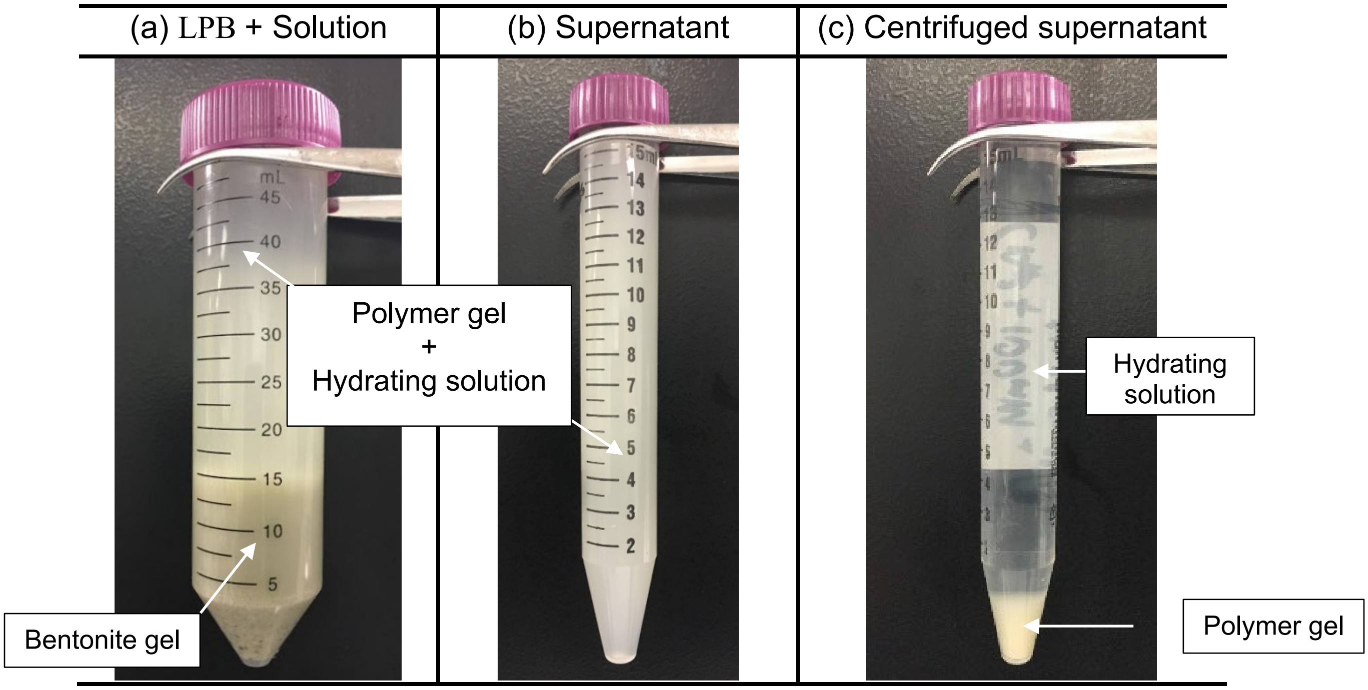
(a) LPB + Solution

(b) Supernatant

(c) Centrifuged supernatant

Figure 33. Method used to prepare the supernatant of the bentonite-polymer composite (BPC) specimens for cation analysis after free swell tests performed on 2 g of bentonite extracted from the PMB GCL using 50 mL of solution.

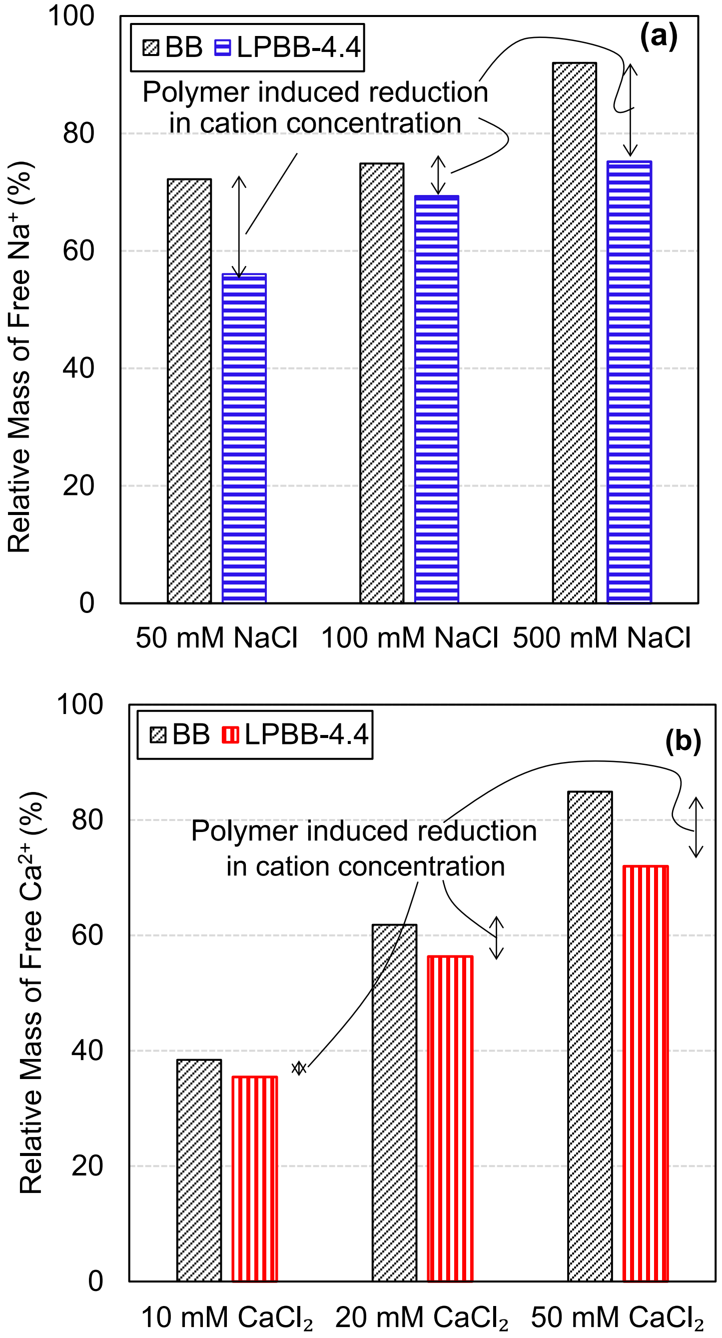

Figure 34. Results of cation analysis performed on supernatant retrieved from the flocculation tests performed by hydrating 2 g of conventional bentonite (CB) and bentonite-polymer composite (PBC) specimens in 50 mL of NaCl (a) or CaCl$_2$ (b) solutions of varying concentrations.

3 Summary and Conclusions

The first objective of this study was to develop new alternative index tests or criteria to predict the long-term hydraulic performance of the PMB GCLs. The second objective was to mechanistically understand how aggressive leachates like MSW-I ash leachate affect the performance of these second generation GCLs. This section showcases how these objectives of the study were achieved.

3.1 Effect of Specimen Preparation on Index Properties of Polymer-Modified Bentonite GCLs

The study presented in Section 2.1 (Section 2.1.1.1 and Section 2.1.1.2) of this report was conducted to investigate how specimen preparation (crushing and sieving) affects the swell index (SI) of PMB GCLs. SI tests were conducted on seven PMBs and the base sodium bentonite (Na-B) obtained from one GCL manufacturer using DI water. The PMBs contained granular Na-B dry blended with proprietary polymer. Based on information provided by the manufacturer, four of the PMBs contained linear polymer (water-soluble polymer), whereas the remaining three contained crosslinked polymer (superabsorbent polymer). The PMBs and Na-B were prepared using the ASTM standard method (D5890) and two alternative methods prior to SI testing. LOI tests were performed to estimate the polymer content of the prepared specimens.

Based on the results of the SI and LOI the following conclusions can be deduced:

1. There are limitations in application of the ASTM D5890 standard procedure for preparing specimens for SI testing, particularly for PMBs. For both the Na-B and PMBs used in the study, <100% of the specimen passed through the #100 sieve regardless of the amount of crushing performed using a mortar and pestle. For the Na-B, 0.2% of the initial mass of the specimen was retained on the #100 sieve, whereas up to ~4% of the specimen was retained on the #100 sieve for the PMBs.
2. The SI and LOI of the portion of the PMBs passing #100 sieve was comparable to that of the Na-B, whereas the portion retained on #100 sieve had high SI (~50 to 550 mL/2 g) and LOI (~40 to 84%). These observations indicate that grinding and sieving of the PMBs per the ASTM D5890 lead to segregation of polymer.

3. Alternative specimen preparation methods investigated in this study showed that unlike Na-B, crushing and sieving have significant influence on the SI of PMBs. However, the effect was more profound for PMBs containing crosslinked polymer due to the high swelling capacity of superabsorbent polymers.
4. The results of this study suggest that, in order to measure representative SI values for PMBs, SI tests should be performed using uncrushed polymerized bentonite received from the manufacturer or retrieved from the GCL.

3.2 Hydraulic Conductivity of Polymer-Modified Bentonite GCLs to MSW-I Ash Leachates

The study presented in Section 2.2 of this report was conducted to evaluate the hydraulic conductivity of PMB GCLs permeated with five synthetic MSW-I ash leachates with ionic strength ranging from 174 mM – 1978 mM, using DI water as a reference solution. Six PMB GCLs containing a dry blend of bentonite and proprietary polymers were used in this study. The polymers used in the PMB GCLs were classified to be either linear polymer (LP) or crosslinked polymer (CP) based on visual analysis of the swelling characteristics of specimens extracted from the GCLs. Bentonite extracted from PMB GCLs containing linear polymer (LPB GCLs) formed a viscous polymer-bentonite gel when hydrated whereas bentonite from PMB GCLs containing crosslinked polymer (CPB GCLs) formed a less-viscous bentonite gel with randomly distributed discrete polymer hydrogels. The polymer loading of the PMB GCLs ranged from 0.5 – 5.5% (by dry mass of the bentonite). Two CB GCLs (one from each GCL manufacturer) were also investigated for comparison. Hydraulic conductivity tests were conducted on GCL specimens hydrated and permeated with synthetic MSW-I ash leachate at average effective stress of 30 kPa – 39 kPa.

Based on the findings of the study, the following conclusions are drawn:

1. Hydraulic conductivity of the PMB GCLs permeated MSW-I ash leachates depends on the ionic strength of leachate, the polymer loading in the GCL as well as the type of polymer (i.e., whether the polymer is linear or crosslinked). The polymer loading

of PMB GCL can be verified by performing loss on ignition (LOI) test on extracted bentonite from the GCL, while a simple free swell test on the extracted bentonite can be used to identify the type of polymer as shown in this study.

2. PMB GCLs used in this study had hydraulic conductivity lower than 1.0×10^{-10} m/s when permeated with the MSW-I ash leachate with ionic strength of 174 mM (regardless of the polymer type or polymer loading), whereas the CB GCLs had hydraulic conductivity greater than 5.0×10^{-8} m/s when permeated with the same leachate.
3. However, all the PMB GCLs used in this study had hydraulic conductivity greater than 3.0×10^{-10} m/s when permeated with MSW-I ash leachate with ionic strength exceeding 600 mM.
4. Similar to CB GCLs, prehydrating PMB GCLs with water improves the compatibility of PMB GCLs to MSW-I ash leachates. Prehydration with water seem to improve the performance of PMB GCL with higher polymer loading.
5. The relationship between swell index (SI) and hydraulic conductivity of PMB GCLs, a strong correlation existed between SI and hydraulic conductivity of PMB GCLs when the PMB specimens used for the SI tests were not subjected to any form of crushing and sieving. Which suggests that SI (measured using polymerized bentonite retrieved from the GCL) can be used to assess the compatibility of PMB GCLs at least qualitatively to MSW-I ash leachates under low effective stress (< 40 kPa) during initial investigations.
6. At similar polymer loading, LPB GCLs have lower hydraulic conductivity than CPB GCLs when permeated with the same MSW-I ash leachate. This is because linear polymers dissolves and diffuse uniformly in the bentonite matrix, therefore are more efficient than crosslinked polymers in blocking flow during permeation.
7. However, polymer elutes from LPB GCLs during permeation, regardless of the chemistry of the permeant solution (i.e. whether permeated with DI water or MSW-I ash leachate). This is because, unlike crosslinked polymers, linear polymers are water-soluble, therefore, easily migrate with the leachate during permeation.

8. Polymer elution affected the hydraulic conductivity of the LPB GCLs used in this study when permeated with MSW-I ash leachates with ionic strength ≥ 622 mM but had small impact on hydraulic conductivity of the LPB GCLs permeated with the MSW-I ash leachate with ionic strength of 174 mM.
9. The results of this study also suggest that the polymer blockage mechanism previously hypothesized to control the hydraulic conductivity of PMB GCLs is only applicable to PMB GCLs containing crosslinked polymer because crosslinked polymers are water-insoluble therefore do not easily migrate with the permeating solution as linear polymers do.

3.3 Investigating Factors Influencing Polymer Elution and the Mechanism Controlling Chemical Compatibility of a Polymer-Modified Bentonite GCL containing linear Polymer

A study was conducted to investigate factors that influence polymer elution and the mechanism controlling chemical compatibility of PMB GCLs containing linear polymer (LPB GCLs) by performing a series of hydraulic conductivity and index tests on one commercially available LPB GCL using DI water, varying concentrations of NaCl and $CaCl_2$ solutions. The LPB GCL contained a blend of granular bentonite and proprietary linear polymer (with 4.4% polymer loading dry mass). Control tests were also conducted on a commercially available CB GCL from the same manufacturer, containing the same untreated bentonite and having the same GCL physical properties (geotextiles and bonding) as the LPB GCL. Polymer elution during permeation was quantified using the TOC concentration in the effluent samples collected during hydraulic conductivity testing of the LPB GCL. Physicochemical factors that affect polymer elution were investigated by performing viscosity tests on slurries of bentonite extracted from the LPB GCL and duplicate hydraulic conductivity tests on LPB GCL using varying average hydraulic gradient (at the same average effective stress).

Based on the findings of the study, the following conclusions are drawn:

1. The linear polymer gel eluted during permeation of the LPB GCL, regardless of the permeant chemistry (i.e. whether with DI water of salt solution). However, the rate at which polymer eluted and the effect of polymer elution had on the final hydraulic conductivity of the LPB GCL depended on the concentration and valence of the dominant cation in the permeant solution.
2. The rate at which polymer eluted from the LPB GCL increased with the cation valance and concentration of the dominant cation in the permeant solution. When permeated with $CaCl_2$ solutions, polymer eluted at a rate nineteen times faster than with the NaCl solutions. This is because divalent cations can contract the polymer chains by crosslinking the functional groups within a polymer chain and/or between individual polymer chains which consequently reduces the polymer ability to absorb water resulting in a lower viscosity polymer gel, which is less resistant to flow.
3. The rate at which polymer eluted also increased with the average hydraulic gradient used during permeation. However, hydraulic gradient did not have any impact of final hydraulic conductivity of the LPB GCL.
4. There was no correlation between the final hydraulic conductivity and the mass of polymer retained in the GCL. For instance, measured hydraulic conductivity of the LPB GCL specimen permeated with 500 mM NaCl was $\sim 1.4 \times 10^{-10}$ m/s, whereas hydraulic conductivity the specimen permeated with 2000 mM NaCl was $\sim 1.7 \times 10^{-8}$ m/s even though twice as much polymer eluted from the specimen permeated with 500 mM NaCl (487.7 mg) compared to the specimen permeated with 2000 mM NaCl (224.0 mg).
5. Moreover, hydraulic conductivity of the LPB GCL specimen permeated with 500 mM NaCl was more than two orders of magnitude lower than the specimen permeated with 500 mM $CaCl_2$ even though similar amount of polymer eluted from both specimens. This suggests that the same LPB GCL can have different hydraulic conductivities even when the same amount of polymer is retained in the GCL. this also implies that the improved chemical compatibility of the LPB GCL can be not attributed to previously hypothesized polymer blockage mechanism.

6. Free swell tests coupled with chemical analysis suggest that the chemical compatibility of the LPB GCL, is due to the ability of the polymer to scavenge cations from the solution, which allows the bentonite to undergo osmotic swelling during the initial hydration period. Analogous to the mechanism for improved hydraulic performance of CB GCLs prehdyrated with water, the dispersed structure of the bentonite fabric and the increase of adsorbed water molecules, attained during osmotic swelling, controls the long-term hydraulic conductivity of the LPB GCL (even after the polymer is eluted).

4 Materials and Methods

4.1 Geosynthetic Clay Liners

Six PMB GCLs were used in this study. The GCLs were supplied by two major manufacturers and contained a dry blend of granular Na-B and proprietary polymer(s).

Two CB GCLs (one from each manufacturer) containing only granular Na-B were also included in this study for comparison. For each independent GCL manufacturer, the PMB GCLs were manufactured using the same bentonite used in the CB GCL. Table 7 summarizes the properties of all the GCLs used in this study.

The polymers used in the PMB GCLs were broadly classified to be either linear polymer (LP) or crosslinked polymer (CP) based on information given by the manufacturers and visual analysis of the swelling characteristics of specimens extracted from the GCLs, even though the name of specific polymers were not disclosed by the manufacturers. The PMB GCLs used in this study are designated herein as LPBA-0.5, LPBA-1.5, LPBA-3.7, LPBB-4.4, CPBA-3.4, and CPBA-5.5, while the CB GCLs are designated as BA and BB. For the first letter(s) in the GCL designation, "B" denotes "bentonite", "LPB" denotes "linear polymer-bentonite", and "CPB" denotes "crosslinked polymer-bentonite", whereas the last letter indicates the manufacturer (A or B). The numerical suffix in the PMB GCL designation is the polymer loading (content). Based on information given by the manufacturers, all the CB GCLs and LPB GCLs commercially available, whereas the CPB GCLs are new line of products that are in the commercialization process. The intended industry application of each GCL is also reported in Table 7.

Table 7. Properties of GCLs used in this study

	Geosynthetic clay liners							
	Conventional		Bentonite-polymer composite					
Property	BA[a]	BB	LPBA-0.5[b]	LPBA-1.5	LPBA-3.7	LPBB-4.4	CPBA-3.4	CPBA-5.5
Upper geotextile	NW	NW	NW	NW	NW	NW	NW	NW
Carrier geotextile	W	SNW	NW	NW	NW	SNW	NW	NW
Reinforcement	NP	NP	NP	NP	NP	NP	NP	NP
Bentonite mass per unit area[c] (kg/m^2)	4.3	4.1	5.4	4.8	5.5	4.1	5.4	4.9
Initial thickness (mm)	6.3	6.3	8.1	6.6	8.0	6.4	7.6	7.8
Initial water content (%)	18.5	7.7	15.8	19.3	17.5	7.4	19.6	19.4
Median granule size, D_{50} (mm)	0.9	0.5	0.7	0.8	0.8	0.5	0.7	0.8
Loss on ignition[d] (%)	1.6	1.6	2.1	3.1	5.3	6.0	5.0	7.1
Polymer loading[e] (%)	-	-	0.5	1.5	3.7	4.4	3.4	5.5
Polymer type[f]	-	-	LP	LP	LP	LP	CP	CP
Intended industry application[g]	CON	CON	CAR	CLR	CLR	CAR	AL	AL

Note: NW = Nonwoven, SNW = Scrim nonwoven, W = Woven, NP = Needle-punched fibers, - = Not applicable, LP = Linear polymer, CP = Crosslinked polymer, CON =Conventional, CAR = Coal ash resistant, CLR = Chloride resistant, AL = Aggressive leachates

[a] In the GCL designation, the first letter(s) indicates: B = Bentonite, LPB = Linear polymer-bentonite, CPB = Crosslinked polymer-bentonite. And the last letter indicates the manufacturer (A or B)

[b] The numerical suffix in the bentonite-polymer composite GCL designation is the polymer loading in percent dry mass

[c] Determined following ASTM D5993

[d] Determined following ASTM D7348

[e] Estimated based on the loss on ignition (LOI) of bentonite-polymer composite after correcting for the LOI of the untreated bentonite

[f] Classified based on visual inspection of swelling characteristics of specimens hydrated with DI water

[g] Based on information provided by the GCL manufacturers

Loss on ignition (LOI) test is commonly used to quantify the polymer loading of bentonite-polymer composites (Scalia et al., 2014; Tian et al., 2016; Scalia and Benson, 2017; Chen et al., 2019; Tian et al., 2019; Wireko et al., 2020). Polymer loading of all the PMB GCLs used in this study was determined using LOI test performed in accordance with ASTM D7348. Specimens extracted from the PMB GCLs were first oven-dried to a constant mass at 105 ± 5 ^{0}C. The specimens then were ignited at 550 ± 5 ^{0}C for 4 h using a muffle furnace. During the LOI test, polymer additives were assumed to be the only constituents that are combusted completely. The average percent mass loss of three replicate specimens sampled from unique locations in the GCL was reported in Table 7 as the LOI. Polymer loading of the PMB GCLs was estimated using of the average LOI of the PMB specimen after correcting for the LOI of the bentonite fraction (i.e. LOI of the bentonite extracted from the CB GCLs). The LOI of the BA and BB reported in Table 7can be attributed to loss of strongly bound water and impurities such as calcite and organic matter (Scalia et al., 2014; Tian et al., 2016; Scalia and Benson, 2017; Tian et al., 2019; Wireko et al., 2020). In addition to the GCLs, manufacturer A also provided samples of the raw bentonite and bentonite-polymer composites used in making the GCLs and specified the measured LOI and polymer loading of the samples. The LOI and polymer loading of the samples matched that of the specimens extracted from the GCLs (reported in Table 7) and manufacturer specified LOI and polymer loading values.

Figure 35a-c shows images of swollen bentonite extracted from BA (no polymer), LPBA-3.4 (containing linear polymers) and CPBA-5.5 (containing crosslinked polymers) after performing a free swell test (ASTM D5890) on 2 g of the as-retrieved specimen (specimen not subjected to any crushing or sieving) using DI water (hydrating for 24 h). Unlike, the untreated bentonite from BA (which formed a non-viscous bentonite gel as shown in Figure 35a), bentonite extracted from PMB GCLs containing linear polymers (LPB GCLs) formed a viscous polymer-bentonite gel when hydrated (compare Figure 35b to Figure 35a). However, bentonite extracted from PMB GCLs containing crosslinked polymers (CPB GCLs) formed a non-viscous bentonite gel with randomly distributed discrete polymer hydrogels as shown Figure 35c. Based on information given by the manufactures, all the CB GCLs and LPB GCLs commercially available, whereas the CPB GCLs are new line of products that are in the commercialization process.

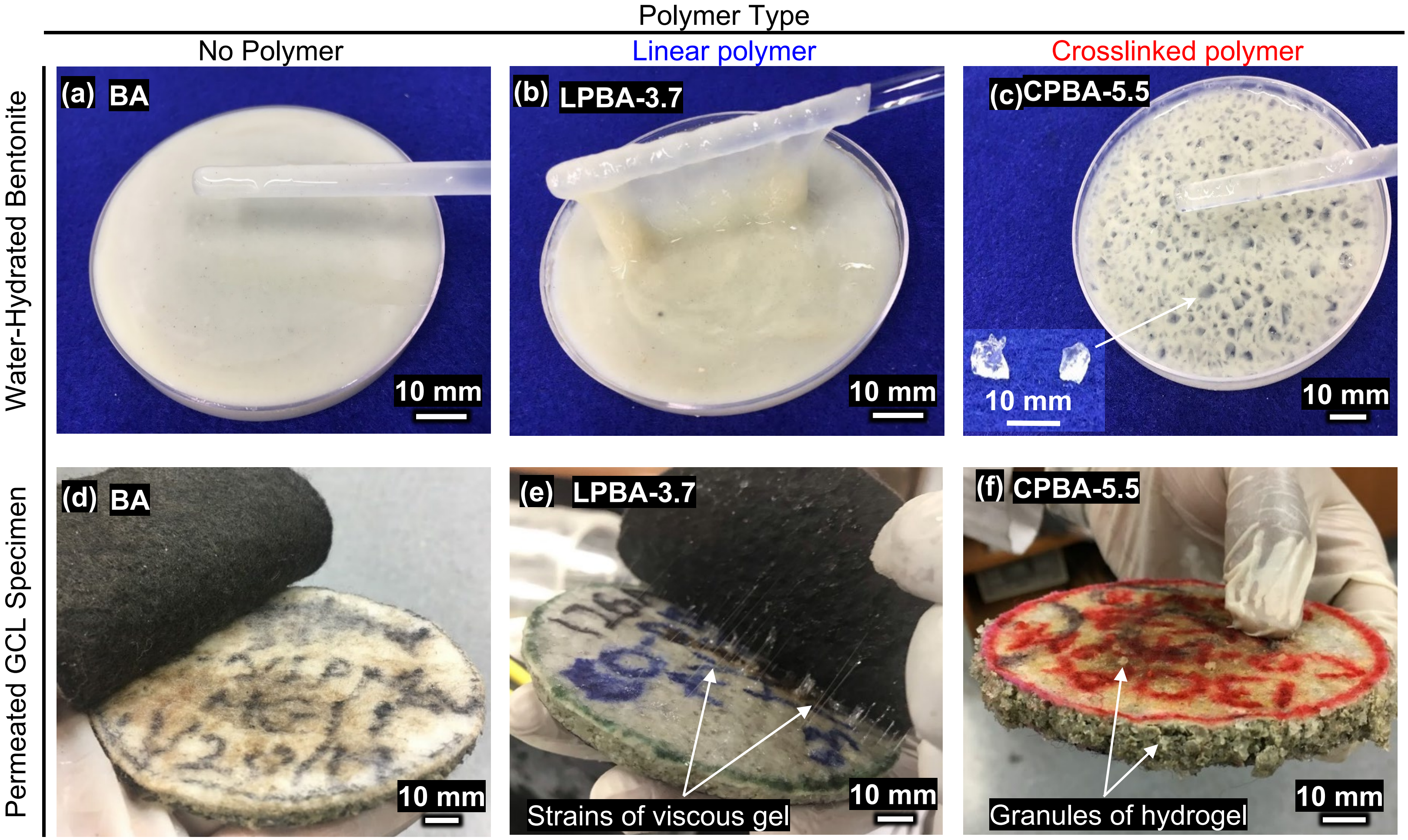

Figure 35. (a-c) Images of water-hydrated bentonite extracted from a conventional bentonite (CB) GCL or a bentonite-polymer composite (BPC) GCL containing linear polymers (LPB GCL) or a PMB GCL containing crosslinked polymers (CPB GCL) and (d-f) images of a CB or LPB or CPB GCL specimens permeated with synthetic incineration ash leachates [Note: The granules of hydrogel on top of the GCL in image (f) were manually extruded from the exposed peripheral of the GCL for visualization purpose. The numerical suffix in the PMB GCL designation is the polymer loading in percent dry mass].

The granule size distribution of bentonite extracted from the GCLs, shown in Figure 36, was obtained through mechanical sieve analysis following ASTM C136/C136M. Based on the Unified Soil Classification System (USCS), bentonite extracted from all the GCLs used in this study had granule size distribution similar to poorly graded sands (i.e. SP). However, the bentonite in the GCLs supplied by manufacturer "A" had a medium granule size (D_{50}) ranging from 0.7 – 0.9 mm, whereas bentonite from GCLs from manufacturer "B" had practically the same granule size distribution with a medium granule size (D_{50}) of 0.5 mm (see Table 7).

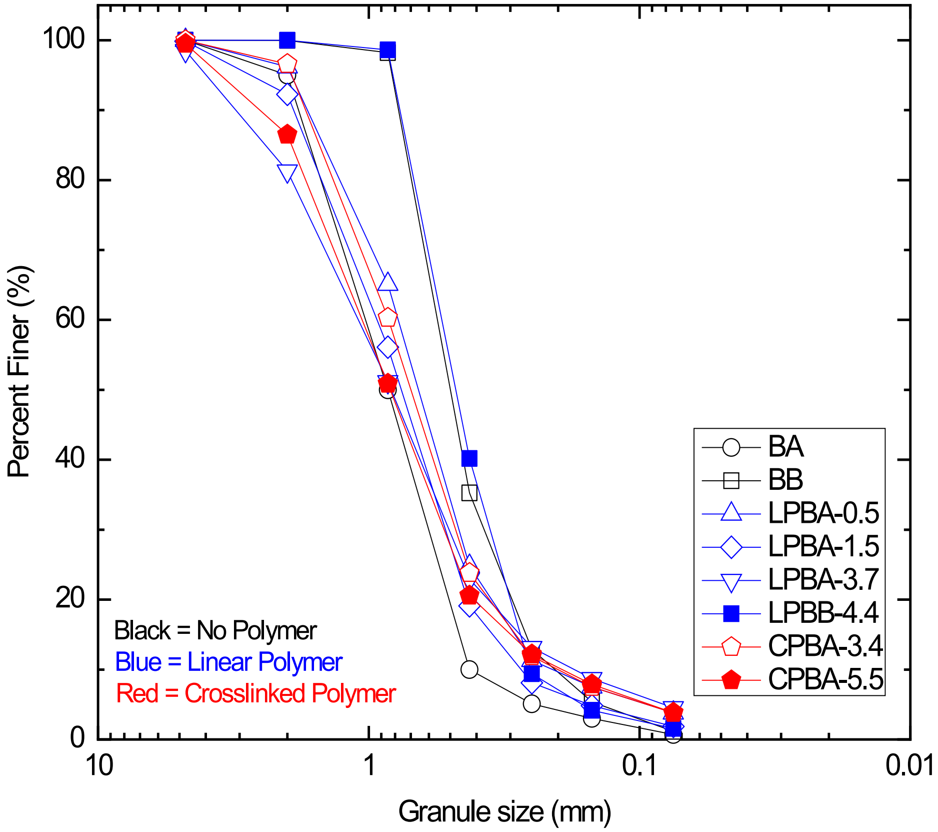

Figure 36. Granule-size distribution of conventional (in black) and bentonite-polymer composite (in color) GCLs (Note: In the GCL designation, the first letter(s) indicates: B = Bentonite, LPB = Linear polymer-bentonite, CPB = Crosslinked polymer-bentonite. The last letter in the GCL designation indicate the manufacturer (A or B), whereas the numerical suffix in the bentonite-polymer composite GCL designation is polymer loading in percent dry mass of bentonite).

4.2 MSW-I Ash Leachates

Five synthetic leachates were created for this study. The synthetic leachates were representative of landfills where MSW-I ash are either disposed alone (i.e. ash monofills) or co-disposed with MSW (i.e. co-disposal landfills). The chemical composition of the synthetic MSW-I ash leachate was determined based on chemical analysis of real MSW-I ash leachates collected and characterized by Li et al. (2019). The predominant cations in real MSW-I ash leachates are Na^+, K^+, and Ca^{2+}, whereas Cl^- is the predominant anion (Townsend et al., 2015; Moody and Townsend, 2017; Li et al., 2019). Therefore, for simplicity, Na^+ and Ca^{2+} were used to represent all monovalent and divalent cations respectively, while Cl^- was the only anion species considered in this study. This was considered conservative because, Tian et al. (2017) and Geng (2018) showed that unlike CB GCLs, solutions containing only Cl^- species have more adverse effect on the hydraulic conductivity of PMB GCLs than solutions containing a mixture Cl^- and other anion species like sulphate (SO_4^{-2}).

Two representative leachates were created for ash monofills (AM) landfills, and three were created for co-disposal (CD) landfills. A summary of the measured chemical properties of the synthetic MSW-I ash leachates used in this study are given Table 8. The target concentration of Na^+ and Ca^{2+} in the synthetic leachates was based on the minimum (MIN), average (AVG) or maximum (MAX) concentrations of monovalent and divalent cations of the overall leachate database for AM or CD leachates, whereas the target organic content of the synthetic leachates was based on measured AVG or MAX total organic carbon (TOC) concentration of AM or CD leachates in the database. The synthetic leachates were prepared by dissolving reagent grade powdered sodium chloride (NaCl) (≥ 99% pure, MilliporeSigma, St. Louis, Missouri), powdered calcium chloride dihydrate ($CaCl_2 \cdot 2H_2O$) (≥ 99% pure, MilliporeSigma, St. Louis, Missouri) in DI water. A technical grade powdered sodium humate (< 90% pure, MilliporeSigma, St. Louis, Missouri) was also added the synthetic leachates to present the TOC. The average carbon fraction of the sodium humate was estimated to be 45.5% (by mass) based on TOC measurements of sodium humate solutions prepared at different concentrations.

The concentrations of major cations in the MSW-I ash leachates were verified using microwave plasma atomic emission spectroscopy (MP-AES 4100, Agilent Technologies, Santa Clara, California), following the ion chromatographic method in Rice et al. (2012). And TOC of the synthetic leachates was measured using a Shimadzu TOC-VWS analyzer, following the APHA method 5310C in Rice et al. (2012). Samples of the synthetic leachates were filtered using 0.45 µm syringe filters before the cation and TOC measurement. Triplicate samples were used in the measurement and the average was reported. The electrical conductivity (EC) and pH of solutions were respectively measured using an Orion 4-cell EC probe (Thermo Fisher Scientific, Waltham, Massachusetts) and a pH sensor (Vernier Software and Technology, Beaverton, Oregon).

Table 8. Chemical properties of synthetic MSW-I ash leachates used in study

Designation	TOC[a] (mg/L)	Measured cation concentration (mM)				Cl^{-}[(b)] (mM)	pH	EC (S/m)	Ionic strength[c] (mM)	RMD[d] ($M^{0.5}$)
		Na^+	K^+	Ca^{2+}	Mg^{2+}					
CD-MIN	40	115.0	0.9	19.0	0.2	154.3	6.8	1.6	173.5	0.8
CD-AVG	40	360.0	0.8	87.0	0.2	535.2	6.1	4.9	622.4	1.2
CD-MAX	119	558.0	1.3	179.0	0.1	863.0	6.1	7.9	1096.6	1.3
AM-AVG	10	551.0	1.4	155.0	0.3	917.5	6.0	6.9	1018.3	1.4
AM-MAX	11	1220.0	2.4	251.7	0.2	1726.2	6.0	12.5	1978.1	2.4

Note: CD = Co-Disposal, AM = Ash monofill, MIN = minimum, AVG = Average, Max =Maximum, TOC = Total organic carbon, EC = Electrical conductivity, RMD = Relative abundance of monovalent and divalent cations in the solution

[a] Represented with a technical grade powdered sodium humate purchased from MilliporeSigma (St. Louis, Missouri)

[b] Estimated based on anion–cation charge balance

[c] Calculated as $I = 0.5 \sum c_i z_i^2$, where I is ionic strength, c_i and z_i are the concentration and the valance of the i-th ion respectively

[d] Calculated as $RMD = M_M / M_D^{0.5}$, where M_M is the total molarity of the monovalent cations and M_D is the total molarity of the divalent cations.

The ionic strength (I) of the MSW-I ash leachates given in Table 8 is calculated as $I = 0.5\ \sum c_i z_i^2$, where c_i and z_i are the concentration and the valance of the i-th ion respectively. Kolstad et al. (2004b) quantified the relative abundance of monovalent and divalent cations by the parameter RMD which is calculated as $RMD = M_M / M_D^{0.5}$, where M_M is the total molarity of the monovalent cations and M_D is the total molarity of the divalent cations.

Figure 37 shows the relationship between ionic strength and RMD of the synthetic leachates used in this study. Data of the MSW-I ash leachates characterized by Li et al. (2019) is also show in Figure 37 along with MSW-I ash leachate data from Ashmawy et al. (2002) and Townsend et al. (2015). MSW leachate data from Bradshaw and Benson (2014) and Townsend et al. (2015) are also plotted on Figure 37 for comparison. As shown in Figure 37, MSW-I ash leachates typically have ionic strength > 100 mM. The ionic strength of the synthetic AM leachates, i.e. AM-MAX and AM-AVG is ~1978 mM and ~1018 mM respectively. And ionic strength of the synthetic CD leachates, i.e. CD-MAX, CD-AVG, and CD-MIN is ~1097 mM, ~622 mM and ~174 mM respectively. The synthetic MSW-I ash leachates (in Table 8 and Figure 37) were classified as either MAX, AVG or MIN only based on ionic strength because all the leachates used in the study had ionic strength > 100 mM. Kolstad et al. (2004b) reported that ionic strength had a greater influence than RMD on hydraulic conductivity of CB GCLs permeated with leachates with ionic strength > 50 mM. Similarly, Chen et al. (2019) reported that for PMB GCLs permeated with CCP leachates with ionic strength ranging from 39.5 mM – 975 mM, ionic strength had a much greater impact on the hydraulic conductivity of the PMB GCLs as compared to RMD for the leachates with ionic strength > 50 mM.

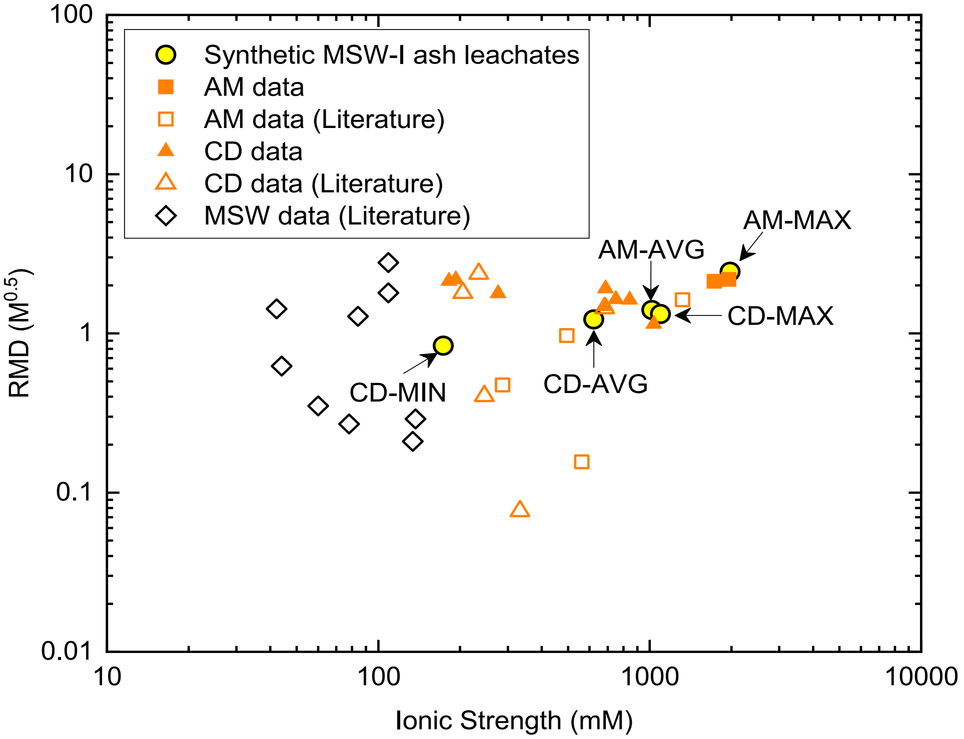

Figure 37. Relationship between RMD and ionic strength of synthetic MSW-I ash leachates used in the study [Note: RMD = Relative abundance of monovalent and divalent cations in the solution, MSW-I ash = MSW incineration ash, CD = Co-Disposal, AM = Ash monofill, MIN = minimum, AVG = Average, Max = Maximum, MSW = Municipal soil waste. AM and CD leachate data from Ashmawy et al. (2002) and Townsend et al. (2015). The classification of the synthetic MSW-I ash leachates as either MIN, AVG or MAX was based on the ionic strength of the leachates. MSW leachate data from Bradshaw and Benson (2014) and Townsend et al. (2015)].

4.3 Hydraulic Conductivity Tests

Hydraulic conductivity tests were conducted on the GCLs in flexible-wall permeameters using the falling headwater-constant tailwater method in ASTM D5084 and ASTM D6766. The permeameters used in this study had ⅛ in tubing and fittings. The GCL specimens were hydrated with tap water or MSW-I ash leachate for 48 h with the effluent line closed. After hydration, the GCLs were permeated with MSW-I ash leachate under an average effective stress of 30 – 39 kPa and average hydraulic gradient of 120 – 310 (depending on the final bulk GCL thickness). High hydraulic gradient (ranging from 50 up to 2800) is frequently used in hydraulic conductivity testing of both CB and PMB GCLs to shorten test duration (Daniel and Shan, 1993; Petrov and Rowe, 1997; Petrov et al., 1997a, b; Ruhl and Daniel, 1997; Shackelford et al., 2000; Shackelford et al., 2010; Tian et al., 2016; Chen et al., 2018; Tian et al., 2019; Zainab and Tian, 2020). Shackelford et al. (2000) showed that hydraulic conductivity of GCLs is not sensitive to hydraulic gradient. Gravity heads were used to apply cell pressure (20 kPa) and hydraulic gradient for long-term testing of the GCL specimen permeated with DI water.

No backpressure was applied during permeation to facilitate the collection of effluents for periodical electrical conductivity (EC) and pH measurements. Termination criteria for the hydraulic conductivity tests were defined according to the ASTM D6766. The hydraulic termination criteria require hydraulic conductivity to be steady and the ratio of outflow to inflow to be within in 1.0 ± 0.25, and chemical termination criteria require that the ratio of effluent to influent EC and pH to fall within 1.0 ± 0.1. All the tests met the hydraulic and chemical termination criteria except for LPBA-3.7 permeated with CD-MIN which is still ongoing and has not met the chemical equilibrium criteria due to low pore volume of flow (PVF). Hydraulic conductivity of the GCLs permeated with DI water was used as reference therefore chemical termination criteria were not deemed important for those specific tests.

4.4 Total Organic Carbon Analysis (Quantification of Polymer Elution)

Effluent from the hydraulic conductivity tests on the PMB GCLs containing linear polymers (LPB GCLs) was visually more viscous than the influent regardless of the chemistry of the permeant solution (i.e. whether permeated with DI water or MSW-I ash leachate), which indicated that polymer eluted from the LPB GCLs during permeation. Similar observations have been reported in the literature for PMB GCLs permeated with leachates and salts solutions (Tian et al., 2016; Tian and Benson, 2017; Tian et al., 2017; Chen et al., 2019; Tian et al., 2019). However, no visual evidence of polymer elution was observed during permeation of the PMB GCLs containing crosslinked polymers (CPB GCLs). Image of one LPB GCL specimen (LPBA-3.7) permeated with a synthetic MSW-I ash leachate is compared in Figure 35 with a CPB GCL specimen (CPBA-5.5) which has also been permeated synthetic MSW-I ash leachate. Image of one CB GCL specimen (BA) permeated with a synthetic MSW-I ash leachate is also shown in Figure 35 d for comparison. As shown Figure 35 e, there are strains of polymer gel between the surface of the LPB GCL specimen and the adjacent geotextile used for flow distribution, which indicates polymer elution. However, for the CPB GCL shown in Figure 35f, no such observed was made. This is because unlike linear polymers, crosslinked polymers are not completely water in soluble (compare Figure 35b and Figure 35 c), so do not migrate during permeation.

To quantify the total mass of polymer eluted from the PMB GCLs during permeation, the total organic carbon (TOC) concentration in each effluent sample was measured using a Shimadzu TOC-VWS analyzer in accordance with APHA method 5310C in Rice et al. (2012). Five calibration standard solutions were prepared by diluting 1000 mg/L anhydrous potassium hydrogen phthalate with DI water. Prior to analysis effluent samples were diluted 25 times in 40 mL glass vials to keep the carbon content within the range of the standard solutions. DI water was randomly place in between samples as check to ensure accuracy of measurements. The measured TOC concentration was corrected to account for the TOC concentration of the influent leachate. And the mass (in mg) of eluted polymer in the effluent sample was calculated as the product of the corrected TOC concentration (in mg/L) and the volume of effluent sample (in L).

4.5 Viscosity Tests

Linear or water-soluble polymers like Na-CMC, PAA and PAM used in polymer-modified bentonites and mixtures proposed for aggressive liquid applications have hydrophilic functional groups such as carboxylic acid and amide groups that have the ability to form coordination bonds, therefore making them soluble in aqueous media (Chatterji and Borchardt, 1981; Rivas et al., 2003; Williams, 2007; Kadajji and Betageri, 2011; Rivas et al., 2018). The conformation of the polymer chains of water-soluble polymers depends on the concentration and the valence of the predominant cation of hydrating liquid, and is directly related to viscosity of the polymer gel (Katchalsky, 1964; Mungan, 1972; Martin, 1975; Muller et al., 1979; Chatterji and Borchardt, 1981; Durst et al., 1981; Billmeyer, 1984; Huber, 1993; Peng and Wu, 1999; Schweins and Huber, 2001; Schweins et al., 2006).

Hence, to investigate the effect of cation valence and concentration on polymer elution, viscosity tests were conducted on bentonite slurries prepare by mixing bentonite extracted from the PMB or CB GCL with NaCl and $CaCl_2$ solutions. A Brookfield Digital Rheometer (Model DV-III+, AMETEK Brookfield, Middleborough, Massachusetts) was used to measure the apparent viscosity of PMB and CB slurries. The viscometer applies torque to rotate a spindle by a motor through a calibrated spring. The deflection of the spring measures the drag on the spindle. The slurries were prepared by gradually adding 20 g of air-dried PMB or CB (in increments of 1 g) to a plastic bottle already filled with 200 mL of the permeant solution and shaking vigorously until the slurry homogenized. No mechanical mixer was used to prevent break down of polymer chains. The slurries were aged for 24h and then shaken vigorously before viscosity was measured. The speed of the viscometer was fixed at 250 RPM and the spindle number was selected so the viscosity reading fall within 10–90% torque as recommended. All the viscosity measurements were performed at room temperature.

5 Acknowledgements

This material is based upon work supported by the Environmental Research and Education Foundation (EREF) and the Colloid Environmental Technologies Co. (CETCO). Any opinions, findings, and conclusions in this material are those of the authors and do not necessarily reflect the views of EREF and CETCO.

6 References

Allegrini, E., Vadenbo, C., Boldrin, A., Astrup, T.F., 2015. Life cycle assessment of resource recovery from municipal solid waste incineration bottom ash. *Journal of Environmental Management* 151, 132-143.

Ashmawy, A.K., El-Hajji, D., Sotelo, N., Muhammad, N., 2002. Hydraulic performance of untreated and polymer-treated bentonite in inorganic landfill leachates. *Clays and Clay Minerals* 50, 546-552.

Athanassopoulos, C., Benson, C.H., Donovan, M., Chen, J.N., 2015. Hydraulic conductivity of a polymer-modified GCL permeated with high-pH solutions. *Proceedings of the Geosynthetics Conference 2015*, Portland, Oregon, USA, Industrial Fabrics Association International, Roseville, MN, USA, pp. 181–186.

Behera, S., Mahanwar, P.A., 2020. Superabsorbent polymers in agriculture and other applications: a review. *Polymer-Plastics Technology and Materials* 59, 341-356.

Billmeyer, F.W., 1984. *Textbook of polymer science*, 3rd ed, Wiley, New York, USA.

Bonaparte, R., Daniel, D.E., Koerner, R.M., 2002. Assessment and recommendations for improving the performance of waste containment systems, Report No. EPA/600/R-02/099, *US Environmental Protection Agency*, Cincinnati, OH.

Bradshaw, S.L., Benson, C.H., 2014. Effect of municipal solid waste leachate on hydraulic conductivity and exchange complex of geosynthetic clay liners. *Journal of Geotechnical and Geoenvironmental Engineering* 140, 1-17.

Bradshaw, S.L., Benson, C.H., Rauen, T.L., 2016. Hydraulic conductivity of geosynthetic clay liners to recirculated municipal solid waste leachates. *Journal of Geotechnical and Geoenvironmental Engineering* 142, 1-12.

Buchholz, F.L., Graham, A.T., 1998. *Modern superabsorbent polymer technology* 152, Wiley New York, USA.

Chai, J.C., Prongmanee, N., 2020. Barrier properties of a geosynthetic clay liner using polymerized sodium bentonite. *Geotextiles and Geomembranes* 48, 392-399.

Chandler, A.J., Eighmy, T.T., Hjelmar, O., Kosson, D., Sawell, S., Vehlow, J., Van der Sloot, H., Hartlén, J., 1997. *Municipal solid waste incinerator residues*. Studies in Environmental Science 67, Elsevier, Amsterdam, Netherlands.

Chatterji, J., Borchardt, J.K., 1981. Applications of water-soluble polymers in the oil field. *SPE-9288-PA* 33, 2042-2056.

Chen, J., 2015. Compatibility of geosynthetic clay liners with leachate from CCP management facilities. PhD Dissertation. University of Wisconsin-Madison.

Chen, J.N., Benson, C.H., Edil, T.B., 2018. Hydraulic conductivity of geosynthetic clay liners with sodium bentonite to coal combustion product leachates. *Journal of Geotechnical and Geoenvironmental Engineering* 144, 1-12.

Chen, J.N., Salihoglu, H., Benson, C.H., Likos, W.J., Edil, T.B., 2019. Hydraulic conductivity of bentonite-polymer composite geosynthetic clay liners permeated with coal combustion product leachates. *Journal of Geotechnical and Geoenvironmental Engineering* 145, 1-12.

Daniel, D.E., Shan, H.Y., 1993. Effects of partial wetting on the performance of the bentonite component of a geosynthetic clay liner. *Proceedings of the Geosynthetics*

93, St. Paul, MN, USA, Industrial Fabrics Association International, Vancouver, BC, Canada, pp. 1482-1496.

Daniel, D.E., Bowders, J.J., Gilbert, R.B., 1997. Laboratory hydraulic conductivity testing of GCLs in flexible-wall permeameters, in: Well, L.W. (Ed.), *Testing and Acceptance Criteria for Geosynthetic Clay Liners*. ASTM International, West Conshohocken, PA, USA, pp. 208-229.

Di Emidio, G., Mazzieri, F., Van Impe, W., 2008. Hydraulic conductivity of a dense prehydrated GCL: impact of free swell and swelling pressure. *Proceedings of the 4th European Geosynthetics Conference*, Golder Associates.

Di Emidio, G., 2010. Hydraulic and chemico-osmotic performance of polymer treated clays. PhD Thesis. Ghent University, Ghent, Belgium.

Di Emidio, G., Van Impe, W., Flores, R.V., 2011. Advances in geosynthetic clay liners: polymer enhanced clays. *Proceedings of the Geo-Frontiers 2011: Advances in geotechnical engineering*, Dallas, TX, USA, ASCE, Reston, VA, USA, pp. 1931-1940.

Donovan, M.S., Valorio, R., Gebka, B., 2017. Polymer enhanced geosynthetic clay liners for bauxite storage. *Proceedings of the 35th International ICSOBA Conference*, Hamburg, Germany, ICSOBA Travaux, Quebec, Canada, pp. 469-478.

Dou, X., Ren, F., Nguyen, M.Q., Ahamed, A., Yin, K., Chan, W.P., Chang, V.W.-C., 2017. Review of MSWI bottom ash utilization from perspectives of collective characterization, treatment and existing application. *Renewable and Sustainable Energy Reviews* 79, 24-38.

Durst, F., Haas, R., Kaczmar, B.U., 1981. Flows of dilute hydrolyzed polyacrylamide solutions in porous media under various solvent conditions. *Journal of Applied Polymer Science* 26, 3125-3149.

Egloffstein, T.A., 2001. Natural bentonites—influence of the ion exchange and partial desiccation on permeability and self-healing capacity of bentonites used in GCLs. *Geotextiles and geomembranes* 19, 427-444.

Fan, R.D., Reddy, R.K., Yang, Y.L., Du, Y.J., 2020. Index properties, hydraulic conductivity and contaminant-compatibility of CMC-treated sodium activated calcium bentonite. *International Journal of Environmental Research and Public Health* 17, 1-18.

Fina, A., Camino, G., 2011. Ignition mechanisms in polymers and polymer nanocomposites. *Polymers for Advanced Technologies* 22, 1147-1155.

Geng, W., 2018. Assessing the performance of polymer-bentonite mixtures for hydraulic barrier applications. PhD Dissertation. University of Wisconsin-Madison.

Grim, R.E., Guven, N., 1978. *Bentonites: geology, mineralogy, properties, and uses*. Developments in sedimentology 24, Elsevier, Amsterdam, The Netherlands.

Guler, E., Ozhan, H.O., Karaoglu, S., 2018. Hydraulic performance of anionic polymer-treated bentonite-granular soil mixtures. *Applied Clay Science* 157, 139-147.

Guyonnet, D., Touze-Foltz, N., Norotte, V., Pothier, C., Didier, G., Gailhanou, H., Blanc, P., Warmont, F., 2009. Performance-based indicators for controlling geosynthetic clay liners in landfill applications. *Geotextiles and Geomembranes* 27, 321-331.

Huber, K., 1993. Calcium-induced shrinking of polyacrylate chains in aqueous solution. *The Journal of Physical Chemistry* 97, 9825-9830.

Jo, H.Y., Katsumi, T., Benson, C.H., Edil, T.B., 2001. Hydraulic conductivity and swelling of nonprehydrated GCLs permeated with single-species salt solutions. *Journal of Geotechnical and Geoenvironmental Engineering* 127, 557-567.

Jo, H.Y., Benson, C.H., Edil, T.B., 2004. Hydraulic conductivity and cation exchange in non-prehydrated and prehydrated bentonite permeated with weak inorganic salt solutions. *clays and clay minerals* 52, 661-679.

Jo, H.Y., Benson, C.H., Shackelford, C.D., Lee, J.M., Edil, T.B., 2005. Long-term hydraulic conductivity of a geosynthetic clay liner permeated with inorganic salt solutions. *Journal of Geotechnical Geoenvironmental Engineering* 131, 405-417.

Joseph, A.M., Snellings, R., Van den Heede, P., Matthys, S., De Belie, N., 2018. The use of municipal solid waste incineration ash in various building materials: A Belgian point of view. *Materials (Basel, Switzerland)* 11, 1-30.

Kadajji, V.G., Betageri, G.V., 2011. Water soluble polymers for pharmaceutical applications. *Polymers* 3, 1972-2009.

Katchalsky, A., 1964. Polyelectrolytes and their biological interactions. *Biophysical journal* 4, 9-41.

Katsumi, T., Onikata, M., Hasegawa, S., Lin, L., Kondo, M., Kamon, M., 2001. Chemical compatibility of modified bentonite permeated with inorganic chemical solutions. *Proceedings of the Third Geoenvironmental Engineering Conference: Geoenvironmental Impact Management*, Edinburgh, UK, Thomas Telford Publishing, London, UK, pp. 419-424.

Katsumi, T., Ogawa, A., Fukagawa, R., 2004. Effect of prehydration on hydraulic performance of geosynthetic clay liners permeated with inorganic chemical solutions. *Proceedings of the The third Asian Regional Conference on Geosynthetics: Now adn Future of Geosynthetics in Civil Engineering*, Seoul, Korea, pp. 937-944.

Katsumi, T., Ishimori, H., Ogawa, A., Yoshikawa, K., Hanamoto, K., Fukagawa, R., 2007. Hydraulic conductivity of nonprehydrated geosynthetic clay liners permeated with inorganic solutions and waste leachates. *Soils Foundations* 47, 79-96.

Katsumi, T., Ishimori, H., Onikata, M., Fukagawa, R., 2008. Long-term barrier performance of modified bentonite materials against sodium and calcium permeant solutions. *Geotextiles and Geomembranes* 26, 14-30.

Koerner, R.M., 2012. *Designing with geosynthetics*, 5th ed, Pearson Prentice Hall, New Jersey, USA.

Kolstad, D.C., Benson, C.H., Edil, T.B., Jo, H.Y., 2004a. Hydraulic conductivity of a dense prehydrated GCL permeated with aggressive inorganic. *Geosynthetics International* 11, 233-241.

Kolstad, D.C., Benson, C.H., Edil, T.B., 2004b. Hydraulic conductivity and swell of nonprehydrated geosynthetic clay liners permeated with multispecies inorganic solutions. *Journal of Geotechnical and Geoenvironmental Engineering* 130, 1236-1249.

Lam, C.H.K., Ip, A.W.M., Barford, J.P., McKay, G., 2010. Use of Incineration MSW Ash: A Review. *Sustainability* 2, 1943-1968.

Lee, J.M., Shackelford, C.D., Benson, C.H., Jo, H.Y., Edil, T.B., 2005. Correlating index properties and hydraulic conductivity of geosynthetic clay liners. *Journal of Geotechnical and Geoenvironmental Engineering* 131, 1319-1329.

Lee, J.M., Shackelford, C.D., 2005. Impact of bentonite quality on hydraulic conductivity of geosynthetic clay liners. *Journal of Geotechnical and Geoenvironmental Engineering* 131, 64-77.

Lee, W.F., Wu, R.J., 1996. Superabsorbent polymeric materials. I. Swelling behaviors of crosslinked poly(sodium acrylate-co-hydroxyethyl methacrylate) in aqueous salt solution. *Journal of Applied Polymer Science* 62, 1099-1114.

Li, L., Tang, Y., Abichou, T., Higgs, B., Wireko, C., Li, R., 2019. Characterization of leachates from landfills containing MSW-I residues. *Journal of Hazardous, Toxic, and Radioactive Waste* 23, 1-12.

Mahon, R., Balogun, Y., Oluyemi, G., Njuguna, J., 2019. Swelling performance of sodium polyacrylate and poly(acrylamide-co-acrylic acid) potassium salt. *SN Applied Sciences* 2, 1-15.

Martin, F.D., 1975. The Effect of Hyrolysis of Polyacrylamide on Solution viscosity, Polymer Retention and Flow Resistance Properties. *Proceedings of the SPE Rocky Mountain Regional Meeting*, Denver, Colorado, Society of Petroleum Engineers, SPE, pp. 8.

McBride, M.B., 1994. *Environmental chemistry of soils*, Oxford University Press, New York, USA.

McRory, J., Ashmawy, A., 2005. Polymer treatment of bentonite clay for contaminant resistant barriers. *Proceedings of the Geo-Frontiers 2005: Waste containment and remediation*, Austin, TX, USA, ASCE, Reston, VA, USA, pp. 1-11.

Mesri, G., Olson, R.E., 1971. Mechanisms controlling the permeability of clays. *Clays and Clay Minerals* 19, 151-158.

Moody, C.M., Townsend, T.G., 2017. A comparison of landfill leachates based on waste composition. *Waste Manag* 63, 267-274.

Moreno-Villoslada, I., Rivas, B.L., 2002. Competition of divalent metal ions with monovalent metal ions on the adsorption on water-soluble polymers. *The Journal of Physical Chemistry B* 106, 9708-9711.

Moreno-Villoslada, I., Rivas, B.L., 2003. Retention of metal ions in ultrafiltration of mixtures of divalent metal ions and water-soluble polymers at constant ionic strength based on Freundlich and Langmuir isotherms. *Journal of Membrane Science* 215, 195-202.

Mukherjee, S., Mukhopadhyay, S., Zafri, M.Z.B., Zhan, X., Hashim, M.A., Sen Gupta, B., 2018. Application of guar gum for the removal of dissolved lead from wastewater. *Industrial Crops and Products* 111, 261-269.

Muller, G., Laine, J.P., Fenyo, J.C., 1979. High-molecular-weight hydrolyzed polyacrylamides. I. Characterization. Effect of salts on the conformational properties. *Journal of Polymer Science: Polymer Chemistry Edition* 17, 659-672.

Mungan, N., 1972. Shear Viscosities of Ionic Polyacrylamide Solutions. *SPE-3521-PA* 12, 469-473.

Norrish, K., 1954. The swelling of montmorillonite. *Discussions of the Faraday society* 18, 120-134.

Oehmig, W.N., Roessler, J.G., Blaisi, N.I., Townsend, T.G., 2015. Contemporary practices and findings essential to the development of effective MSWI ash reuse policy in the United States. *Environmental Science & Policy* 51, 304-312.

Olphen, H.v., 1963. *An introduction to clay colloid chemistry: for clay technologists, geologists, and soil scientists*, Interscience Publishers, New York, USA.

Olphen, H.V., 1977. *An introduction to clay colloid chemistry*, Wiley, New York, USA.

Olsta, J.T., Chung, J.H., Daniel, D.E., 2004. Various aspects of sodium bentonite testing, in: Mackey, R.E., von, K.M. (Eds.), *Advances in geosynthetic clay Liner technology: 2nd symposium*. ASTM International, West Conshohocken, PA, USA, pp. 3-10.

Onikata, M., Kondo, M., Kamon, M., 1996. Development and characterization of a multiswellable bentonite. *Proceedings of the Second International Congress on Environmental Geotechnics*, Osaka, Japan Taylor and Francis, Boca Raton, FL, USA, pp. 587-590.

Onikata, M., Kondo, M., Hayashi, N., Yamanaka, S., 1999. Complex formation of cation-exchanged montmorillonites with propylene carbonate: Osmotic swelling in aqueous electrolyte solutions. *Clays and Clay Minerals* 47, 672-677.

Oren, A.H., Aksoy, Y.Y., Onal, O., Demirkiran, H., 2018. Correlating the hydraulic conductivities of GCLs with some properties of bentonites. *Geomechanics and Engineering* 15, 1091-1100.

Ozhan, H.O., 2018. Effects of Temperature Increase in 0.5 M MgCl2 Solution on Hydraulic Capability of Anionic Polymer–Treated Geosynthetic Clay Liners Used as Barriers. *Journal of Environmental Engineering* 144, 1-11.

Pandey, M.R., Badiger, S., Sivakumar Babu, G.L., 2019. Effects of bentonite and polymer soil amendment on contaminant transport parameters. *Journal of Hazardous, Toxic, and Radioactive Waste* 23, 1-11.

Peng, S., Wu, C., 1999. Light Scattering Study of the Formation and Structure of Partially Hydrolyzed Poly(acrylamide)/Calcium(II) Complexes. *Macromolecules* 32, 585-589.

Petrov, R.J., 1995. Swelling and compatibility characteristics of a geosynthetic clay liner. Master of Science Thesis. University of Western Ontario.

Petrov, R.J., Rowe, R.K., Quigley, R.M., 1997a. Selected factors influencing GCL hydraulic conductivity. *Journal of Geotechnical and Geoenvironmental Engineering* 123, 683-695.

Petrov, R.J., Rowe, R.K., Quigley, R.M., 1997b. Comparison of laboratory-measured GCL hydraulic conductivity based on three permeameter types. *Geotechnical Testing Journal* 20, 49-62.

Petrov, R.J., Rowe, R.K., 1997. Geosynthetic clay liner (GCL)-chemical compatibility by hydraulic conductivity testing and factors impacting its performance. *Canadian Geotechnical Journal* 34, 863-885.

Prongmanee, N., Chai, J.C., Shen, S., 2018. Hydraulic Properties of Polymerized Bentonites. *Journal of Materials in Civil Engineering* 30, 1-10.

Prongmanee, N., Chai, J.C., 2019. Performance of geosynthetic clay liner with polymerized bentonite in highly acidic or alkaline solutions. *International Journal of Geosynthetics and Ground Engineering* 5, 1-12.

Qian, X., Koerner, R.M., Gray, D.H., 2001. *Geotechnical aspects of landfill construction and design*, Prentice Hall, New Jersey, USA.

Razakamanantsoa, A.R., Barast, G., Djeran-maigre, I., 2012. Hydraulic performance of activated calcium bentonite treated by polyionic charged polymer. *Applied Clay Science* 59-60, 103-114.

Razakamanantsoa, A.R., Djeran-Maigre, I., 2016. Long term chemo-hydro-mechanical behavior of compacted soil bentonite polymer complex submitted to synthetic leachate. *Waste Manag* 53, 92-104.

Reybrock, W., 2018. Methods for Testing the Effect of Hydraulic Gradient on the Polymer Elution of Polymer GCLs. Master of Science. University of Wisconsin-Madison

Rice, E.W., Bridgewater, L., Eston, A.D., Clesceri, L.S., 2012. *Standard Methods for the Examination of Water and Wastewater*, 22nd ed, American Public Health Association, Washington D.C., USA.

Rivas, B.L., Moreno-Villoslada, I., 2000. Effect of the Polymer Concentration on the Interactions of Water-Soluble Polymers with Metal Ions. *Chemistry Letters* 29, 166-167.

Rivas, B.L., Pereira, E.D., Moreno-Villoslada, I., 2003. Water-soluble polymer–metal ion interactions. *Progress in Polymer Science* 28, 173-208.

Rivas, B.L., Aguirre, M.d.C., 2007. Arsenite retention properties of water-soluble metal–polymers. *Journal of Applied Polymer Science* 106, 1889-1894.

Rivas, B.L., Pereira, E., Maureira, A., 2009. Functional water-soluble polymers: polymer–metal ion removal and biocide properties. *Polymer International* 58, 1093-1114.

Rivas, B.L., Pereira, E.D., Palencia, M., Sánchez, J., 2011. Water-soluble functional polymers in conjunction with membranes to remove pollutant ions from aqueous solutions. *Progress in Polymer Science* 36, 294-322.

Rivas, B.L., Urbano, B.F., Sánchez, J., 2018. Water-Soluble and Insoluble Polymers, Nanoparticles, Nanocomposites and Hybrids With Ability to Remove Hazardous Inorganic Pollutants in Water. *Frontiers in Chemistry* 6, 1-13.

Rosin-Paumier, S., Touze-Foltz, N., Pantet, A., Monnet, P., Didier, G., Guyonnet, D., Norotte, V., 2010. Swell index, oedopermeametric, filter press and rheometric tests for identifying the qualification of bentonites used in GCLs. *Geosynthetics International* 17, 1-11.

Rowe, R.K., 2020. Geosynthetic clay liners: Perceptions and misconceptions. *Geotextiles and Geomembranes* 48, 137-156.

Ruhl, J.L., Daniel, D.E., 1997. Geosynthetic clay liners permeated with chemical solutions and leachates. *Journal of Geotechnical and Geoenvironmental Engineering* 123, 369-381.

Sabbas, T., Polettini, A., Pomi, R., Astrup, T., Hjelmar, O., Mostbauer, P., Cappai, G., Magel, G., Salhofer, S., Speiser, C., Heuss-Assbichler, S., Klein, R., Lechner, P., 2003. Management of municipal solid waste incineration residues. *Waste Management* 23, 61-88.

Salemi, N., Abtahi, S.M., Rowshanzamir, M., Hejazi, S.M., 2018. Geosynthetic clay liners: Effect of structural properties and additives on hydraulic performance and durability. *Environmental Earth Sciences* 77, 1-13.

Salihoglu, H., 2015. Behavior of polymer-modified bentonites with aggressive leachates. Master of Science. University of Wisconsin-Madison

Salihoglu, H., Chen, J.N., Likos, W.J., Benson, C.H., 2016. Hydraulic conductivity of bentonite-polymer geosynthetic clay liners in coal combustion product leachates. *Proceedings of the Geo-Chicago 2016: Sustainable Geoenvironmental Systems*, Chicago, IL, USA, ASCE, Reston, VA, USA, pp. 438-447.

Sato, K., Barast, G., Razakamanantsoa, A.R., Djeran-Maigre, I., Katsumi, T., Levacher, D., 2017. Comparison of prehydration and polymer adding effects on Na activated Ca-bentonite by free swell index test. *Applied Clay Science* 142, 69-80.

Scalia, J., Benson, C.H., Bohnhoff, G.L., Edil, T.B., Shackelford, C.D., 2014. Long-term hydraulic conductivity of a bentonite-polymer composite permeated with aggressive inorganic solutions. *Journal of Geotechnical and Geoenvironmental Engineering* 140, 1-13.

Scalia, J., Benson, C.H., 2016. Evaluation of Na-Bentonite-polyacrylte mixtures to enhance the chemical resistance of geosynthetic clay liners. *Proceedings of the Geo-Chicago 2016: Sustainable Geoenvironmental Systems*, Chicago, IL, USA, ASCE, Reston, VA, USA, pp. 388-397.

Scalia, J., Benson, C.H., 2017. Polymer fouling and hydraulic conductivity of mixtures of sodium bentonite and a bentonite-polymer composite. *Journal of Geotechnical and Geoenvironmental Engineering* 143, 1-13.

Scalia, J., Bohnhoff, G.L., Shackelford, C.D., Benson, C.H., Sample-Lord, K.M., Malusis, M.A., Likos, W.J., 2018a. Enhanced bentonites for containment of inorganic waste leachates by GCLs. *Geosynthetics International* 25, 392-411.

Scalia, J., Benson, C.H., Finnegan, M., 2018b. Alternate procedures for swell Index testing of granular bentonite from GCLs. *Geotechnical Testing Journal* 42, 1169-1184.

Schweins, R., Huber, K., 2001. Collapse of sodium polyacrylate chains in calcium salt solutions. *The European Physical Journal E* 5, 117-126.

Schweins, R., Goerigk, G., Huber, K., 2006. Shrinking of anionic polyacrylate coils induced by Ca2+, Sr2+ and Ba2+: A combined light scattering and ASAXS study. *European Physical Journal E -- Soft Matter* 21, 99-110.

Setz, M.C., Tian, K., Benson, C.H., Bradshaw, S.L., 2017. Effect of ammonium on the hydraulic conductivity of geosynthetic clay liners. *Geotextiles and Geomembranes* 45, 665-673.

Shackelford, C.D., Benson, C.H., Katsumi, T., Edil, T.B., Lin, L., 2000. Evaluating the hydraulic conductivity of GCLs permeated with non-standard liquids. *Geotextiles and Geomembranes* 18, 133-161.

Shackelford, C.D., Sevick, G.W., Eykholt, G.R., 2010. Hydraulic conductivity of geosynthetic clay liners to tailings impoundment solutions. *Geotextiles and Geomembranes* 28, 149-162.

Shen, S.Q., Du, Y.J., Wang, F., Ren, W.W., 2016. Hydraulic conductivity of polymer modified bentonite filter cakes in calcium chloride solutions. *Proceedings of the Geo-Chicago 2016: Sustainable Geoenvironmental Systems*, Chicago, IL, USA, ASCE, Reston, VA, USA, pp. 428-437.

Tian, K., Benson, C.H., Likos, W.J., 2016. Hydraulic conductivity of geosynthetic clay liners to low-level radioactive waste leachate. *Journal of Geotechnical and Geoenvironmental Engineering* 142, 1-12.

Tian, K., Benson, C.H., 2017. Chemical compatibility of geosynthetic clay liners to aggressive bauxite liquor. *Proceedings of the 35th International ICSOBA Conference*, Hamburg, Germany, ICSOBA Travaux, Quebec, Canada, pp. 479-484.

Tian, K., Benson, C.H., Likos, W.J., 2017. Effect of an anion ratio on the hydraulic conductivity of a bentonite-polymer geosynthetic clay liner. *Proceedings of the Geotechnical Frontiers 2017*, Orlando, FL, USA, ASCE, Reston, VA, USA, pp. 180-189.

Tian, K., Likos, W.J., Benson, C.H., 2019. Polymer elution and hydraulic conductivity of bentonite-polymer composite geosynthetic clay liners. *Journal of Geotechnical and Geoenvironmental Engineering* 145, 1-12.

Townsend, T.G., Meeroff, D.E., Darioosh, R., Moody, C., Wally, J., 2015. Assessing options for on-site leachate management at Florida landfills, Report, *Hinkley Center for Solid and Hazardous Waste Management*.

Vasko, S., Jo, H.Y., Benson, C.H., Edil, T.B., Katsumi, T., 2001. Hydraulic conductivity of partially prehydrated geosynthetic clay liners permeated with aqueous calcium chloride solutions. *Proceedings of the Geosynthetics Conference 2001*, Portland, OR, USA, Industrial Fabrics Association International, Roseville, MN, USA, pp. 685-699.

Wang, B., Xu, J., Chen, B., Dong, X., Dou, T., 2019. Hydraulic conductivity of geosynthetic clay liners to inorganic waste leachate. *Applied Clay Science* 168, 244-248.

Williams, P.A., 2007. *Handbook of industrial water soluble polymers*, Blackwell Publishing Ltd, Oxford, UK.

Wireko, C., Zainab, B., Tian, K., Abichou, T., 2020. Effect of specimen preparation on the swell index of bentonite-polymer GCLs. *Geotextiles and Geomembranes*.

Xia, Y., Zhang, H., Phoungthong, K., Shi, D.X., Shen, W.H., Shao, L.M., He, P.J., 2015. Leaching characteristics of calcium-based compounds in MSWI Residues: From the viewpoint of clogging risk. *Waste Management* 42, 93-100.

Xu, X., Liu, X., Oh, M., Park, J., 2018. Swelling Capacity and Hydraulic Conductivity of Polymer-Modified Bentonite under Saline Water Conditions. *Applied Sciences* 8.

Yu, C., Liao, R., Cai, X., Yu, X., 2019. Sodium polyacrylate modification method to improve the permeant performance of bentonite in chemical resistance. *Journal of Cleaner Production* 213, 242-250.

Zainab, B., Tian, K., 2020. Hydraulic conductivity of bentonite-polymer geosynthetic clay liners to coal combustion product leachates. *Proceedings of the Geo-Congress 2020: Engineering, Monitoring, and Management of Geotechnical Infrastructure*, Minneapolis, MN, USA, ASCE, Reston, VA, USA, pp. 579-586.

Zhu, Q., Barney, C.W., Erk, K.A., 2014. Effect of ionic crosslinking on the swelling and mechanical response of model superabsorbent polymer hydrogels for internally cured concrete. *Materials and Structures* 48, 2261-2276.

Zohuriaan-Mehr, M.J., Kabiri, K., 2008. Superabsorbent polymer materials: a review. *Iranian polymer journal* 17, 451-477.

7 Appendices: List of Publications and Conference Presentations

7.1 Publications

Wireko, C., Zainab, B., Tian, K., Abichou, T., 2020. Effect of specimen preparation on the swell index of bentonite-polymer GCLs. *Geotextiles and Geomembranes* https://doi.org/10.1016/j.geotexmem.2020.06.006.

Wireko, C., Abichou, T., Tian, K., Zainab, B., Zhang Z., 2020. Effect of Incineration Ash Leachates on the Hydraulic Conductivity of Bentonite-Polymer Composite Geosynthetic Clay Liners. *Waste Management* (Under Review)

Wireko, C., Abichou, T., 2020. Investigating the Mechanism Controlling the Chemical Compatibility and Hydraulic Conductivity of a Bentonite-Polymer Composite GCL. *Geotextiles and Geomembranes* (Under Review)

7.2 Conference Presentations

Wireko, C., Abichou, T. (presented 2019, June). *Effect of Organic Matter on Index Swell Properties of a Conventional and Bentonite-Polymer GCL*. Environmental Geotechnology, Recycled Waste Materials, and Sustainable Engineering 2019, Chicago, Illinois. (International)

Abichou, T., Wireko, C, (presented 2020, January). Assessment of Long-Term Performance of Linear Polymer Modified Bentonite (LPMB) GCLs. Keynote presentation in Chungsik Yoo (South Korea), Kent von Maubeuge (Germany) (Chair), *IGS TC-Barrier Systems Workshop*. Symposium conducted at the meeting of The International Geosynthetics Society, Barcelona, Spain. (International)

Wireko, C., Abichou, T. (presented 2020, February). *Effect of Inorganic Salts Solutions on Polymer Elution from a Bentonite-Polymer GCL*. Presentation at Global Waste Management Symposium, Environmental Research Education Foundation (EREF), Palm Springs California. (International)